Wilfrid Laurier University

Scholars Commons @ Laurier

Theses and Dissertations (Comprehensive)

2010

Insights Into The World of Pea Nodulation Using the Low Nodulator R50

Scott Clemow
Wilfrid Laurier University

Recommended Citation

Insights into the World of Pea Nodulation Using the Low Nodulator R50

by

Scott Clemow

Bachelor of Science Honours, Wilfrid Laurier University, 2008

THESIS

Submitted to the Faculty of Science

Department of Biology

In partial fulfillment of the requirements for

Master of Science in Integrative Biology

Wilfrid Laurier University

2010

I hereby declare that I am the sole author of this thesis

I authorize Wilfrid Laurier University to lend this thesis to other institutions or individuals for the purpose of scholarly research

I further authorize Wilfrid Laurier University to reproduce this thesis by photocopying or by other means, in total or in part, at the request of other institutions or individuals for the purpose of scholarly research

Abstract

Cytokinin oxidase (CKX) is the enzyme responsible for the degradation of cytokinin, a class of adenine-based plant hormones that stimulate cell division, among other physiological processes. The pea mutant R50 is characterized by having a pale leaf phenotype, dwarf stature, few lateral roots, low nodule formation, and elevated levels of endogenous cytokinins in its shoots, roots and nodules. When compared to that of the wild-type Sparkle, total CKX activity is low but the transcript levels of PsCKX1 are significantly higher. In this study, I investigated the expression of PsCKX1 throughout the development of a nodule and the localization of PsCKX1 in the nodules of Sparkle and R50. To achieve this goal, a spot-inoculation technique was developed to capture different stages of nodule organogenesis. Sparkle nodules developed as expected. The nodules of R50, however, were delayed with root hairs exhibiting abnormal waving. Furthermore, an accumulation of starch grains was noticeable in the mature nodules which formed. Transcription of PsCKX1 was up-regulated upon inoculation, reaching a plateau for Sparkle but continuously increasing for R50. There were no differences in the localization of PsCKX1 between the two lines, but the immunofluorescence signal was much higher in the mutant. Finally, a protocol for the creation of composite plants was worked out with the goal of using the technique for later complementation of R50. All evidence allowed me to suggest that R50 produces a defective PsCKX1 protein which maybe the cause of abnormal nodulation.

Acknowledgements

Table of Contents

Table of Figures

Chapter 1

Chapter 2

Chapter 3

Chapter 4

List of Tables

CHAPTER 1

General Introduction

Introduction

After World War II, a major agricultural transformation took place to "help feed the hungry" (Lockwood, 1999). In summary, the agricultural revolution called for the removal of dynamic natural ecosystems in favour of simplified ones (e.g., growing crops in monocultures without crop rotation) and for the development of crop plants that produced greater yields with higher protein content (Dimitri et al., 2005). These agricultural methods ignored the complex ecological relationships between cultured crops and their environments which led to the rapid depletion of soil nutrients (Thomas and Kevan, 1993). To maintain high crop yields, farmers were forced to apply synthetic nutrients in the form of fertilizers to agricultural fields. The dependency upon fertilizers has since been continually on the rise; 91 million tons of nitrogen-based fertilizers were applied to fields worldwide in 2007 (IFA, 2007). Unfortunately, more than half of these fertilizers are lost from agricultural fields to the environment where they contaminate ground water leading to eutrophication of aquatic ecosystems (Thomas and Kevan, 1993). Although these agriculture methods have been successful at producing food, there are concerns about their sustainability because of their negative environmental impacts as well as their dependency on fossil fuels needed to produce fertilizers (Jensen and Hauggaard-Nielsen, 2003). The chemical process whereby nitrogen is converted from its molecular form (N_2), which is biologically unavailable to eukaryotes, into bio-available nitrogenous compounds, such as ammonia (NH_4), is called nitrogen fixation. It may occur industrially but also naturally via the activity of prokaryotes (Mylona et al. 1995) and the most efficient nitrogen-fixers are those that can establish a symbiosis with plant members from the family Fabaceae (Mylona et al. 1995). Thus, one strategy that can

potentially improve crop yields while reducing the use of nitrogen-based fertilizers is the optimization of the naturally-existing symbiotic nitrogen-fixation process (Salon *et al.* 2001).

For nitrogen fixation to occur a complex and intricate program of events involving the exchange of molecular signals between a host legume plant and a specific group of bacteria, collectively known as rhizobia, has evolved. This relationship is mutualistic: the plant provides to the rhizobia energy in the form of photosynthates and an anaerobic environment for the nitrogen to be fixed while the bacteria supply the plant with the excess ammonia they produce (reviewed by Brewin, 1991).

Pisum sativum and Model Legumes

Nodulation has been investigated scientifically for over 100 years using a few select legumes, such as *Pisum sativum* (pea) (e.g. Frank, 1891 in Langenheim and Thimann, 1982). Mendel's extensive genetic analysis of pea in the 19th century provided a key model organism to study plant physiological processes, including nodulation. However, the popularity of pea as a model organism declined over the past few decades because the advancements in molecular technologies have not been easily implemented into this species. Transformation and spot-inoculation of roots are two techniques routinely used in the field of nodulation; these techniques permit the study of gene function and events of early nodule organogenesis, respectively. However, no straightforward methods have been established in pea because of its characteristics: it has a large size that restricts its growing conditions to large spaces (i.e. pea cannot be grown in petri dishes); it has a large genome comprised of approximately 4×10^9 bp (yet to be sequenced), a relatively long life-cycle (~80 days); and it appears to be recalcitrant to a

few molecular techniques such as transformation (Ellis and Poyser, 2001). Researchers ultimately developed two new model plants, *Lotus japonicus* and *Medicago truncatula* (barrel medic) to study nodulation (e.g., Szczyglowski and Stougaard, 2008 and Young and Udvardi, 2009, respectively). These plants have a rapid generation time and prolific seed production, allowing propagation to be completed easily and creating a short window of delay when plants are not experimentally ready (Cook, 1999). Their small stature and small root system permit for growth in restricted spaces such as petri plates (Cook, 1999). These species have small genomes that are almost sequenced, providing an opportunity for many molecular studies (Cannon *et al.* 2006). Also, their small size and small genome allow transformation at a relatively high success rate (Cook, 1999). Knowledge about nodulation has been greatly extended in the last 20 years because of the study of these two legume model plant systems. However, because barrel medic and *Lotus* are not used as major agricultural crops, it is important to complement the information learned from these model systems with that obtained with agriculturally-relevant plants such as pea (Young and Udvardi, 2009). Even with the knowledge that the new model plants brought forth, there is still much to be learned about how the plant coordinates and regulates the required processes for a nodule to develop.

Nodule Organogenesis

The proper recognition and the subsequent interaction between the plant and its microsymbiont result in the formation of a nodule, a novel root organ that fixes N_2. The plant species dictates the architecture and organization of the nodule (reviewed by Guinel, 2009) and therefore each plant-symbiont relationship is unique. But most nodules can be

classified into two types: the indeterminate nodules, that arise from root cortical cells located near the root endodermis, have a long-lived meristem, and the determinate (recently coined by Sprent as desmodioid) nodules, that arise from root cortical cells closer to the epidermis and have a short-lived meristem (Hirsch, 1992). Desmodioid nodules are found on plants such as *Glycine max* (soybean) and the model plant *Lotus japonicus*. Indeterminate nodules are exhibited by plants such as pea and the model barrel medic; these nodules will be concentrated on in this thesis because they are the type of nodules studied in our lab. What follows is an explanation of the nodule organogenesis in barrel medic but I will mention wherever possible what we know of the events in pea.

The series of events is initiated with the secretion of chemicals called flavonoids from the plant roots (Cohn *et al.* 1998). In pea, the two flavonoids, hesperetin and naringenin, are known to act as chemoattractants; they specifically attract *Rhizobium leguminosarum* bv. *viciae*, a common soil bacterium, toward the roots (Begum *et al.* 2001). They also act as transcription activating and non-activating compounds that compete for the binding site of the bacterial protein NodD (Peck *et al.* 2006). NodD is the product of the nodulation (nod) gene *nodD*, the only *nod* gene to be constitutively expressed by rhizobia (Fisher and Long, 1992). The coupling of an activating flavonoid with NodD promotes the binding of the complex to a conserved 55-bp region known as the *nod* box located on the sym plasmid of the bacterium (Rostas *et al.* 1986). This interaction triggers the transcription of a set of *nod* genes which encode several enzymes that contribute to the production of lipo-chito-oligosaccharides or Nod factors (NF) (Fisher and Long, 1992). NFs are responsible for the initiation of two simultaneous developmental programs in legume roots: the epidermal program that prepares the root

cells for bacterial infection and the cortical program that reactivates cell division in the root cortex for nodule formation (Guinel and Geil, 2002).

The Epidermal Program

In pea, *PsSYM10* and *PsSYM37* encode epidermal receptors that perceive the NFs released from the bacteria (Madsen *et al.* 2003 and Zhukov *et al.* 2008, respectively). The plant's recognition of NFs induces, among other things, calcium spiking in the nuclei of epidermal root hair cells (Ehrhardt *et al.* 1996). This activates a calcium-calmodulin-dependent protein kinase (CCaMK) encoded by PsSYM9, two GRAS proteins (NSP1 and NSP2 (PsSYM7), and an ERF transcription factor (reviewed by Oldroyd and Downie, 2008). This response to NFs is essential for the activation and expression of genes required for successful rhizobial infection. NFs promote also root hair curling which results in the entrapment of the rhizobia; those grow into a micro-colony within the curl. The pressure they exert on the epidermal cell wall of the root hair (van Spronsen *et al.* 1994) and the combined release of digestive enzymes result in a localized cell-wall erosion which creates a portal for rhizobia to enter the cell (Robledo *et al.* 2008).

The Cortical Program

Simultaneous to their epidermal action, NFs prime the cells of the pericycle, i.e., the outermost cell layer of the stele, and of the cortex which divide anticlinally first and periclinally later (Timmers *et al.* 1999; Voroshilova *et al.* 2009). Indeed, mutations in the genes responsible for NF receptor proteins prevent the plant from perceiving the rhizobial

signals inhibiting nodule initiation. The sites of cell divisions are located opposite the developing infections usually in front of a xylem pole (Smit *et al.* 1995). Once the pericycle cells have divided, the innermost cortical cells follow suite; they produce square-shaped cells, which as a group are referred to as the initial nodule primordium (Timmers *et al.* 1999). Subsequent divisions extend the nodule primordium to the middle cortex where the nodule meristem is formed (Monahan-Giovanelli *et al.* 2006). In indeterminate nodules the outer cortical cells do not play a role in the formation of the nodule primordium but are nevertheless involved in nodule organogenesis. The outer cortical cells undergo cytoskeletal rearrangement creating a path for the infection threads to migrate towards the developing nodule (Timmers *et al.* 1999). The resulting structure, first observed in pea and known as a pre-infection thread, forms just ahead of the infection thread (van Brussel *et al.* 1992). It is a cytoplasmic bridge that traverses the central vacuole of cells not yet infected; it forms an effective corridor to the developing nodule for the bacteria within the infection thread (van Brussel *et al.* 1992).

Integration of the Two Programs

The integration of the epidermal and cortical programs is essential for a nodule to develop and function properly. The release of bacteria from the infection threads is mediated by the formation of infection droplets which bud from the host-cell plasma membrane into the infected cell of the nodule (Brewin, 1994). This endocytotic process results in the creation of a symbiosome which consists of a plant cell membrane surrounding a bacterium (Monahan-Giovanelli *et al.* 2006). The internalized bacteria undergo global changes in gene expression as they differentiate into bacteroids; certain genes involved in their basic necessities are down-regulated while genes involved in the

7

symbiosis and nitrogen fixation are up-regulated (Becker *et al.* 2004). In indeterminate nodules, symbiosomes generally contain only one bacteroid and are capable of dividing by fission (reviewed by Prell and Poole, 2006).

Morphology of an Indeterminate Nodule

Four distinct histological regions within the nodule have been described (Vasse *et al.* 1990): the bacteria-free meristematic zone (I); the infection zone (II) where bacteria are released from the infection thread; the nitrogen-fixing zone (III), where bacteria are fully differentiated into bacteroids and nitrogen fixation takes place; and a senescent zone (IV), which is usually appearing 5 weeks after inoculation. Vasse *et al.* (1990) also describe a small transition zone, Zone II-III, where the conversion from bacteria to bacteroid occurs. This is also the region for the induction of many plant nodulin genes, such as the symbiotic leghemoglobins (Soupène *et al.* 1995). Timmers *et al.* (2000) described a fifth zone (V) within the nodule called the saprophytic zone, where some intracellular bacteria which did not differentiate into bacteroids remain alive and take advantage of the symbiosis for their exclusive benefit. The central zones afore described are enclosed by peripheral tissues consisting of an outer cortex, i.e., a protective layer (2-5 layers) of thin-walled cells originating from the root, and a nodule parenchyma which originates from the nodule meristem (Hirsch, 1992). Within the nodule parenchyma, a network of vascular strands surrounded by a sheath of vascular endodermis is evident (reviewed by Guinel, 2009). Separating the vascular tissue from the vascular endodermis are pericycle cells, with wall ingrowths, specialized in the exchange of compounds between the infected tissue and the nodule parenchyma (Newcomb, 1981). Encasing the nodule

parenchyma is a nodule endodermis with casparian strips (reviewed by Guinel, 2009). The outer cortex is the only tissue to surround the nodule meristem as all other peripheral tissues originate from it and thus are located below it (Bond, 1948).

Hormones Involved in Nodule Organogenesis

Although nodulation is beneficial to the legume, it needs a large amount of energy for the plant to construct the nodule *de novo* and to supply the residents with photosynthates essential for nitrogenase activity. It requires sixteen molecules of ATP for the production of 2 molecules of ammonia. The plant must balance the benefits of establishing this relationship with normal nutritional needs for growth and development and periods of stress. Thus, both the epidermal and cortical programs are under the tight control of phytohormones (e.g. Guinel and Geil, 2002). Their involvement in nodule development is complicated and not fully understood. The difficulty in elucidating each hormone's function arises because hormone actions are deeply intertwined in the nodulation process. Complicating the matter further are the subtle differences in nodule regulation between indeterminate and determinate nodules. Although most of the nodulation stages between indeterminate and determinate nodules are similar, salicylic acid (SA) for instance can block indeterminate nodule formation while having no effect on determinate nodule formation (van Spronsen, 2003). What follows is a brief description of the hormones known to be involved in nodule development, with no special focus on the type of nodule.

Negative Regulators

Ethylene, jasmonic acid (JA), SA, and abscisic acid (ABA) all inhibit nodule initiation, i.e., the signals involved in the epidermal program. First, ethylene suppresses

the NF signal transduction; the result is the inhibition of root hair deformation, calcium-spiking, bacterial infection, expression of early nodulin genes and ultimately nodule number (Oldroyd *et al.* 2001). Second, JA, when applied, inhibits the transcription of two early nodulin genes, *ENOD11* and *RIP* (Ding and Oldroyd, 2009). It is known as a synergistic partner to ethylene converging through the transcription factor ERF1 (Lorenzo *et al.* 2003). However, JA has also effects opposite to those of ethylene on calcium spiking whereby ethylene shortens and JA prolongs the spike period (Sun *et al.* 2006). Third, exogenous SA treatment of alfalfa roots result in both reduced and delayed nodule development (Martinez-Abarca *et al.* 1998). SA levels are known to be increased during the plant defence response. Interestingly, rhizobia release their unique salicylate hydroxylase enzymes which reduce endogeneous SA levels thereby repressing the plant defence response. An overexpression of the rhizobial salicylate hydroxylase (NahG) gene in both *Lotus* and barrel medic increased rhizobial infection and nodule numbers (Stacey *et al.* 2006). Fourth, ABA have similar effects to those of ethylene on nodule formation; however, their regulation of nodulation appears to be independent of one another (Ding *et al.* 2008). ABA can abolish the formation of spontaneous nodules resulting from the gain-of-function mutations CCaMK, suggesting that ABA also inhibits early steps in the *Lotus* cortical program by suppressing the cytokinin activation of cell division (Ding *et al.* 2008).

Positive Regulators

Brassinosteroids, gibberellins, auxins and cytokinins are positive regulators of nodulation. Mutations that diminish the levels of brassinosteroid and gibberellin result in

the reduction of the number of nodules produced by the plant (Ferguson *et al.* 2008). However, there has been little investigation on how these hormones affect the formation of a nodule. Auxins and cytokinins are known to be antagonistic partners in the development of organs; for example, high levels of auxin and low levels of cytokinin promote cell division for lateral root development. The opposite is true for the first cell divisions leading to the formation of a nodule; cytokinin levels are high as auxin flow is temporarily inhibited, resulting in a localized suppression of auxin transport (Mathesius *et al.* 2008). Interestingly, plants with high levels of endogenous auxin have an increased nodule number (van Noorden *et al.* 2006) indicating that auxin is essential for nodule organogenesis once the nodule primordium is established. Although all of the aforementioned hormones are required and their actions deeply intricated in nodule organogenesis, cytokinin will be discussed in greater depth as the pea mutant R50 studied here accumulates it in large quantities.

Cytokinin

Cytokinins are a class of adenine-based plant hormones that are important for cell division and therefore essential for the establishment of any primordium (Mok and Mok, 2001). Cytokinin signaling has been studied in depth in the model plant system *Arabidopsis thaliana*. Cytokinin acts through a complex two-component system which involves receptor kinases (AHK4, AHK3 and AHK2), histidine phosphotransfer proteins (AHPs) and response regulators (reviewed by Ferreira and Kieber, 2005). In short, cytokinin binding to a receptor kinase on the plasma membrane stimulates the transfer of one of its phosphate groups to an AHP protein (Imamura *et al.* 1999), triggering the

translocation of this protein into the nucleus (Hwang and Sheen, 2001) where the gained phosphate is passed to a response regulator (Imamura *et al.* 2001). This transfer relieves the repression of type-B *Arabidopsis* response regulators (ARRs) leading to the induction of the cytokinin responses as well as the expression of type-A ARRs (Heyl *et al.* 2008) that function as negative regulators of cytokinin responses (To *et al.* 2008).

Many aspects of plant growth and development are regulated by cytokinin, including nodulation. Cytokinin signaling was recently demonstrated to be of prime importance to nodule organogenesis as a gain-of-function mutation in the *Lotus* cytokinin receptor LHK1, an ortholog to the *Arabidopsis* AHK4, resulted in spontaneous nodule formation (Tirichine *et al.* 2007). Conversely, a loss-of-function in the cytokinin receptor LHK1 repressed the formation of nodule primordia (Murray *et al.* 2007). In pea, a dose-response has been observed between treatment of exogenous cytokinin and nodule formation as cytokinin stimulates nodule production but inhibits it at concentration greater than 1 μM (Lorteau *et al.* 2001). The hallmark of a plant hormone is its ability to affect physiological processes at concentrations far below the levels that vitamins and nutrients would affect these processes (Davies, 2004). Thus, since these hormones influence changes in minute quantities, they need to be tightly regulated.

Cytokinin Oxidase

The active cytokinin pool of a plant cell is controlled by its rate of import, biosynthesis, inactivation and degradation. Cytokinin homeostasis is regulated by cytokinin oxidase (CKX) which catalyzes the irreversible degradation of the hormone by cleaving the unsaturated isoprenoid side chains, releasing an adenine molecule and

aldehyde side-chain products (reviewed by Werner *et al.* 2006). In higher plants, CKX proteins are encoded by a small family of CKX genes. Seven CKX-encoding genes have been discovered in *Arabidopsis* (Werner *et al.* 2001); so far 11 CKX members have been identified in *Oryza sative* (rice), 13 for *Triticum* (wheat) and *Hordeum vulgare* (barley) and 2 CKX members have been identified in pea (Held *et al.* 2008). CKX is a flavoprotein that contains a covalently-bound FAD molecule as a cofactor. Although oxygen was originally classified as the electron acceptor for CKX, it was recently discovered that CKX preferentially acts as a dehydrogenase (Frébortová *et al.* 2004), as all seven AtCKX enzymes had increased activity when an electron acceptor other than oxygen was present (Galuzka *et al.* 2007). Therefore the enzyme was reclassified and is now called cytokinin oxidase/dehydrogenase.

CKX knock-outs plants have been difficult to study because of the functional redundancy of the members of the CKX gene family, although a couple of studies have been completed. On one hand, Ashikari *et al.* (2005) were able to knock-out *OsCKX2*, resulting in an increased grain number in rice, while a decrease in grain number was observed with its overexpression. On the other hand, Zalewski *et al.* (2010) silenced the *HvCKX1* gene in barley leading to higher plant productivity.

Gain-of-function mutations in *Arabidopsis* resulting in the overexpression of CKX have been utilized to decrease cytokinin content with the intention of unraveling the physiological processes of cytokinin. Cytokinin-deficient plants have decreased shoot-apical meristem activity, reduced formation of leaf primordia and vascular development (eventually resulting in shoot meristem activity arrest), delayed flowering and enhanced root growth (Werner *et al.* 2001; Yang *et al.* 2003). Most of these phenotypic traits can

be also observed in cytokinin receptor mutants (Higuchi *et al.* 2004; Nishimura *et al.* 2004; Riefler *et al.* 2006). However, a few differences have been identified between plants with reduced cytokinin content and cytokinin receptor mutant plants. Shoot meristem arrest and delayed flowering were not observed in the cytokinin signalling mutants. One other difference was that the triple cytokinin receptor mutants have reduced root systems compared to those in plants with decreased cytokinin content (Higuchi *et al.* 2004; Nishimura *et al.* 2004; Riefler *et al.* 2006).

R50

A good tool to study the effects that cytokinin has on growth and development in pea is the mutant R50 (Figure 1.1) which accumulates cytokinins (Ferguson *et al.* 2005). R50 (*sym16*) is a pleiotropic recessive mutant, obtained by gamma radiation of the seeds of Sparkle, which was screened for low nodulation at 21 days after planting (Kneen and LaRue, 1988). It exhibits a total CKX enzymatic activity lower than that of wild-type (WT) Sparkle in its roots, shoots and nodules; interestingly, PsCKX1 and PsCKX2 transcripts are up-regulated in its shoots and nodules (Held *et al.* 2008).

R50 has been characterized as possessing a small root system, short internodes, and a short stature, and displaying a pale leaf colour when compared to the wild-type (Guinel and Sloetjes, 2000). Physiological processes such as flowering time and nodulation also appear to be delayed in R50. In addition, the vasculature in its roots has been described as abnormal as the primary root and lateral roots contain an extra and one fewer vascular pole than Sparkle, respectively (Pepper *et al.* 2007). The vasculature of R50's nodule also contains 1 additional vascular strand, 3 in total, with the strands being

highly diverse in length compared to the vasculature found in Sparkle nodules (Pepper *et al.* 2007). R50 nodulation phenotype is unique in that the number of infections is normal,

Figure 1.1. Sparkle versus R50. The wild-type (WT), Sparkle, and the mutant R50 at 21 days after planting. R50 is the result of a single recessive mutation at *sym16*. R50 is stunted in its growth and has pale leaves compared to Sparkle.

R50   WT
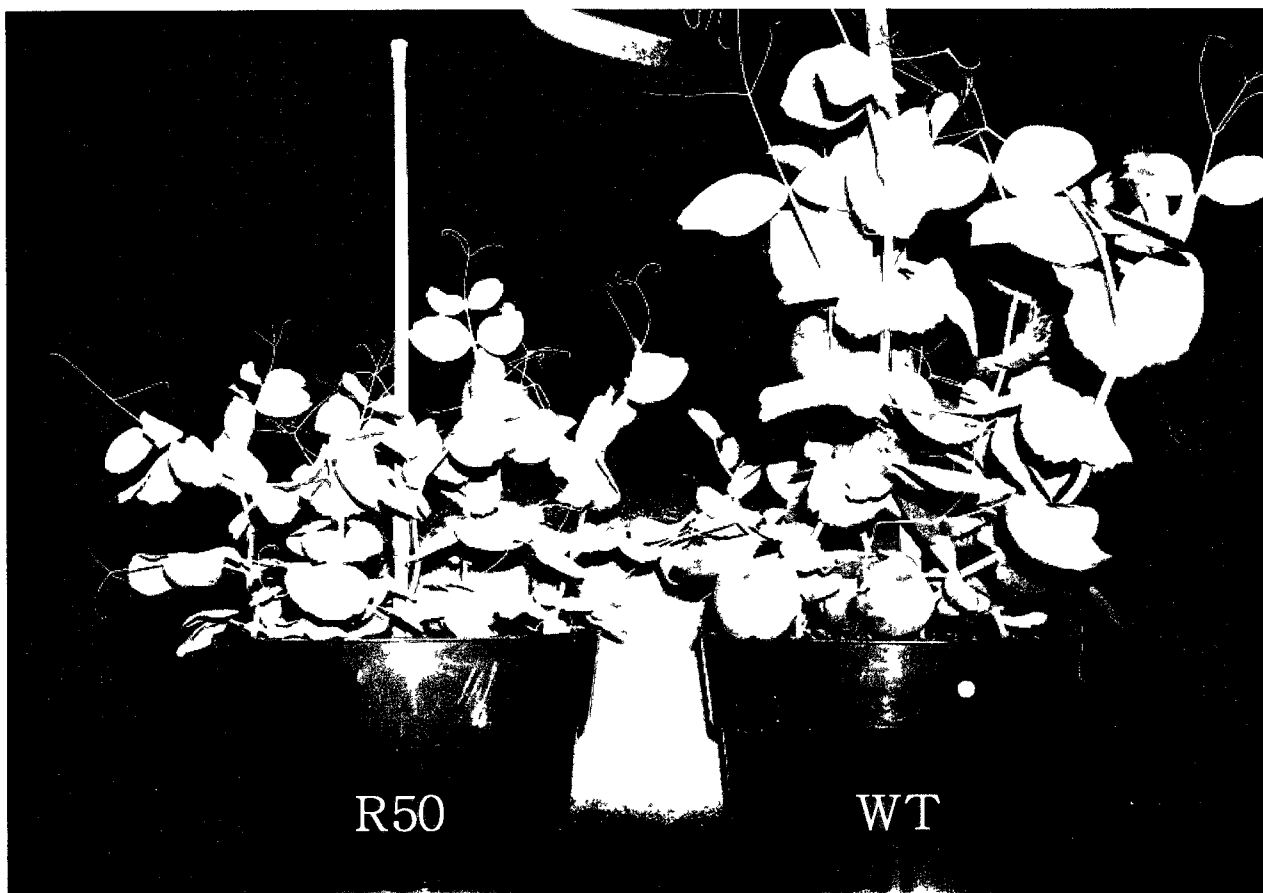
i.e., similar to that of Sparkle, but the periclinal divisions of the inner cortical cells which should usually follow the anticlinal divisions do not occur to form a nodule primordium (Guinel and Sloetjes, 2000). Furthermore, the infection threads seem to be misguided in their growth as they do not proceed directly toward the nodule primordium and appear as coiled masses. The few nodules that do form are rather flat and appear white in colour compared to the oblong pink nodules observed on wild-type roots (Guinel and Sloetjes, 2000). Interestingly, treatments of WT pea with cytokinin levels greater than 1μM result in a nodulation phenotype similar to that of R50, i.e., coiled infection threads and flattened nodule primordia (Lorteau *et al.* 2001).

Objectives

In this research, I studied the nodule organogenesis of *Pisum sativum* (pea) at the molecular level to determine the role of cytokinin oxidase in a developing nodule. Specifically, I aimed at:

- Developing a spot-inoculation method to examine early infection events.

- Generating the expression profile of *PsCKX1* transcripts throughout developing nodules.

- Localizing the protein of PsCKX1 in the nodule.

I also developed a protocol to obtain composite pea plants to insert or silence genes known to be essential for nodulation. Specifically, I aimed at:

- Promoting the synchronous formation of lateral roots from a callus in a decapitated pea plant.

- Obtaining healthy composite plants.

References

Begum, A., Leibovitch, S., Migner, P., and Zhang, F. 2001. Specific flavonoids induced Nod gene expression and pre-activated nod genes of *Rhizobium leguminosarum* increased pea (*Pisum sativum* L.) and lentil (*Lens culinaris* L.) nodulation in controlled growth chamber environments. *Journal of Experimental Botany.* **52**: 1537-1543.

Bond, L. 1948. Origin and developmental morphology of root nodules of *Pisum sativum*. *Botanical Gazette.* **109**: 411-434.

Brewin, N. 1991. Development of the legume root nodule. *Annual Review Cell Biology.* **7**: 191-226.

Cannon, S. B., Sterck, L., Rombauts, S., Sato, S., Cheung, F., Gouzy, J., Wang, X., Mudge, J., Vasdewani, J., Schiex, T., Spannagl, M., Monaghan, E., Nicholson, C., Humphray, S. J., Schoof, H., Mayer, K. F. X., Rogers, J., Quétier, F., Oldroyd, G. E., Debellé, F., Cook, D.R., Retzel, E. F., Roe, B. A., Town, C. D., Tabata, S., Van de Peer, Y., and Young, N. D. 2006. Legume genome evolution viewed through the *Medicago truncatual* and *Lotus japonicus* genomes. *Proceedings of the National Academy of Sciences.* **103**: 14959-14964.

Cohn, J., Day, B., and Stacey, G. 1998. Legume nodule organogenesis. *Trends in Plant Science.* **3**: 105-110.

Cook, D. 1999. Medicago truncatula – a model in the making! *Biotic Interactions.* **2**: 301-304.

Ding, Y., Kalo, P., Yendrek, C., Sun, J., Liang, Y., Marsh, J. F., Harris, J. M., Oldroyd, G. E. D. 2008. Abscisic acid coordinates Nod Factor and cytokinin signaling during the regulation of nodulation in *Medicago truncatula*. *The Plant Cell.* **20**: 2681-2695.

Ding, Y., and Oldroyd, G.E.D. 2009. Positioning the nodule, the hormone dictum. *Plant Signaling and Behavior.* **4**: 89-93.

Dimitri, C., Effland, A., and Conklin, N. 2005. The 20th century transformation of U.S. agriculture and farm policy. USDA.

Ehrhardt, D. W., Wais, R., and Long, S. R. 1996. Calcium spiking in plant root hairs responding to *Rhizobium* nodulation signals. *Cell.* **85**: 673-681.

Ellis, T., and Poyser, S. 2002. An integrated and comparative view of pea genetic and cytogenetic maps. *New Phytologist.* **153**: 17-25.

Ferguson, B.J., Wiebe, E.M., Emery, N., and Guinel, F.C. 2005. Cytokinin accumulation and an altered ethylene response mediate the pleiotropic phenotype of the pea nodulation mutant R50 (*sym16*). *Canadian Journal of Botany.* **83**: 989-1000.

Ferreira, F. J., and Kieber, J. J. 2005. Cytokinin signaling. *Current Opinion in Plant Biology*. **8**: 518-525.

Fisher, F., and Long, S. 1992. *Rhizobium*-plant signal exchange. *Nature*. **357**: 655-660.

Galuszka, P., Popelkova, H., Werner, T., Frebortova, J., Pospisilova, H., Mik, V., Kollmer, I., Schmulling, T., Frebort, I. 2007. Biochemical characterization of cytokinin oxidases/dehydrogenases from *Arabidopsis thaliana* expressed in *Nicotiana tabacum* L. *Journal of Plant Growth and Regulation*. **26**: 255-267.

Guinel, F.C. and Sloetjes, L.L. 2000. Ethylene is involved in the nodulation phenotype of *Pisum sativum* R50 (*sym16*), a pleiotropic mutant that nodulates poorly and has pale green leaves. *Journal of Experimental Botany*. **51**: 885-894.

Heyl, A., Ramireddy, E., Brenner, W. G., Riefler, M, Allemeersch, J., and Schmulling, T. 2008. The transcriptional repressor ARR1-SRDX suppresses pleiotropic cytokinin activities in *Arabidopsis*. *Plant Physiology*. **147**: 1380-1395.

Hwang, I., and Sheen, J. 2001. Two-component circuitry in *Arabidopsis* cytokinin signal transduction. *Nature*. **413**: 383-389.

IFA. May 2007. International Fertilizer Association. Fertilizer—Use Statistics. www.fertilizer.org/ifa/statistics.asp.

Jensen, E. S., and Hauggaard-Nielsen, H. 2003. How can increased use of biological N_2 fixation in agriculture benefit the environment? *Plant and Soil*. **252**: 177-186.

Kneen, B. E., and LaRue, T. A. 1988. Induced symbiosis mutants of pea (*Pisum sativum*) and sweetclover (*Melilotus alba annua*). *Plant Science*. **58**: 177-182.

Langenheim, J. H. and Thimann, K. V. 1982. Botany – Plant biology and its relation to human affairs. John Wiley and Sons, New York. pp 145-159.

Lockwood, A. J. 1999. Agriculture and biodiversity: Finding our place in the world. *Agriculture and Human Values*. **16**: 365-379.

Lorenzo, O., Piqueras, R., Sánchez-Serrano, J. J., and Solano, R. 2002. ETHYLENE RESPONSE FACTOR1 integrates signals from ethylene and jasmonate pathways in plant defence. *The Plant Cell*. **15**: 165-178.

Lorteau, M-A., Ferguson, B.J., and Guinel, F.C. 2001. Effects of cytokinin on ethylene production and nodulation in pea (*Pisum sativum*) cv. Sparkle. *Physiologia Plantarum*. **112**: 421-428.

Monahan-Giovanelli, H., Pinedo, C., and Gage, D. 2006. Architecture of infection thread networks in developing root nodules induced by the symbiotic bacterium *Sinorhizobium meliloti* on *Medicago truncatula*. *Plant Physiology*. **140**: 661-670.

Mylona, P., Pawlowski, K., and Bisseling, T. 1995. Symbiotic nitrogen fixation. *The Plant Cell*. **7**: 869-885.

Peck, M., Fisher, F., and Long, R. 2006. Diverse flavonoids stimulate NodD1 binding to *nod* gene promoters in *Sinorhizobium meliloti*. *Journal of Bacteriology*. **188**: 5417-5427.

Pepper, A.N., Morse, A.P., Guinel, F.C. 2007. Abnormal root and nodule vasculature in R50 *(sym 16)*, a pea nodulation mutant which accumulate cytokinin. *Annals of Botany*. **99**: 765-776.

Rostas, K., Kondorosi, E., Horvath, B., Simoncsits, A., and Kondorosi, A. 1986. Conservation of extended promoter regions of nodulation genes in *Rhizobium*. *Proceedings of the National Academy of Sciences*. **83**: 1757-1761.

Smit, G., de Koster, C., Schripsema, J., Spaink, H., van Brussel, A., and Kijne, J. 1995. Uridine, a cell division factor in pea roots. *Plant Molecular Biology*. **29**: 869-873.

Szczyglowski, K., and Stougaard, J. 2008. *Lotus* genome: pod of gold for legume research. *Trends in Plant Science*. **13**: 515-517.

Timmers, A., Auriac, M. and Truchet, G. 1999. Refined analysis of early symbiotic steps of the *Rhizobium-Medicago* interaction in relationship with microtubular cytoskeleton rearrangements. *Development*. **126**: 3617-3628.

Timmers, A., Soupene, E., Auriac, A.C., de Billy, F., Vasse, J., Boistard, B., and Truchet, G. 2000. Saprophytic intracellular rhizobia in alfalfa nodules. *Molecular Plant-Microbe Interactions*. **13**: 1204-1213.

Thomas, V. G. and Kevan P.G. 1993. Basic principles of agroecology and sustainable agriculture. *Journal of Agriculture and Environment*. **6**: 1-19.

van Brussel, A., Bakhuizen, R., Van Spronsen., Spaink, H.P, Tak, T., Lugtenberg, Ben., Kijne, J.W. 1992. Induction of pre-infection thread structures in the leguminous host plant by mitogenic lipo-oligosaccharides of *Rhizobium*. *Science*. **257**: 70-72.

van Spronsen, P., Bakhuizen, R., van Brussel. A., and Kijne, J. 1994. Cell wall degradation during infection thread formation by the root nodule bacterium *Rhizobium leguminosarum* is a two-step Process. *European Journal of Cell Biology*. **64**: 88-94.

Young, N.D., and Udvardi, M. 2009. Translating *Medicago truncatula* genomics to crop legumes. *Current Opinion in Plant Biology*. **12**: 193-201.

CHAPTER 2

Spot-inoculation of *Pisum sativum*

Methodology

Protocol: A "stress-free" spot-inoculating method for *Pisum sativum*

Scott R. Clemow and Frédérique C. Guinel

Department of Biology, Wilfrid Laurier University, 75 University Avenue West, Waterloo, N2L 3C5, Ontario, Canada.

[§]Corresponding author – FCG

Email addresses:
>   SRC: clem5940@mylaurier.ca
>   FCG: fguinel@wlu.ca

Abstract

Background

The symbiotic nodule is a unique plant organ that develops on the legume root through the exchange of signaling molecules between the plant and host-specific bacteria called rhizobia. This structure provides the necessary conditions for atmospheric nitrogen to be effectively converted by the rhizobia into plant-usable nitrogenous compounds. Model legumes, such as *Medicago* and *Lotus*, and techniques that have recently become available made it possible to investigate the molecular events required for nodule formation. To study the initial events of nodule organogenesis, the precise location of rhizobial infection is essential. Towards this goal, a technique called spot-inoculation had been developed for soybean and had been implemented in the model legumes; however, it turned out to be difficult to apply to pea.

Results

We present a fine-tuned spot-inoculation method for pea and its delayed nodulation mutants which allows us to observe the early events of the formation of a nodule and follow its development to maturity. Seeds were pre-germinated, transferred to growth pouches, and inoculated with a minute drop of *Rhizobium leguminosarum* in the root zone that is most susceptible to infection. Spot-inoculation was successful only when light was completely eliminated from roots, low nutrient solution with micronutrients provided, and the bottom of the pouch cut for the filter paper to draw water from the vermiculite to maintain the root system in a moist environment.

Conclusions

The adaptation of this technique for pea allows the visualization of the time course of nodule organogenesis and, in combination with molecular tools, will aid in the dissection of nodule regulation. The method permits the precise and speedy study of early nodulation events and should be transferable to the study of all kinds of symbiotic mutants. This protocol overcomes key problems in the spot-inoculation method because it is geared toward lateral root infection and the long-term health of the plant.

Introduction

Pisum sativum (pea) was once a promising model organism for plant research; however, it has lagged behind other plants in becoming the model organism to study nodulation. Reasons for this stem from the fact that pea is a large plant. It requires for its growth large spaces that cannot be reduced to the scale of Petri dishes and it has a relatively long life-cycle ($\sim$ 80 days). It has a large genome (yet to be sequenced) making many molecular techniques difficult to use [1], and it has been difficult to transform pea for the study of nodulation gene function. However, the agricultural and economic importance of pea has been on the rise since the mid 1970's. Canada, the world's largest producer and exporter of pea, is responsible for 28% of the world's 11, 914, 230 metric tons of dry pea [2]. Pea production is expected to increase further as farming practises are changing, with farmers once again utilizing the benefits of crop rotation to decrease fertilizer applications.

Two legumes, *Lotus japonicus* and *Medicago truncatula* (barrel medic), have been used as model plants to study the plant-rhizobial relationship that leads to the fixation of nitrogen [e.g., 3, 4]. These model organisms have helped advance our understanding of the molecular dialogue between plants and rhizobia and the signaling pathway which ensues. The early symbiotic events in the root that lead to nodule organogenesis are a subject of great interest, but have been difficult to study [5]. Complications arise in finding the sites of developing nodules within non-translucent and thick roots [5]. Furthermore, specific events that lead to the formation of a nodule occur within the root not only after but also before bacteria enter the root [5]. In short, for an indeterminate nodule such as that formed on barrel medic and pea, cell dedifferentiation occurs in the

27

inner cortex, triggering the development of the nodule primordium. Meanwhile pre-infection threads form to prepare the progression of the rhizobia across the root cortex [6]. Once the bacteria have penetrated the inner cortex, the nodule primordium develops into a nodule meristem and soon a nodule emerges from the root [7]. Nevertheless, there is still much to be learned about the early events required for a nodule to form.

Spot-inoculation is a technique that can be exploited to induce the formation of a nodule at a known location, and it has been utilized to identify many of the events mentioned previously. It permits the easy capture of the first stages of nodule organogenesis, including the pre-infection events. This technique also enables one to know precisely the age of the developing or mature nodule, permitting a possible linkage between gene expression and a particular developmental stage. Spot-inoculation is now a common practice in the model legumes *Lotus* and *Medicago* whereby plants are grown on agar plates with varying nutrients [8-11]. Yet this method has not been widely used to spot-inoculate larger plants such as pea, likely because these are difficult to work with under these conditions. To accommodate this technique to pea, we had to adapt the protocol from Turgeon and Bauer of 1983 [12].

Materials

Plant Material

Pisum sativum L. cv. Sparkle plants were grown under incandescent (OGE 600 hour, 60 – 120 W, 120 Volts, General Electric) and cool white fluorescent lights (Watt-Miser GE, F96TIZ-CW-HO-WM) in a growth-room with a 22h/18h, 16°C/8°C hour, light/dark regime. The total light intensity received by the plants was 280 μmol·m-2·s-1.

Bacterial Strain

Rhizobium leguminosarum bv. *viciae* 128C53K (gift from Dr. S. Smith, EMD Crop Bioscience, Milwaukee, WI) was cultured, from a rhizobial slant kept at -20°C, in 20 mL of yeast-mannitol broth (YMB) consisting of (g/L) mannitol 10.0, K_2HPO_4 0.5, $MgSO_4$ 0.2, NaCl 0.1, yeast extract 0.4 and adjusted to a pH of 6.8. The broth inoculated with a loop-full of a culture was grown at 25°C in Erlenmeyer flasks on an orbital shaker at 100 rpm. Cells were grown to late log phase (48 hours) and the viable cell density was 1.2 x 10^6 colony forming units (CFUs)/ mL.

Reagents and Consumables

Growth pouches (Mega International, West St. Paul, MN)

Sterile low nitrogen nutrient solution containing (mM) KH_2PO_4 2.00, $Ca(NO_3)_2$ 0.50, K_2SO_4 2.00, $MgSO_4 \cdot 7H_2O$ 1.00, Fe III EDTA 0.20, and microelements (μM) KCl 0.05, H_3BO_3 25.0, $MnSO_4 \cdot H_2O$ 2.0, $ZnSO_4 \cdot 7H_2O$ 2.0, $CuSO_4 \cdot 5H_2O$ 0.5, $Na_2MoO_4 \cdot 2H_2O$ 0.5.

Lab tape (VWR International, Arlington Heights, IL)

Sterile water

Sterile serological pipette

Sterile filter paper

Vermiculite – medium-sized grain (Plant Products Company Ltd., Brampton, ON)

Cuvette

Equipment

Micro-pipette – an Eppendorf™ pipette with a range of $0.1 - 2.5\mu L$.

Tweezers

Razor blade

Scissors

Water-proof marker

Dissecting microscope

Orbital shaker incubator (New Brunswick Scientific, Edison, NJ)

7.5 and 15 cm width pots

Cary 50 UV-visible spectrophotometer (Varian, Inc. Mississauga, ON)

Protocol

Background

Substrate Choice

Fåhraeus (1957) developed a technique that permits the periodic observation of the *Trifolium repens* (white clover) rhizobial infection [13]. It relied on the cultivation of seedlings on nutrient-filled microscope slides (a.k.a. Fahraeus slides). Reports have been made in which pea has been successfully spot-inoculated utilizing Fahraeus medium [14] or agar-filled plates [6, 15]. However, in our lab we have never been able to grow healthy pea plants in agar, and other labs in the past have reported similar problems [16]. Pea has a large root system which out-grows plates rapidly, making it difficult to cultivate the plant over a long period of time, and impractical to study nodule development, especially in pea mutants with delayed nodulation. Likely to avert this problem, to our knowledge, pea spot-inoculation techniques have all been performed on primary roots. Although in this species nodules occasionally form on primary roots, they most often develop on lateral roots [17, 18]. The fact that pea primary and lateral roots have different anatomy [19] could have an unforeseen effect on nodule development.

With filter paper within a pouch as a substrate, one can avoid the finicky growth of large plants on agar plates. Turgeon and Bauer [12] grew *Glycine max* (soybean) in germination pouches held in an upright position in plastic trays with high walls and spot-inoculated them with one nL drop of inoculum, which they placed in the root zone that is most susceptible to infection [20]. The pouches needed to be checked daily to determine if watering was required. In our attempts to replicate this technique for pea, the roots

either tended to dry rapidly or became easily water-logged, thus stunting the growth of the plant and preventing the formation of any nodules even with high humidity conditions. The pouches at times needed to be watered twice a day, and if a careful eye was not kept on them the roots dried quickly making a prolonged study unfeasible. With the protocol outlined below, plants in pouches can be left unattended for 4-5 days, or longer.

Inoculum Delivery

Diaz *et al.* [17] reported successful nodulation on the primary root of pea spot-inoculated with a drop of an inoculum made of a mixture of rhizobia and 0.15% agar. Employing the technique of Diaz *et al.* [17], van Brussel *et al.* [6] were in fact able to observe the first described pre-infection threads. However, when we tried this method, the agar-mixed rhizobia impeded root growth (drying the root in some cases) in the area of application and no nodules were observed. Other spot-inoculation techniques were attempted. First, a small strip of parafilm™ was used to hold the drop of inoculum in place at the desired location [20]. Second, a rhizobial-india ink suspension was essayed [20]. Bhuvaneswari *et al.* [20] used both techniques to determine the zone of soybean root that is the most susceptible to infection. Finally, glass micro-carriers which were successful in spot-inoculating alder with *Frankia* [21] were used to transfer rhizobia to the root and to prevent the inoculum drop from moving away from the desired location. The above techniques not only were tedious and time-consuming, but they failed to produce nodules via spot-inoculation on pea, i.e. the nodules did not form where the inoculum was originally placed.

With the technique presented here, the spot-inoculation of pea is easily accomplished. It is possible to determine the exact age of the nodule from the time of

inoculation to 28 days thereafter, although it may be possible to examine older nodules. It offers the plants a stress-free environment, eliminating potential artifacts caused by plant stress responses. It also reduces the amount of attention required from the researcher to care for the plants.

Growth and Spot-Inoculation of Pea

It is important to follow the steps outlined below with the usual precautions to reduce the probability of contamination, namely by using a sterile hood or a flame. Figure 2.1 highlights important steps in the protocol for successful spot-inoculation.

1| Surface-sterilize seeds in 8% bleach for 5 minutes to eliminate microbial and fungal contamination during germination. Wash seeds in three rinses of sterile water for 1 minute each and store them in sterile water in darkness for 12 to 15 hours to imbibe.

2| Plant seeds in 7.5 cm pots filled with sterile vermiculite and let grow for 3 days (Figure 2.1, A). Growing seeds in vermiculite is crucial to obtain plants with straight roots for easy transfer to pouches.

3| Three days later, prepare to transfer one seedling per germination pouch. Make a hole in the trough centre of the pouch with a clean blade, so that the root is placed through the trough but the cotyledons do not fall through the hole. It is important to allow the pea seedlings to develop for 3 days as the length of the radicle is optimal at this time.

Figure 2.1 - Schematic representation of important steps in the protocol for pea spot-inoculation

A. Imbibed seeds placed in vermiculite and kept for 3 days; B. Seedling radicle placed in trough of trimmed pouch; C. Cotyledons and epicotyls protruding from tightly-closed pouches; D. Pots, with pouches inside, filled with vermiculite; E. Inoculation 5 days later with bacteria placed in the most susceptible zone to infection; F. Pouches returned to pots; and G. Healthy plants allowed to grow until harvest.
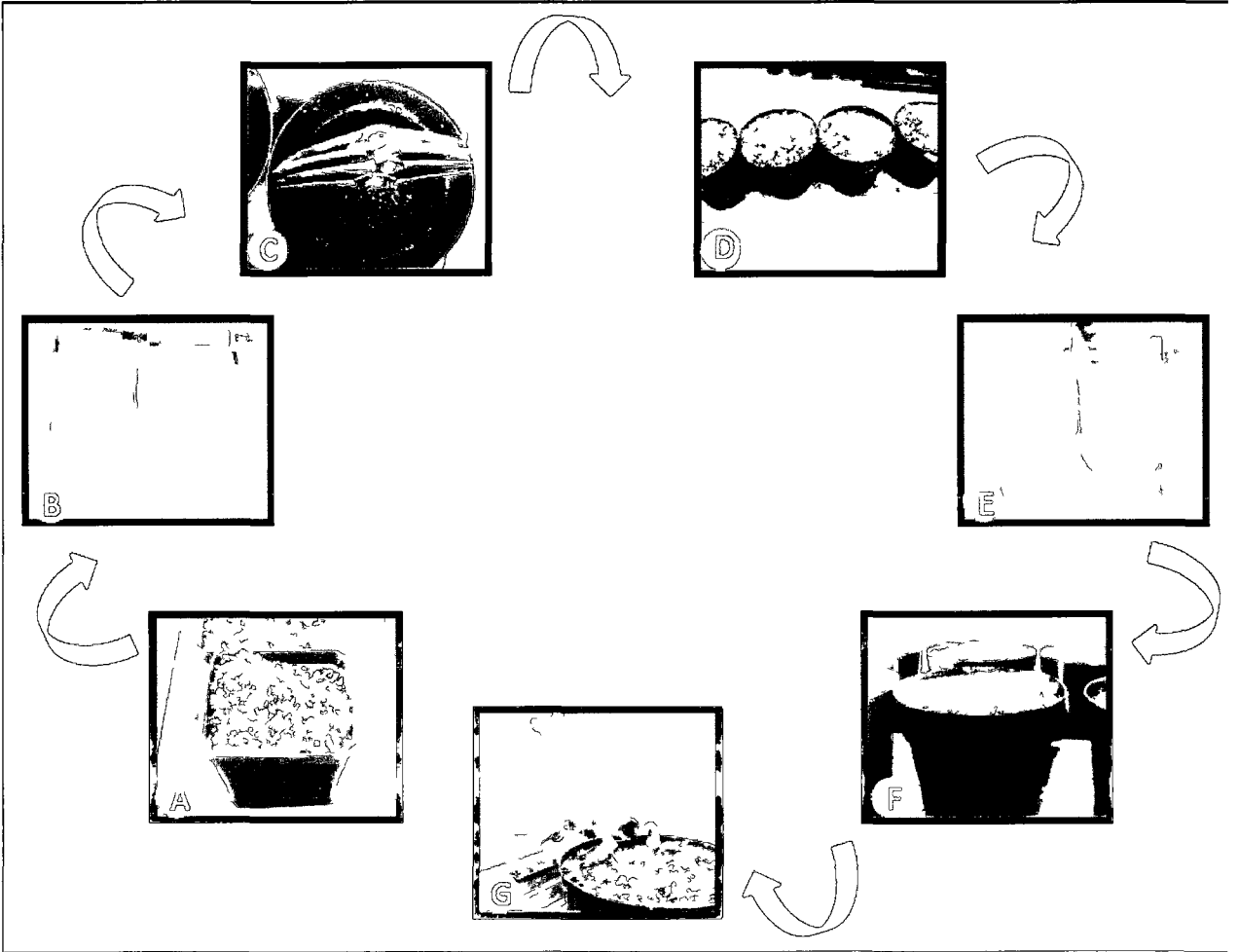
4| Wet pouch with sterile low-nitrogen nutrient solution until the entire surface of the filter paper has absorbed liquid (~ 7mL). Micro-nutrients such as boron are required for nodules to develop [22]. It is important to supply these nutrients instead of water alone as the seedling will not have access to them in a soil-free environment.

5| Gently remove the seedlings from the pots, carefully remove the seed-coat with forceps, and place the primary root through the hole previously made (Figure 2.1, B). The root must be in contact with the moist filter paper of the growth pouch.

6| Tape the top of the pouch closed, leaving a hole for the shoot to emerge (Figure 2.1, B). Taping the pouch helps to maintain a moist inner environment preventing the roots from drying out. It also prevents vermiculite from entering the pouch (see below).

7| Cut a piece of the growth pouch 2.5cm from its bottom with a pair of scissors (Figure 2.1, B). The filter paper within the pouch will thus be in contact with the moist vermiculite (see below); this will ensure a constant supply of water to the developing roots while at the same time prevent any water-logging. The sides of the pouch can also be trimmed for a better fitting when the pouches are inserted into the pots.

8| Place the growth pouches with the seedlings in 15 cm diameter pots (Figure 2.1, C) and fill those with sterile vermiculite to cover completely the pouches (Figure 2.1, D). Covering the pouch with vermiculite prevents light from coming in contact with the roots; this is important as exposure to light inhibits pea nodulation [23].

9| Dampen the vermiculite with water and place the pots in trays in a controlled growth room. Water the plants by adding water to the tray. The vermiculite maintains a humid environment for the pouch and filter paper.

10| Two days before inoculation, grow a bacterial culture in YMB, pH 7.0, at 25°C. Do not water the plants during this time to reduce the amount of residual water in the pouch. If the pouches are too wet, the inoculum drop will not remain on the root. It is of prime importance to time the earlier watering so that at this stage the pouches are only damp.

11| After 5 days of growth in the pouches, lateral roots will be of an optimal length for spot-inoculation (Figure 2.1, E). Remove the pouches from the pots and find under the dissecting microscope the zone that is the most susceptible to infection, i.e., the region where roots hairs are starting to emerge from the root. This location is usually 0.5-1cm away from the root tip.
NOTE: Condensation on the inside of the plastic pouch can impede the viewing of roots. Gently lift the top layer of the pouch from the bottom and use a sterile filter paper to remove the water droplets.

12| Mark the zone of the most susceptibility on the outside of the pouch with a water-proof marker (Figure 2.1, E). Do not damage the root when applying the marker; if needed, hold the top surface of the pouch away from the root and apply the mark to the desired location.

13| Lift the top plastic sheet at the bottom end and apply with a micro-pipette a 0.5 µL drop of 5% rhizobial solution (viable cell density of 6.4 x 10^4 CFUs/ mL).

14| Return the pouches to the pots and cover with vermiculite (Figure 2.1, F). Water the plants when needed; a good indication to do so is given when the colour of the pouch changes as it starts to dry. Harvest at the desired time (Figure 2.1, G).

15| In our experiments carried out under the described conditions, we observed nodulation events as early as 24 hours after spot-inoculation; pink nodules are seen at 10 days after inoculation.

Comments

We found many uses for this technique. 1. The clear plastic of the pouch allows the developing root system with its nodules to be followed over time by macro-photography (Figure 2.2), so that the dynamic growth of lateral roots with their nodules can be followed. 2. Roots can be cut on either side of the inoculated spot for assessment of gene expression, with mock-inoculated roots used as a control, so that expression can be correlated to specific symbiotic events. 3. In the case where rhizobia transformed with a lacZ gene are used to perform spot-inoculation, root segments may be fixed and cleared to follow rhizobial progression. 4. Nodules developing at the inoculated spot can be studied structurally and histochemically. The root can be cut 0.5 cm on either side of the spot at any time after inoculation and sectioned (fresh or fixed) to study specific nodule ages (Figure 2.3).

We see one great advantage of our method over those performed earlier. In contrast to prior techniques which have relied on the primary root of pea for spot-inoculation, our method utilizes its lateral roots which are where this species develops the majority of its nodules. It was estimated that a nodule formed within ~0.5 cm from the intended location in 95-100% of the treatments. Some roots failed to develop properly because they did not grow in contact with the paper of the pouch; these were not used (Figure 2.2 D).

If we had to mention one inconvenience with our technique, it would be that it does not limit nodule production to one specific location as nodules occasionally developed on the root system where rhizobia were not applied. However, since we were interested in knowing the precise age of a developing/nodule, we did not take into account

39

Figure 2.2 - Macro-photography of developing nodules

A. An overview of an 8 day-old spot-inoculated plant. B. A close-up of the pouch focussed on the plant roots 5 days after inoculation. The unfocussed black dots are located on the surface of the pouch and correspond to the different inoculation sites. In C to F, two nodules (arrowheads) can be seen developing over time. The nodules are five-days old (C), seven-days old (D), 10 days-old (E) and 14-days old (F). In D, two roots (arrows) which did not grow in contact with the filter paper of the pouch dried out. In C to F, one of the nodules appears much larger than the others; in F, it is evident that this large nodule has multiple meristems (*) when compared to the others.
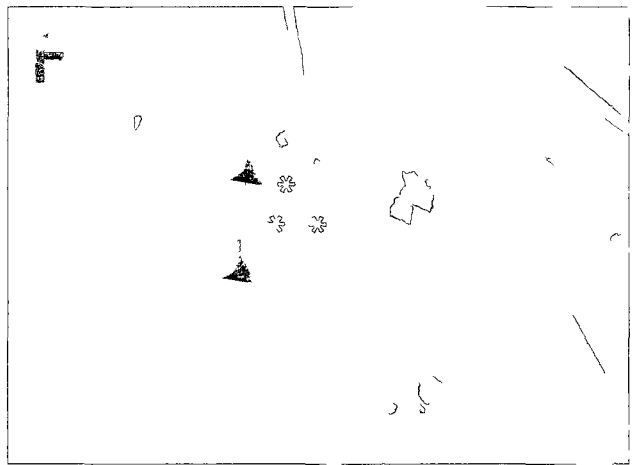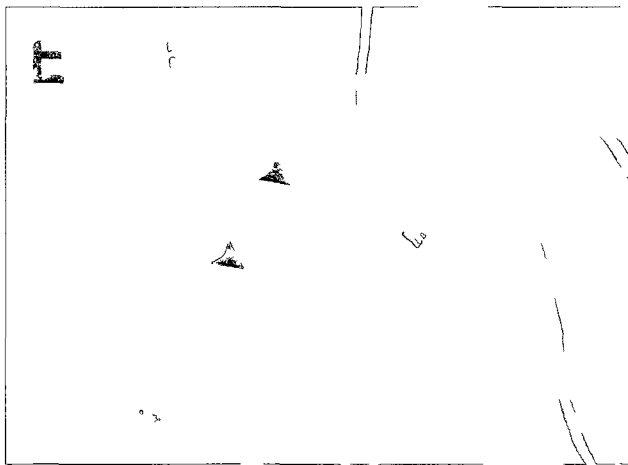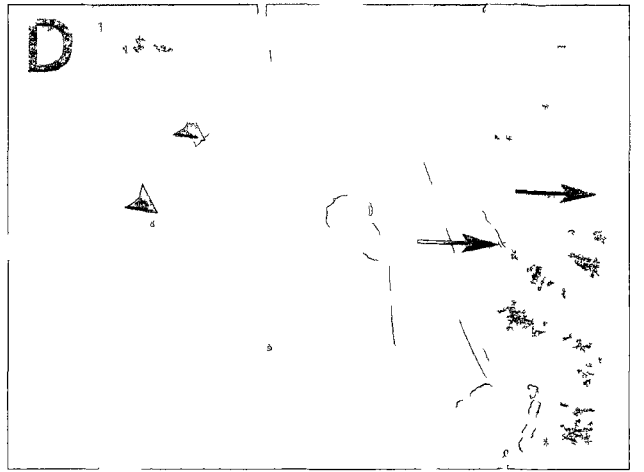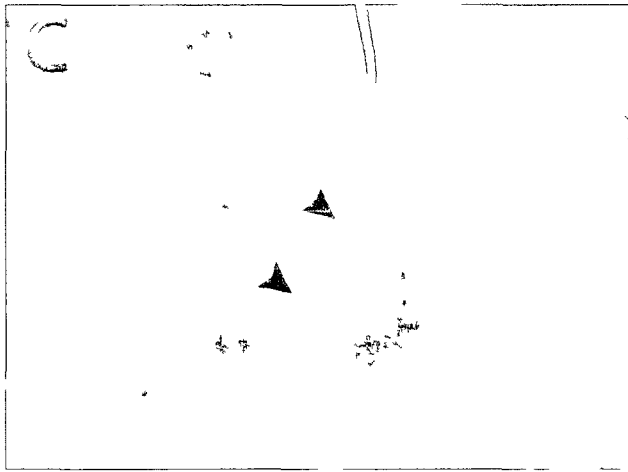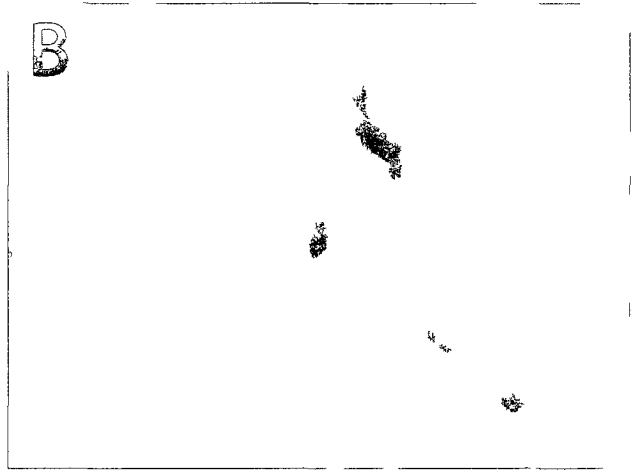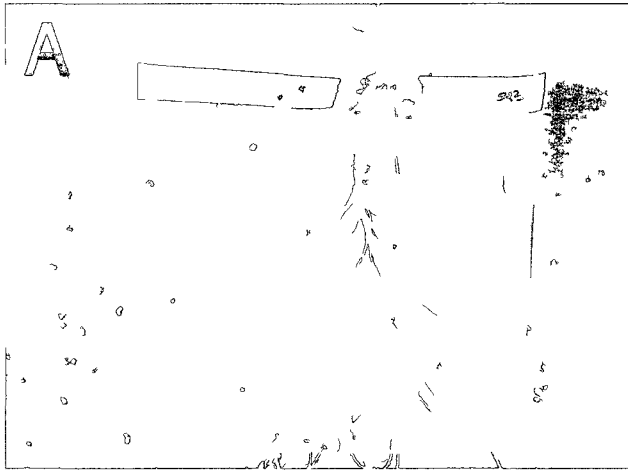
Figure 2.3 – Longitudinal sections of spot-inoculated lateral roots.

A. An unstained longitudinal section of a spot-inoculated lateral root 24 hours after inoculation showing anticlinal divisions in the inner cortex (arrows), and in the pericycle (asterisks), located adjacent to a xylem pole (X). B. A close-up on the area indicated in Figure A. Metabolically active cells, one with a large nucleus (arrowhead), exhibiting anticlinal divisions. C. A longitudinal section of a spot-inoculated root three days after inoculation and stained with toluidine blue to reveal the nodule meristem (NM), which has passed the mid-point of the root cortical region. Note that for all the photographs, there was no indication of nodule emergence and it was only because of the spot-inoculation of the root that these events were easily captured. All sections were made with a vibratome. Scale bar in A and C = 100 μm. Scale bar for B = 10 μm.

A

B

NM

C
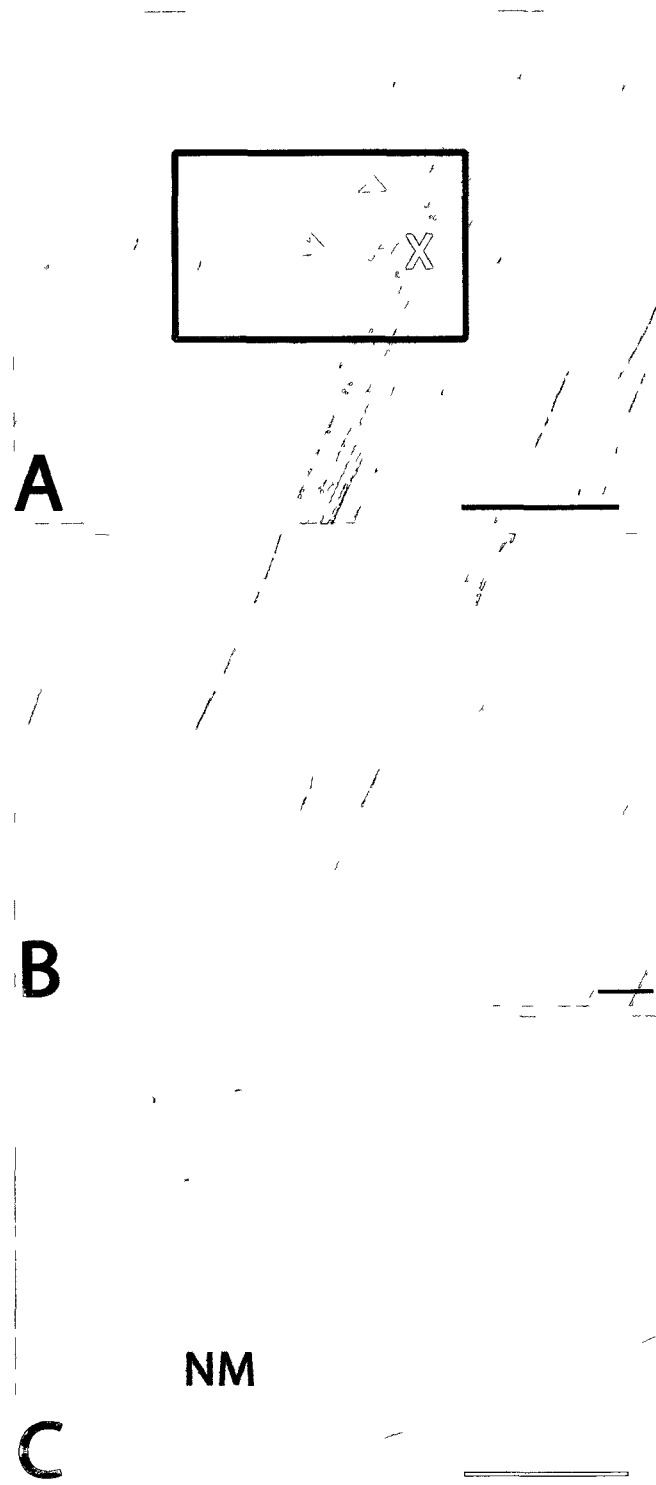
these "straggling" nodules. Also, occasionally spot-inoculated roots develop more than

one nodule in the inoculated area.

Competing interests

The author(s) declare that they have no competing interests.

Authors' contributions

SRC conceived, designed and carried out all experiments in the presented paper. SRC drafted the manuscript.

Acknowledgements

References

1. Ellis, THN, and Poyser, SJ: An integrated and comparative view of pea genetic and cytogenetic maps. *New Phytologist* 2002, **153**: 17-25.

2. Ratnayake, WS, Hoover, R, Warkentin, T: Pea starch: composition, structure and properties – A review. *Starch* 2002, **54**: 217-234.

3. Szczyglowski, K, and Stougaard, J: *Lotus* genome: pod of gold for legume research. *Trends in Plant Science* 2008, **13**: 515-517.

4. Young, ND, and Udvardi, M: Translating *Medicago truncatula* genomics to crop legumes. *Current Opinion in Plant Biology* 2009, **12**: 193-201.

5. Timmers, ACJ, Auriac, M-C, Truchet, G: Refined analysis of early symbiotic steps of the *Rhizobium-Medicago* interaction in relationship with microtubular cytoskeleton rearrangements. *Development* 1999, **126**: 3617-3628.

6. van Brussel, AAN, Bakhuizen, R, Van Spronsen PC, Spaink, HP, Tak, T, Lugtenberg, BJJ, Kijne, JW: Induction of pre-infection thread structures in the leguminous host plant by mitogenic lipo-oligosaccharides of *Rhizobium*. *Science* 1992, **257**: 70-72.

7. Guinel, FC: Getting around the legume nodule: I. The structure of the peripheral zone in four nodule types. *Botany* 2009, **87**: 1117-1138.

8. Niwa, S, Kawaguchi, M, Imaizumi-Anraku, H, Chechetka, SA, Ishizaka, M, Ikuta, A, Kouchi, H: Responses of a model legume *Lotus japonicus* to lipochitin oligosaccharide nodulation factors purified from *Mesorhizobium* loti JRL501. *Molecular Plant-Microbe Interactions* 2001, **14**: 848-856.

9. Mathis, R, Grosjean, C, de Billy, F, Huguet, T, Gamas, P: The early nodulin gene *MtN6* is a novel marker for events preceding infection of *Medicago truncatula* roots by *Sinorhizobium meliloti*. *Molecular Plant-Microbe Interactions* 1999, **12**: 544-555.

10. van Noorden, GE, Kerim, T, Goffard, N, Wiblin, R, Pellerone, FI, Rolfe, BG, Mathesius, U: Overlap of proteome changes in *Medicago truncatula* in response to auxin and *Sinorhizobium meliloti*. *Plant Physiology* 2007, **144**: 1115-1131.

11. Coba de la Peña, T, Cárcamo, CB, Almonacid, L, Zaballos, A, Lucas, MM, Balomenos, D, Pueyo, JJ: A salt stress-responsive cytokinin receptor homologue isolated from *Medicago sativa* nodules. *Planta* 2008, **227**: 769-779.

12. Turgeon, BG, Bauer, WD: Spot inoculation of soybean roots with *Rhizobium japonicum*. *Protoplasma* 1983, **115**: 122-128.

13. Fåhraeus, G: The infection of clover root hairs by nodule bacteria studied by a simple glass slide technique. *Journal of General Microbiology* 1957, **16**: 374-381.

14. Geurts, R, Heidstra, R, Hadri, A-E, Downie, JA, Franssen, H, van Kammen, A, Bisseling, T: Sym2 of pea is involved in a nodulation factor-perception mechanism that controls the infection process in the epidermis. *Plant Physiology* 1997, **115**: 351-359.

15. Albrecht, C, Geurts, R, Lapeyrie, F, Bisseling, T: Endomycorrhizae and rhizobial Nod factors both require SYM8 to induce the expression of the early nodulin genes *PsENOD5* and *PsENOD12A*. *The Plant Journal* 1998, **15**: 605-614.

16. Fred, EB, Haas, ARC: The etching of marble by roots in the presence and absence of bacteria. *The Journal of General Physiology* 1919, **1**:631-638.

17. Díaz, CL, van Spronsen, PC, Bakhuizen, R, Logman, GJJ, Lugtenberg, EJJ, Kijne, JW: Correlation between infection by *Rhizobium leguminosarum* and lectin on the surface of *Pisum sativum* L. roots. *Planta* 1986, **168**: 350-359.

18. Guinel, FC, LaRue, TA: Light microscopy study of nodule initiation in *Pisum sativum* L. cv Sparkle and in its low-nodulating mutant E2 (*sym 5*). *Plant Physiology* 1991, **91**: 1206-1211.

19. Pepper, AN, Morse, AP, Guinel, FC: Abnormal root and nodule vasculature in R50 *(sym16)*, a pea nodulation mutant which accumulates cytokinins. *Annals of Botany* 2007, **99**: 765-776.

20. Bhuvaneswari, TV, Turgeon, BG, Bauer, WD: Early events in the infection of soybean (*Glycine max* L. Merr) by *Rhizobium japonicum*. I. Localization of infectible root cells. *Plant Physiology* 1980, **66**: 1027-1031.

21. Vergnaud, L, Chaboud, A, Prin, Y, Rougier, M: Preinfection events in the establishment of *Alnus-Frankia* symbiosis: Development of a spot inoculation technique. *Plant and Soil* 1985, **87**: 67-78.

22. Brenchley, WE, Thornton, HG: The relation between the development, structure and functioning of the nodules on *Vicia faba*, as influenced by the presence or absence of boron in the nutrient medium. *Proceedings of the Royal Society of London B* 1925, **98**: 373-399.

23. Lee, KH, LaRue, TA: Ethylene as a possible mediator of light- and nitrate-induced inhibition of nodulation of *Pisum sativum* L. cv Sparkle. *Plant Physiology* 1992, **100**: 1334-1338.

CHAPTER 3

A comparison between R50 and Sparkle: early nodule events, *PsCKX1* transcript profile, and the localization of its product in mature nodules

Introduction

Cytokinin is a phytohormone that promotes cell division and differentiation. It regulates many aspects of plant growth and development including symbiotic interactions such as that occurring between legumes and rhizobia. A role for cytokinin in nodule organogenesis was first suggested by Syôno and Torrey (1976) who studied pea nodules. Cytokinin content in the nodule meristem increased as the nodule developed; cytokinin reached peak concentrations two weeks after inoculation and decreased thereafter (Syôno *et al.* 1976). From these observations, it was hypothesized by Syôno and others that cytokinin was essential for the proper establishment of a nodule. The importance of cytokinin signaling during nodule development was recently demonstrated by analyzing the gain-of-function mutant LHK1 in *Lotus*. LHK1, an ortholog to AHK4, is a cytokinin receptor and its mutation results in spontaneous nodule formation (Tirichine *et al.* 2007). Futhermore, a loss-of-function in LHK1 prevents the formation of nodule primordia (Murray *et al.* 2007).

The active cytokinin pool of a plant cell is controlled by its rate of import, biosynthesis, inactivation and degradation. Cytokinin is irreversibly degraded by cytokinin oxidases (CKX) (reviewed by Mok and Mok, 2001; Schmülling *et al.* 2003) which in higher plants are encoded by a family of *CKX* genes. The inactivation of cytokinin occurs in a single step with CKX cleaving the isoprenoid side chain resulting in the production of adenine/adenosine and the corresponding side chain aldehyde (Brownlee *et al.* 1975; McGaw and Horgan, 1983). Seven CKX-encoding genes have been discovered in *Arabidopsis* (Galuszka *et al.* 2004) and many CKX members have been identified in maize, *Oryza sativa* (rice), *Triticum aestivum* (wheat), *Hordeum*

vulgare (barley), *Dendrobium sonia* (reviewed by Werner *et al.* 2006) and 2 CKX members have been identified in pea (Held *et al.* 2008).

The transformation of *Arabidopsis* to create gain-of-function mutations by overexpressing CKX to decrease the cytokinin content of the plant has been utilized to unravel the physiological effects of cytokinin. Such a decrease in cytokinin content results in the reduced activity of the shoot apical meristem, and a reduction in leaf vascular development. Furthermore, delayed flowering and an increase in root growth were noted (Werner *et al.* 2003; Yang *et al.* 2003). The over-expression of *AtCKX3* and *ZmCKX1* in Lotus led to increased production of lateral roots but fewer nodules developed on those roots (Lohar *et al.* 2004).

Exogenous cytokinin promotes nodule formation in pea up until 1μM but inhibits it at higher concentrations (Lorteau *et al.* 2001). The nodulation phenotype of the treated wild-type at these higher concentrations was similar to that of the pea mutant R50. R50 is characterized, among other traits, by delayed nodule formation and elevated levels of endogenous cytokinins in its shoots, roots and nodules (Kneen *et al.* 1994; Guinel and Sloetjes, 2000; Ferguson *et al.* 2005). When compared to that of the wild-type, the total CKX enzymatic activity of R50 was low, but in all organs measured, except the flowers, the transcript levels of PsCKX1 were significantly higher, especially in the nodules.

The goal of this study was to identify why the mutant R50 has elevated transcripts of *PsCKX1* but a lower CKX total enzymatic activity compared to its wild-type Sparkle. A *PsCKX1* transcript profile was obtained for developing nodules of Sparkle and R50. I also examined the level of *PsCKX1* protein on a western blot and determined its localization within sections of nodules.

Methods

Plant Materials and Inoculation

Seeds of pea (*Pisum sativum* L. cv. Sparkle) and R50 were surface-sterilized in 8% bleach for 5 minutes, washed three times in sterile water, and imbibed in the dark. The seeds were planted in sterile vermiculite and placed in a controlled growth-room and grown under incandescent (OGE 600 hour, 60 – 120 W, 120 Volts, General Electric) and cool white fluorescent lights (Watt-Miser GE, F96TIZ-CW-HO-WM) in a growth-room with a 22h/18h, 16°C/8°C hour, light/dark regime. The total light intensity received by the plants was 280 $\mu mol \cdot m-2 \cdot s-1$. After three days, the plants were moved to germination pouches (Mega International, Minnesota) and spot-inoculated five days later when lateral roots were of optimal size with a 0.5 μL drop of 5% *Rhizobium leguminosarum* biovar *viciae* 128C53K following the protocol given in Chapter 2.

CKX1 Profile

Lateral roots (1, 7, 14 and 21 DAI) from Sparkle and R50 were cut into 1-2 cm segments comprising the spot-inoculated areas. These segments were harvested from 10 lateral roots per plant and at least 3 different plants were used. All segments were pooled to obtain 100 mg of tissue for total RNA isolation using the Qiagen RNeasy plant mini kit (Qiagen); younger plants required more plants to obtain 100 mg of tissue. An on-column treatment with DNase 1 (Qiagen) was used to remove any contaminating DNA. RNA concentration was estimated by measuring the absorbance at 260 nm (A260) using a spectrophotometer (Varian, Inc., Mississauga, ON). The ratio of A260 to A280 was

calculated to estimate RNA purity. Two μg of RNA was used for first-strand cDNA synthesis using the Omniscript RT kit (Qiagen). The primers for CKX1 were designed by Chengli Long (Master Thesis, Wilfrid Laurier University, 2010). PCR reactions were prepared using hot-start master mix (Qiagen) and 2 μL of template cDNA. The linear range of amplification for *PsCKX1* and *PsActin* was determined (by removing tubes from the PCR machine in 4-cycle intervals starting at cycle 16 and ending at cycle 48) to be 26 cycles at 94°C for 30s (denaturation), 56°C for 1 min (annealing) and 72°C for 1 min (extension) followed by a final 6-min extension at 72°C. The PCR products were run on an agarose (Bioshop) gel for 1 hour at 110V and analyzed by Quantity One software (Biorad) to determine the relative abundances of *PsCKX1* to the control actin.

Purification of Recombinant PsCKX1

The plasmid with *PsCKX1* insert prepared by Bozdarov (2008) was isolated and purified using the Qiagen Plasmid Midi Kit (Qiagen), following the guideline of the manufacturer. Recombinant PsCKX1 was produced in *Escherichia coli* BL21 using the pET expression system. The expression vector pET-21a(+) (Novagen) containing sub-cloned *PsCKX1* was transformed into *E.coli* BL21 via electroporation. A 250 mL Luria Burtani (Bioshop, Burlington, Ontario) culture of *PsCKX1* pET-21a(+) with ampicillin (100 μg/mL) was grown at 37°C on an orbital shaker (220 rpm) until the absorbance at 600 nm was between 0.4 and 0.6 on a spectrophotometer. Recombinant PsCKX1 was induced by adding 500 μL of 200 μM IPTG (isopropyl β-D-1-thiogalactopyranoside) and the protein expressed for 4 hours at 37°C at 100 rpm. After 10 min on ice the culture was centrifuged at 6000 x g for 10 min to pellet the bacteria and the supernatant was

discarded. The pellet was resuspended in 25mL binding buffer (50 mM Tris-HCl, pH 8.0, 50 mM potassium acetate, 2 mM $CaCl_2$, 1 mM $MgSO_4$ and 20 mM imidazole) and incubated in 200 µg/mL of lysozyme (Bioshop) for 20 min at room temperature. PsCKX1 was isolated in the insoluble protein portion of the cell lysate and was suspended in a 6M urea extraction buffer and run through a nickel resin column. The purified recombinant PsCKX1 protein was used to generate polyclonal antibodies from rabbit (Sacri antibody services, Calgary).

Light Microscopy

Fresh spot-inoculated lateral root segments, 1, 2, 3, 5, 7, 14 and 21 DAI, were dried on a filter paper to remove excess moisture and embedded in 5% agar. I noticed that dry tissue enables a better seal in agar. Sections were obtained on a vibratome (Leica VT1000P, Bannockburn, IL) and viewed under bright-field optics (Axiostar, Zeiss) (Karas *et al.* 2005). A few sections were stained with 0.05% (w/v) toluidine blue O (TBO; Fisher Scientific Company, Fair Lawn, NJ) in benzoate buffer (pH 4.4) (Pepper *et al.* 2007). Potassium iodine (1% iodine, 2% potassium iodine, 97% water) (Ward's natural science, St.Catharines, ON) was added to some sections to visualize starch. Pictures were captured on a Canon Powershot A600 and processed with Axiovision 4.7 (Zeiss).

Immunolocalization of PsCKX1

Spot-inoculated root segments (14 and 21 DAI) were fixed in 4% para-formaldehyde in PEM buffer (50 mM PIPES, 5 mM EGTA, 5 mM MgSO4), placed under vacuum for 1 hour, and rinsed three times in fresh PEM buffer (Vincent and Brewin, 2000). Fixed root

segments were sectioned (~30 μm thick) using a vibratome. The sections were mounted on γ-aminopropyltriethoxysilane-coated (APTES, Sigma-Aldrich) slides for better adherence (Vincent and Brewin, 2000) and a hydrophobic ring was drawn around a group of sections using a PAP pen to restrict the diluted antibodies (Rockland KHP001). They were treated with 0.05% (w/v) cellulase (Onzuka, Yakult Honsha, Tokyo) in PEM buffer for 10 min and then blocked for 1 hour in PEM buffer with 3% (w/v) bovine serum albumin (Rockland BSA-50) (Vincent and Brewin, 2000). Primary antibodies were diluted 1:1000 in PEM buffer with 2% BSA and the sections incubated overnight at 4°C in humid glass chambers. Sections were washed with three 15 min rinses of PEM buffer with 1% (w/v) BSA and then incubated with the secondary antibody AlexaFluor 635 (Invitrogen A31574) or AlexaFluor 488 (A11070) raised in goat against rabbit immunoglobulins. This antibody was diluted 1:1000 in PEM buffer with 1% (w/v) BSA and the sections were incubated for 2 hours at room temperature. Sections were again washed with three 15 min rinses of PEM buffer with 1% (w/v) BSA. Sections were incubated for 15 min with SYTO 13 (Invitrogen S7575) in PEM (1 μL/mL) buffer to stain the nucleic acids of the bacteroids and plant nuclei (Haynes, et al. 2004). In a fume hood, slides were dipped into xylene to remove the hydrophobic rings and cover-slips were mounted on the slides using ProLong® Gold antifade reagent mounting medium (Invitrogen P36930). The slides were allowed to cure for 24 hours before being viewed on a laser-scanning confocal microscope (Olympus Fluoview FV1000). Fluorescent excitation and emission wavelengths of 495 nm and 519 nm were used for AlexaFluor 488 and SYTO 13. AlexaFluor 635 required wavelengths of 633 nm for excitation and

647 nm for emission. Images were captured in single slice using objective lenses: 10x, 20x, 60x (oil immersion), and 100x (oil immersion).

Western Blot

Total protein was extracted from spot-inoculated roots (100 mg) of the two pea lines 21 DAI in 3mL of extraction buffer (6 M urea, 50 mM tris-HCl pH 8.0, 50 mM potassium acetate, 5 mM $MgSO_4$, 2 mM $CaCl_2$, 0.5 M DTT and 10 percent protease inhibitor cocktail (Bioshop)) (Held *et al.* 2008). The protein extract was centrifuged for 5 min at 12 000 rpm to remove cell debris. The concentration of the protein was measured using a Bicinchoninic protein assay (BCA kit, Pierce) and 80 μg of the total protein was run on 10% SDS gel. The protein was transferred onto a polyvinylidene fluoride (PVDF) membrane (Biorad) at 15V for 40 min. The membrane was blocked in 5% skim milk for 2 hours and polyclonal anti-PsCKX1 antibodies were diluted 1:1000 in 5% skim milk at 4°C overnight. The blot was washed in three 15 min rinses of Tris-buffered saline Tween-20 (TBS-T) and incubated with horseradish peroxidase (HRP) secondary antibody (Rockland) diluted 1:10,000 for 2 hours. The blot was visualized with an ECL kit (GE Healthcare) and the blot was exposed to film (GE Healthcare) for 10, 20 and 30 seconds in a dark room for imaging.

Results

Light Microscopy – Early Nodule Development

The reader is referred to Table 3.1 for a summary of the observations made from sectioning spot-inoculated roots.

The root hairs of Sparkle were deformed 24 hours after spot-inoculation (HAI) (Figure 3.1 A and B) and infection threads or bacterial colonies in root hairs were evident 48 HAI (Figure 3.1 C and D, respectively). Periclinal cell divisions were visible in the pericycle cells in front of the protoxylem poles 24 HAI (Figure 3.2 A and C). Anticlinal cell divisions were later observed in the pericycle cells 48 HAI (Figures 3.2 B, D and E); at that time, anticlinal cell divisions extended into the inner cortical cells followed by periclinal divisions (Figure 3.2 B, E and F). Although infection threads were occasionally evident in the roots hairs two DAI, only occasionally were they observed extending into the cortical cells, i.e., crossing the epidermal interface (Figure 3.1 C). However, no pre-infection threads were observed in any of the sections examined although as reported by van Brussel *et al.* (1992), they should have existed. As expected, the infections were most of the time facing the xylem poles, but in some cases, they were seen facing a phloem pole (Figure 3.3). Three DAI, infection threads extending from the root surface into the middle cortex (Figure 3.3 B) were seen progressing towards the nodule primordium (Figure 3.3 A). Small bumps on the root surface were observed five DAI as the nodule emerged through the root epidermis (refer to Figure 2.2 C). At this stage, the specialization of cell types could already be observed. An infection thread was caught

Table 3.1 – Summary of nodule development in Sparkle and R50 based on the two

developmental programs (A: epidermal program and B: cortical program) described by

Guinel and Geil (2002).

A: Epidermal program				
Time	**Sparkle**		**R50**	
	Observations	**Figure**	**Observations**	**Figure**
24 HAI	Root hairs deformed	3.1 A and B	Root hairs long and straight	3.4 A
48 HAI	Root hairs curled; infection threads in root hairs and occasionally outer cortical cells.	3.1 C and D	Root hairs have wavy appearance	3.4 B and C
3 DAI	Infection threads caught extending into the middle cortex and entering dividing cells of the developing nodule.	3.3 B	No sign of infection	N/A
5 DAI	Infection threads enter an emerging nodule	3.3 C and D	Coiled infection threads observed in the outer cortical cells	3.4 D and E
14 DAI	N/A	N/A	Coiled infection threads seen reaching the inner cortical cells	3.5 E and F

B: Cortical program				
Time	**Sparkle**		**R50**	
	Observations	**Figure**	**Observations**	**Figure**
24 HAI	Periclinal divisions in pericycle cells	3.2 A and C	No cell divisions in pericycle	3.5 A
48 HAI	Anticlinal division observed in pericycle cells; anticlinal and periclinal divisions observed in inner cortical cells.	3.2 B and D	No cell divisions in pericycle	N/A
3 DAI	Anticlinal divisions followed by periclinal divisions in the cortical cells.	3.3 A	No cell division in pericycle or inner cortical cells	3.5 B
5 DAI	An emerging nodule with some cell specialization (i.e. Infected cells and nodule vasculature)	3.3 C, D and E	No cell divisions caught but it most likely occurs	3.4 D and E
7 DAI	Nodule with Zone I, II, II-III and Zone III established	3.6 A	N/A	N/A
10 DAI	N/A	N/A	A developing nodule within the root. Coiled infection thread evident and a few cells in the middle which could be infected.	3.5 C and D
14 DAI	A mature nodule	3.6 B	A nodule with a few infected cells and abnormal vasculature	N/A

Figure 3.1 - Inoculated roots of Sparkle 24 HAI (A and B) and 48 HAI (C and D).

A: An unstained whole-mount displaying deformed and branched root hairs. B: A close-up of one of the branched root hairs. C: An unstained cross-section exhibiting an infection thread (arrow) in a root hair and outermost cortical cell layer facing a phloem pole. No cell division of the inner cortical cells was observed. D: A trapped rhizobial micro-colony (arrow) within a curled root hair. Thickness of sections was ~ 30 μm. Scale bar for A and C = 100 μm. Scale bar for B and D = 20 μm.
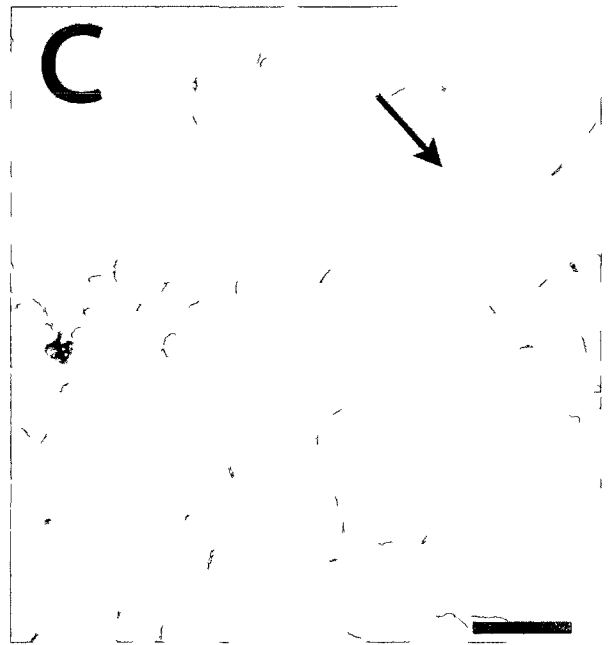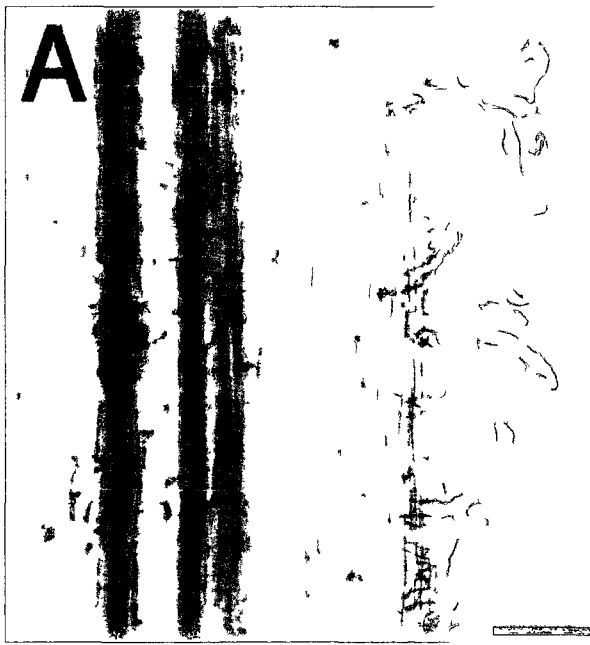
Figure 3.2 - Inoculated roots of Sparkle 24 HAI (A and C) and 48 HAI (B, D, E and F).

A: An unstained cross-section showing the periclinal divisions in the first layer of pericycle (P) cells facing a xylem pole (X). B: An unstained cross-section exhibiting the dividing pericycle (P) cells in front of a xylem pole. The inner cortical cell layer (C), endodermis (E), and pericycle layers are identified in front of a different xylem pole. C: A close-up of A showing the periclinal divisions (arrows) in the pericycle cells. D: A magnified image of the developing nodule in B. Periclinal (arrow) and anticlinal (arrowheads) divisions are observed in the pericycle cells. Also there are anticlinal divisions (*) in the cells adjacent to the xylem pole. E: Anticlinal divisions (arrowhead) are observed in the first layer of pericycle cells and periclinal divisions are seen extending into the second layer of pericycle cells. Cells adjacent to the xylem pole are observed dividing anticlinally (*). F: Anticlinal (arrowhead) and periclinal (arrow) cell divisions are observed in front of a xylem pole. Scale bar = 20 μM.
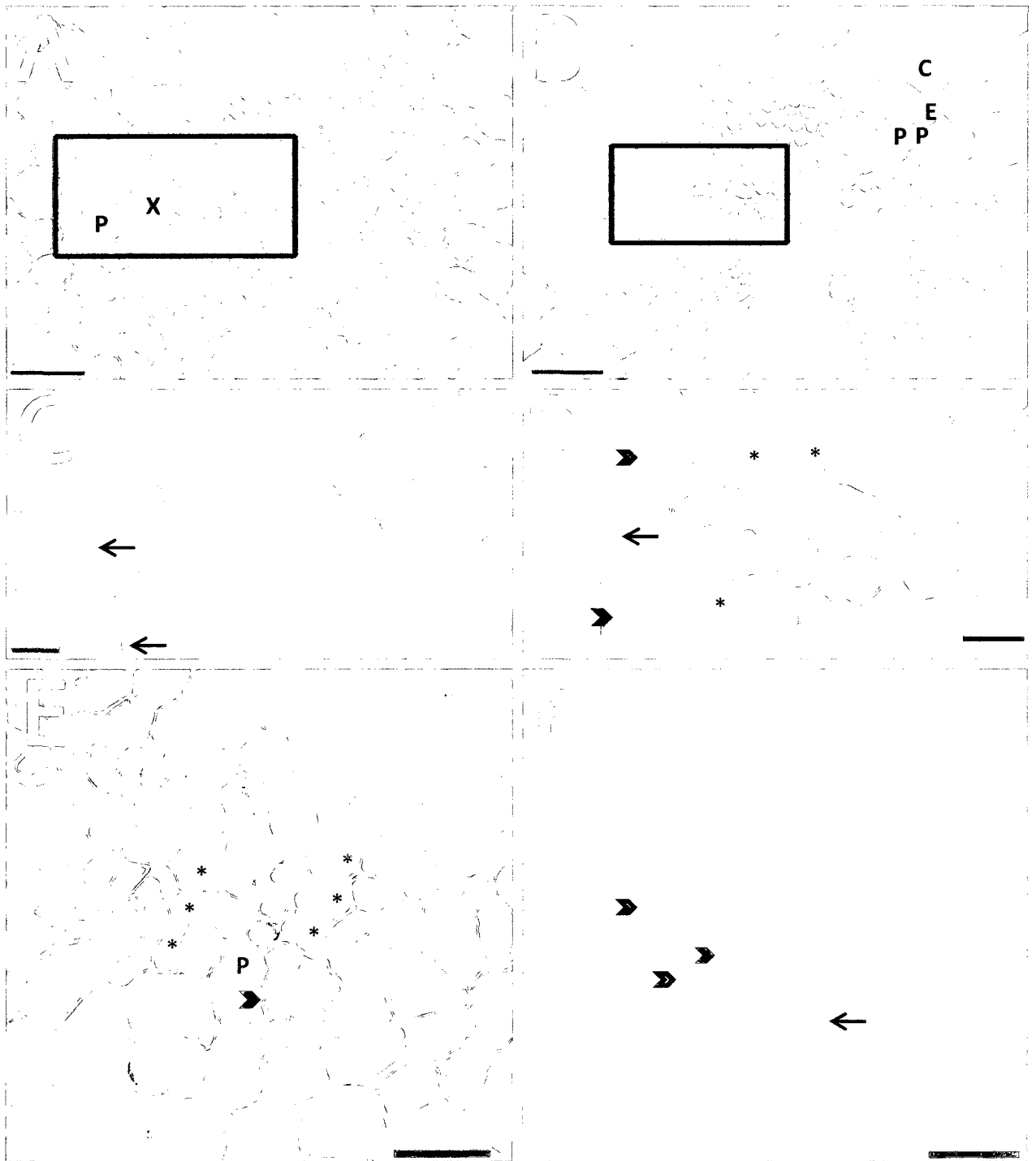
Figure 3.3 - Inoculated roots of sparkle 3 DAI (A and B) and 5 DAI (C, D and E).

A: An unstained cross-section of cells dividing anticlinally (arrow) and periclinally (arrowhead) in front of a phloem pole. This sequence of division generates square-shaped cells in the cortex (C). B: At a different plane of the same section, infection threads (arrows) could be observed. C: Emerged nodule formed opposite a phloem pole (Pl), note the off-center establishment of the infection thread in the nodule. The meristem (M), infected cells (I), and the nodule vasculature (V) begin to become established in the developing nodule. D: A close-up of the infection thread in C (box) which can be seen crossing the epidermal layer and the nodule peripheral tissue. E: A magnified view of the root vasculature (X for xylem) seen in C (box) that is embracing the nodule. A Scale bar for A, B, D and E = 20 μm. Scale bar for C = 100 μm.

A

B

D →

M

C

D

I

P

E
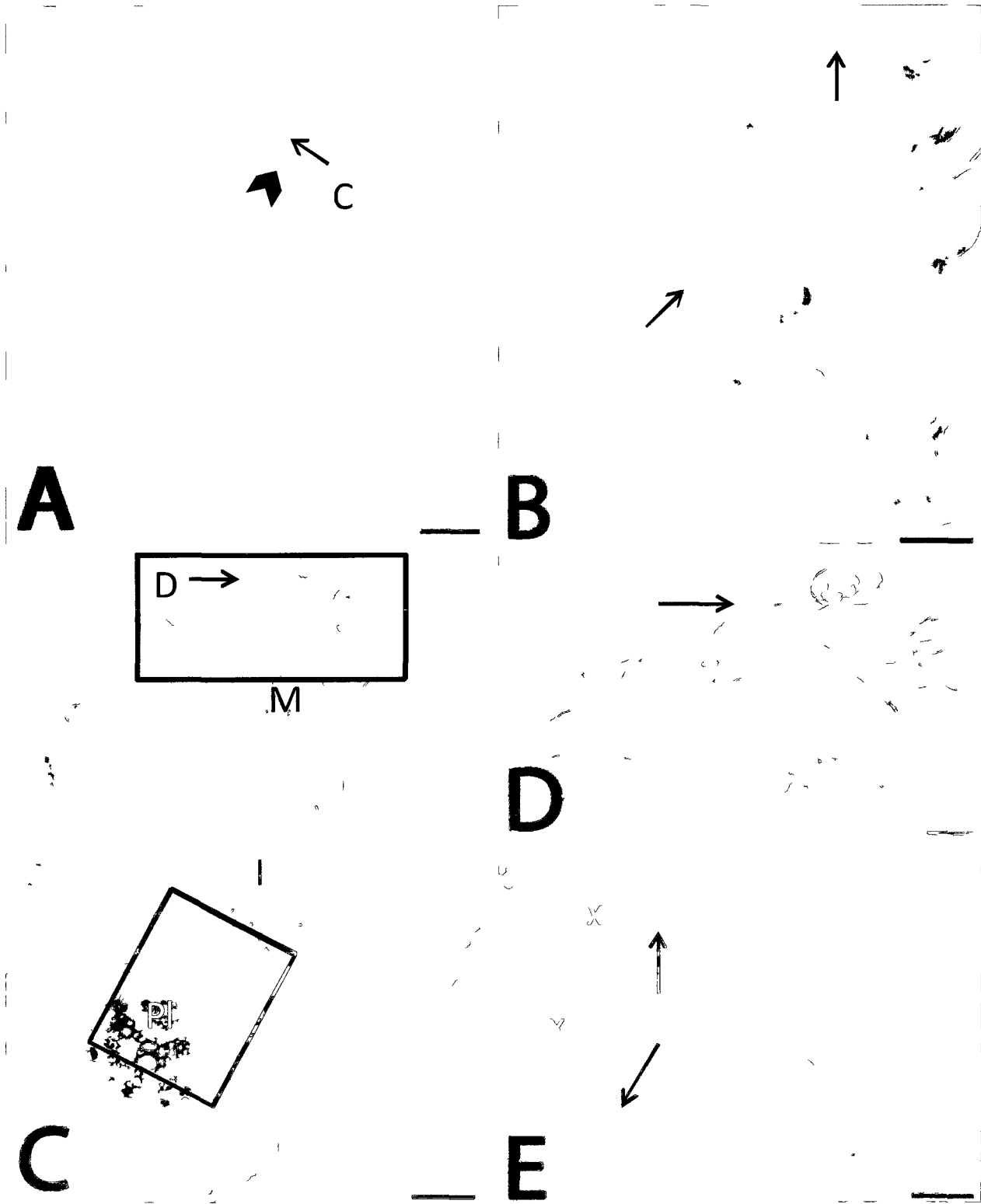
opposite of a phloem pole and seen extending into the developing nodule (Figure 3.3 C and D) where the process of rhizobia exocytosis was well under way as indicated by the presence of a small pocket of infected cells within the middle of the nodule (I in Figure 3.3 C). Note the infection thread in Figure 3 C is entering the nodule on an off-centered axis as described by Vorishilova *et al.* (2009). The nodule vasculature was already in place in the periphery of the nodule (Figure 3.3 C and E). Since the developing nodule is in front of a phloem pole, the nodule vasculature will develops from the two xylem poles embracing the phloem pole (Guinel, 2009).

The spot-inoculation of lateral roots and the subsequent sectioning and microscopy of R50 revealed that many of the events that led to the formation of nodules in the mutant were delayed compared to Sparkle (Table 3.1). It was difficult to pinpoint the exact timing of events for the development of R50 nodules as the mutant is known to be a low nodulator (Guinel and Sloetjes, 2000). In R50, root hairs 24 or 48 HAI did not resemble those observed in Sparkle (i.e., root hairs did not deform and did not curl) (Figure 3.4 A), but many, however, had a wavy appearance (Figure 3.4 B and C). Infection threads were first evident in the cortical cells 5 DAI (Figure 3.4 D and E). These infection threads were abnormal as they were coiled and branched many times as already described by Guinel and Sloetjes (2000). No divisions were observed in cells of the pericycle at 1 and 3 DAI (Figure 3.5 A and B). A developing nodule about to emerge through the root epidermis was caught 10 DAI (Figure 3.5 C and D). At 14 DAI, some spot-inoculated roots exhibited an extensive network of infection threads reaching the middle cortical cells but these threads were not associated with cell divisions (Figure 3.5 E and F) suggesting that the epidermal and cortical programs had been uncoupled (Guinel

Figure 3.4 – Inoculated root of R50 24 HAI (A), 48 HAI (B and C) and 5 DAI (D and E).

A: An unstained whole-mount showing that root hairs were not deformed 24 HAI as observed in Sparkle (Figure 3.1 A). B and C: An unstained whole-mount showing that root hairs of R50 exhibited an abnormal wavy-like appearance (arrows). D: An unstained longitudinal root section illustrating the coiled infection threads (arrows) in R50 in the outer cortical cell layers. E: An unstained longitudinal root section showing a branched infection thread (arrow) in the outer cortical cell layers. Scale bar for A, B and C = 100 μm. Scale bar for D and E = 20 μm.
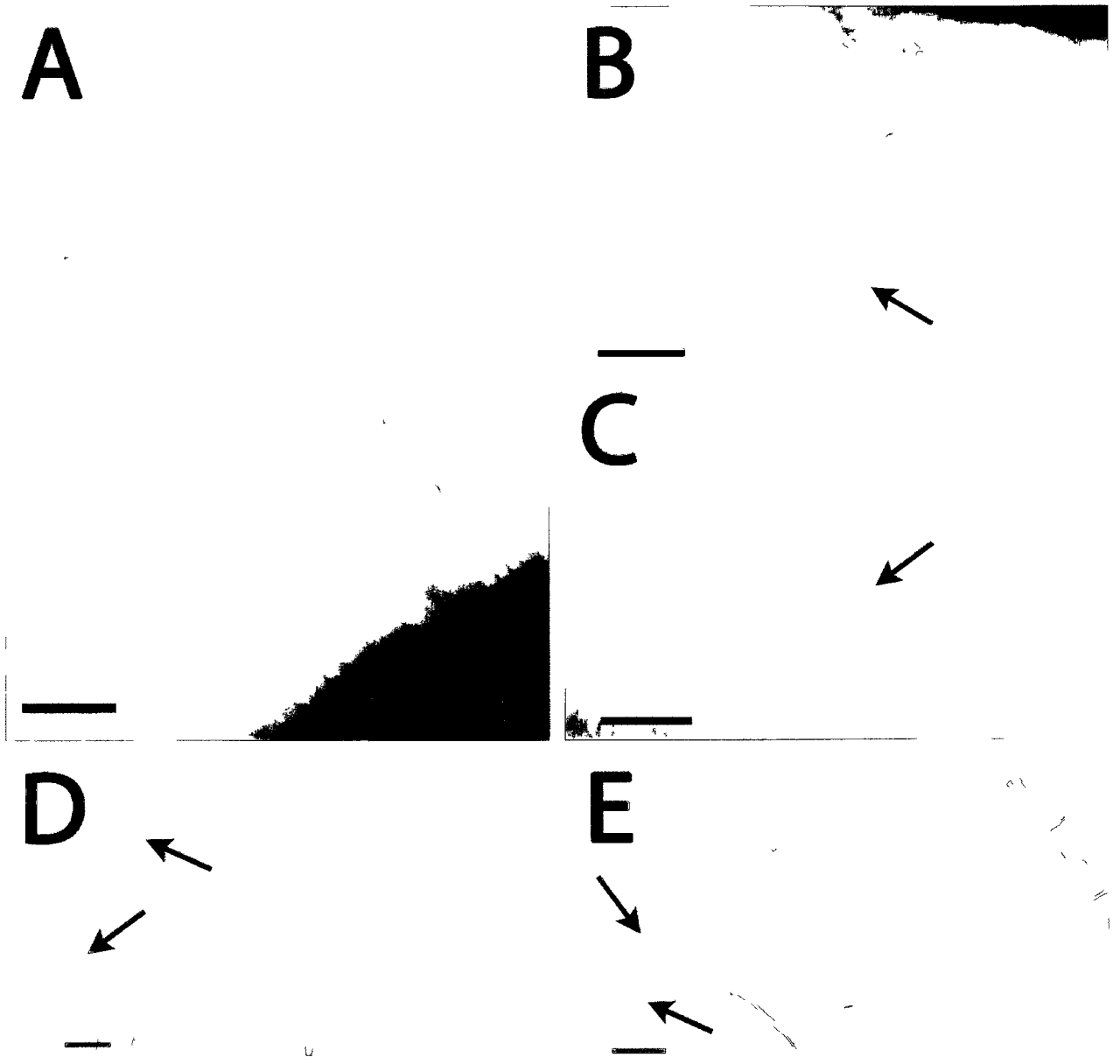
Figure 3.5 – Inoculated root of R50 24 HAI (A), 3 DAI (B), 10 DAI (C and D) and 14 DAI (E and F)

A: An unstained cross-section with no cell divisions of the pericycle. B: A cross-section of a spot-inoculated root with no cell divisions. In front of a xylem pole (X) 3 layers of pericycle cells (P), 1 layer of endodermal cells (E), and multiple layers of cortical cells (C) are evident. C: An unstained sagittal section of a developing nodule; a coiled mass of infection threads (arrow) can be seen entering the cells of the nodule. D: A close-up of the inner cortical and pericycle cells in C (box) showing anticlinal and periclinal divisions. E: A coiled mass of infection threads (arrow) that appear to be blocked in the root cortex. No inner cortical cell (C) divisions are apparent near the vasculature (V). F: A magnified picture of E (box) showing the abnormal infection threads (arrow) and no cells divisions of the cortical cells (C) or pericycle (P) near the vasculature (V). Scale bar for A, B, C, D and F = 20 μm. Scale bar for E = 100 μm.

A

B

C

D

X
P
E
C

E

F

V

C

P
V
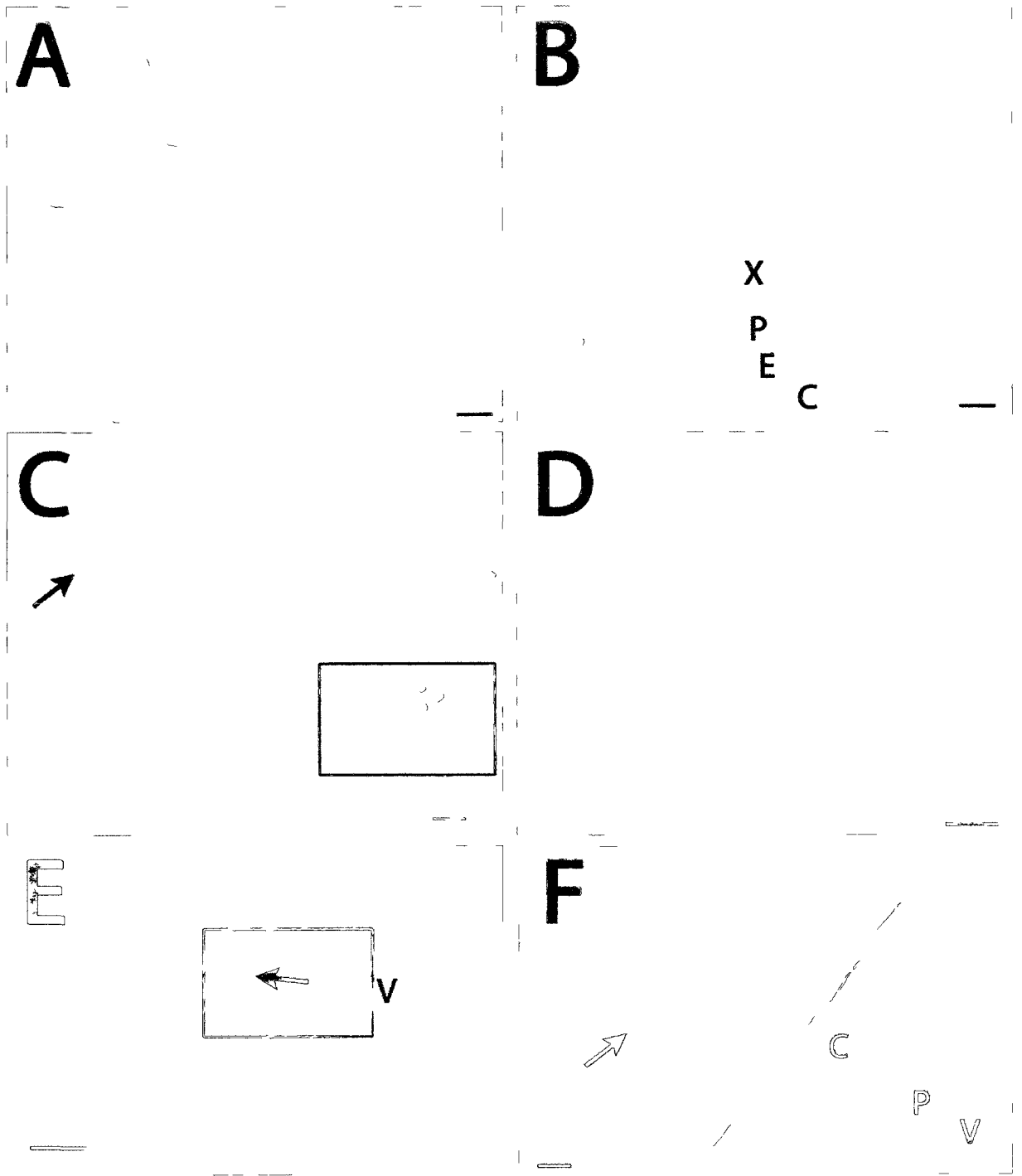
and Geil, 2002). However, at that time, a few nodules with abnormal vascular strands were also present (Pepper *et al.* 2007); these nodules were generally smaller in size and delayed in development compared to those of Sparkle at the same stages.

Light Microscopy – Established Nodules and Starch

Where possible the different zones that comprise a nodule as classified by Vasse *et al.* (1990) will be used to describe the orientation of sectioned nodules. In Sparkle, 7 DAI, the nodules were pink (refer to Figure 2.2 D) (indicating an abundance of leghemoglobin), the meristematic zone (zone I), the infection zone (zone II), and the nitrogen fixation zone (Zone III) were well established (Figure 3.6 A), and the vascular strands extended up to the nodule meristem. Finally, mature nodules were evident 14 DAI (Figure 3.6 B). The senescent zone was not observed as it would develop as the nodule continues to age.

Mature 21 day-old nodules were investigated focusing on the obvious differences between Sparkle and R50 nodules, specifically the quantity and size of the starch grains (Figure 3.7 – Figure 3.10). R50 nodules appear to have a higher density of starch grains; these were also much larger than those observed in Sparkle nodules (Figures 3.7 and 3.8). These observations were confirmed by potassium iodine staining. In both Sparkle and R50, starch grains were located in infected and non-infected cells. The grains in the infected cells were arranged in an organized pattern, generally around the periphery of the cell, and were usually much smaller than those in non-infected cells (Figures 3.9 and 3.10). The infected cells in zone II-III (zone of bacteroid differentiation, Vasse *et al.*, 1990) contain the majority of the starch grains with the exception of the cortical cells located in close proximity to the vascular strands (Figure 3.9 A, Figure 3.10 A). While I

71

Figure 3.6 – Nodules of Sparkle 7 DAI (A) and 14 DAI (B).

A. A sagittal section of a 7 DAI nodule stained with toluidine blue. The meristematic zone (I) is evident with the infection zone located beneath it (II). Infected cells can be seen within the nitrogen fixation zone (III) and the nodule vasculature (arrows) extends around the periphery of the cell. B. An unstained longitudinal section of a nodule 14 DAI with the meristematic zone (I), infection zone (II), and nitrogen fixation zone (III) fully developed. Scale bar = 100 μm.
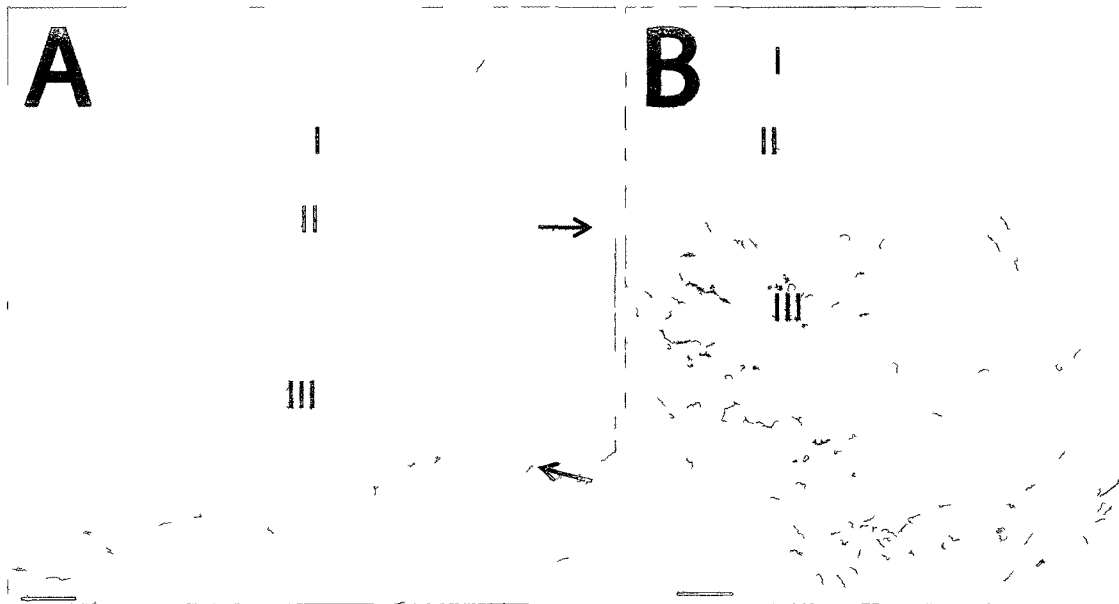
Figure 3.7 – Sagittal sections of Sparkle nodules 21 DAI viewed with differential interference contrast optics

A: Starch grains (arrow) are evident in cortical cells located in between the vasculature (*) and the infected cells (I). B: Starch grains (arrow) of the cortical cells near the nodule vasculature. C: Starch grains (arrows) in one or more uninfected (NI) cells which are surrounded by infected cells (I). D: A group of small starch grains (arrow) in a non-infected cell (NI) and starch grains (arrowheads) can be seen in the infected cells (I). Scale bar for A = 50 μm. Scale bar for B, C and D = 20 μm.
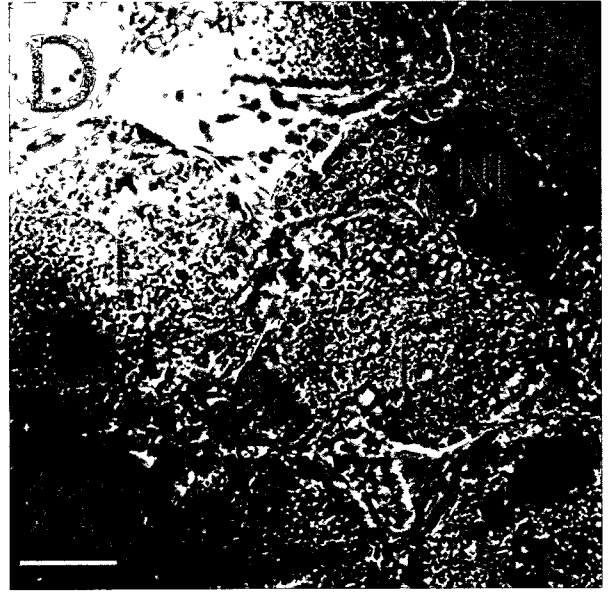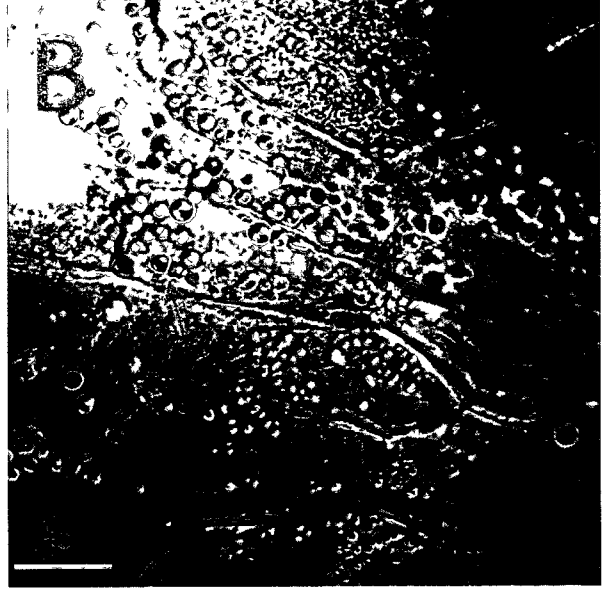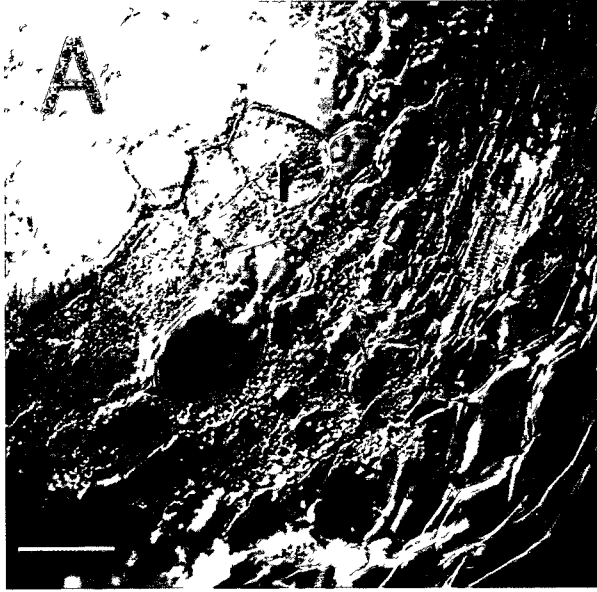
Figure 3.8 - Sagittal sections of R50 nodules 21 DAI viewed with differential interference contrast optics

A: An unstained section of a multi-lobed R50 nodule. The larger portion of the nodule was photographed with the nodule meristem (M) oriented toward the bottom of the page. Starch grains can be seen lining the cortical cells (C) near the vasculature (*). Clumps of starch grains (arrow) are also evident in and around the infected cells (I). B: Clumps of starch grains (arrow) in uninfected cells (NI) in close proximity to infected cells (I). Uninfected cells with no starch grains (NI-x) are also evident. C: A group of non-infected (NI) cells in close proximity to the cortical cells (C). A group of non-infected cells filled with starch grains (arrow) surrounds one uninfected cell without any starch grains. D: Two uninfected cells that appear empty (NI-x). An infected cell (I) with smaller and fewer starch grains (arrowhead) than those observed in the uninfected cells (NI). Scale bar for A = 100 μm. Scale bar for B, C and D = 20 μm.

Figure 3.9 - Sagittal sections of 21 day-old Sparkle nodules stained with potassium iodine

A: The meristematic zone (I), the infection zone (II), the bacteroid diffentiation zone (II-III) and the nitrogen-fixation zone (III) (according to Vasse *et al.* 1990). Starch grains do not appear in zones I and II. The density of starch grains is the highest in zone II-III compared to all other zones. The starch grains in the cells of this zone appear around the cell periphery. B: In zone III, large starch grains (arrowhead) are abundant in the uninfected (NI) cells and small starch grains (arrow) are located in the infected cells (I). An uninfected cell with no starch grains (NI-x) situated beside an uninfected cell with starch grains. C: Starch grains (arrows) within infected cells (I). Scattered amongst the infected cells are uninfected cells (NI) that contain larger starch grains (arrowhead) than those of infected cells. There is also two uninfected cell without starch grains (NI-x). D: An organized pattern of starch grains (box) can be observed around the vacuole (V) of an infected cell (I). Scale bar for A = 100 μm. Scale bar for B, C and D = 50 μm.
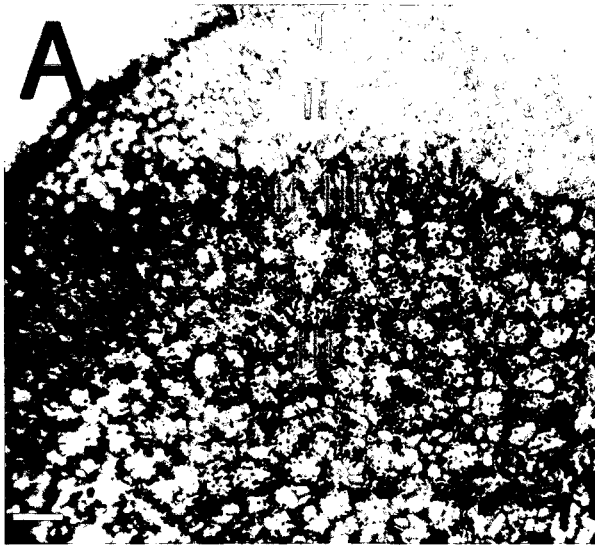
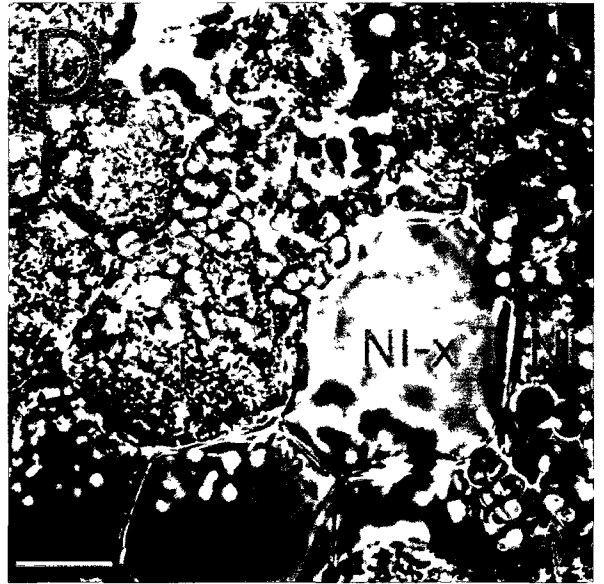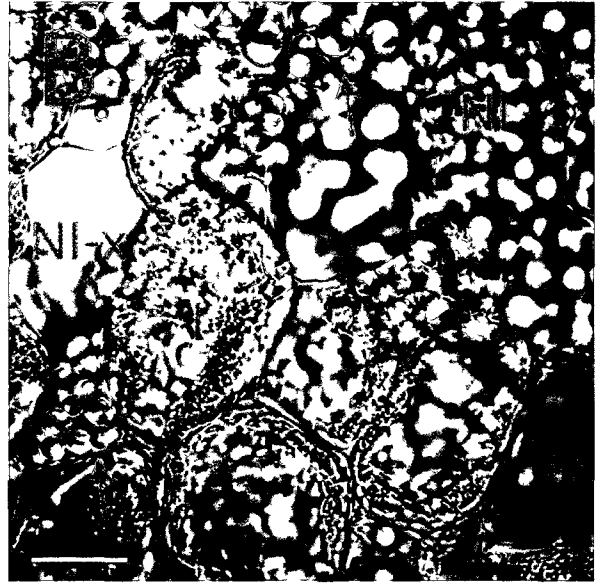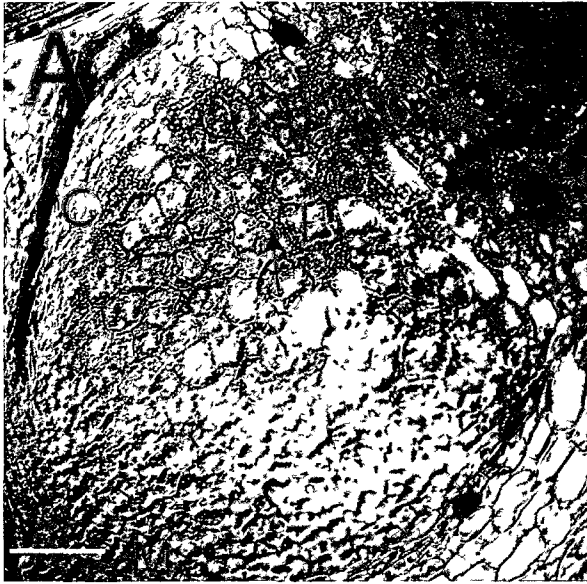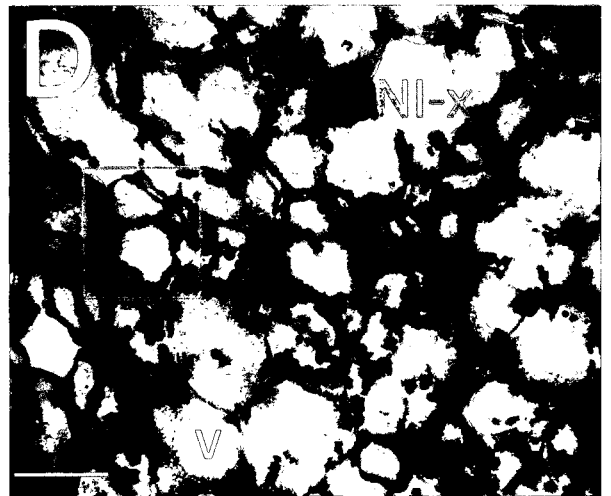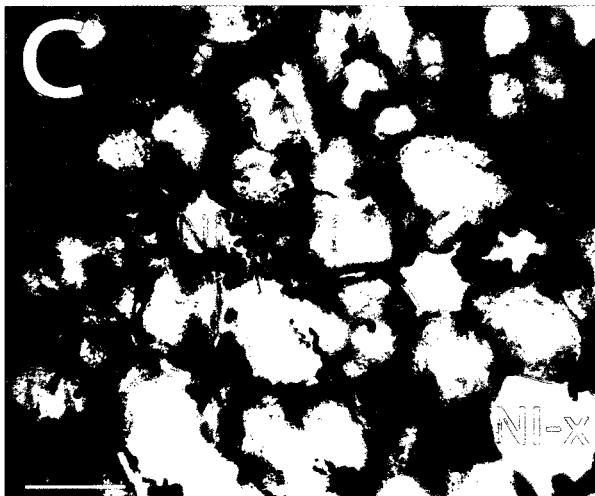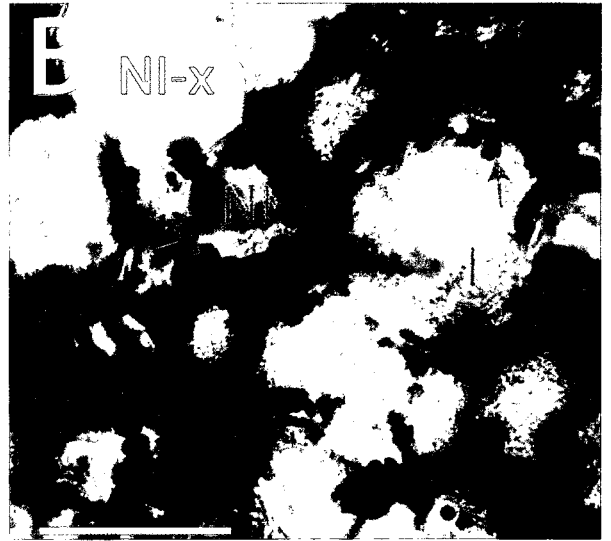**Figure 3.10 - Sagittal sections of 21 day-old R50 nodules stained with potassium iodine**

A: The infection zone (II), the bacteroid diffentiation zone (II-III) and the nitrogen-fixation zone (III). The letter in each box corresponds to the respective panel within this plate. Similar to Sparkle (refer to figure 3.8 for comparison), an abundance of starch grains is observed in zone II-III and in the cortical cells within close proximity to the vasculature (not shown). B: An uninfected cell with no starch grains (NI-x) is sandwiched between uninfected cells (NI) with large starch grains. An organized pattern of starch grains (arrows) arranged around vacuoles (V) of the infected cell (I). C: Uninfected cells with no starch grains (NI-x) and uninfected cells with starch grains (NI) are observed. An organized pattern of starch grains (arrow) can be seen arranged around the vacuole (V). D: Many uninfected cells (NI) filled with large starch grains. Infected cells show starch grains organized within the cytoplasmic strands enveloping the vacuole (V) of the infected cells (I). Scale bar for A = 100 μm. Scale bar for B, C and D = 50 μm.
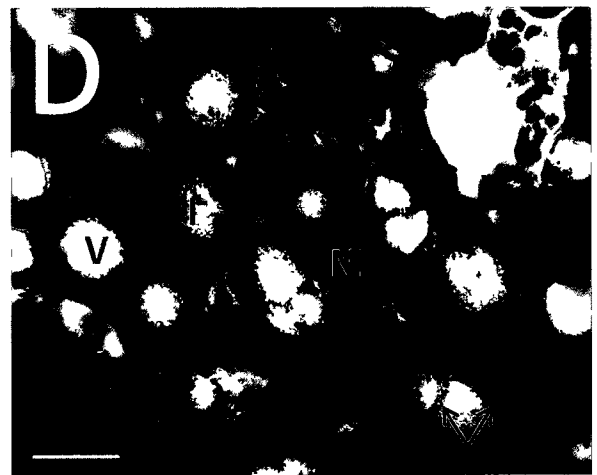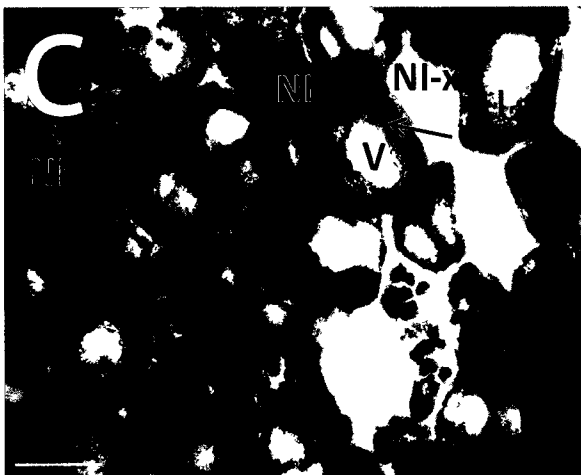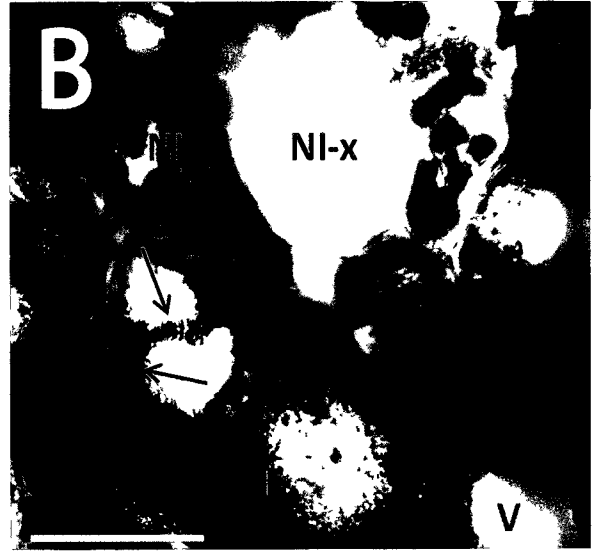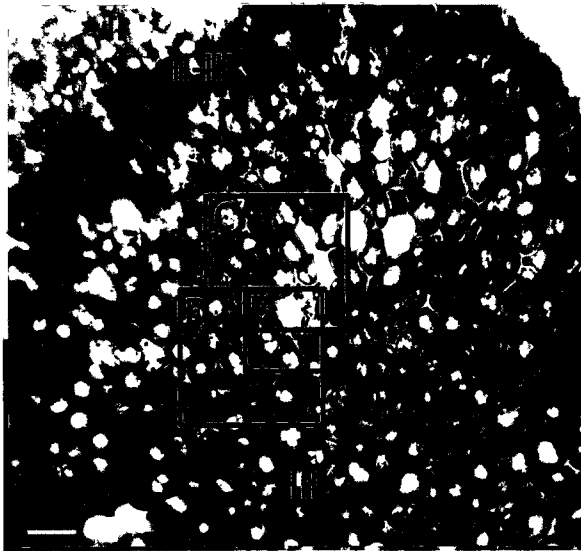
was investigating the starch grains of R50 nodules, it became apparent that two different kinds of uninfected cells may exist; those that contain starch grains and those that do not (Figure 3.10). This observation was also made later in Sparkle nodules (Figure 3.9). Finally, the uninfected cells of R50 appeared to be more numerous and larger than the uninfected cells of Sparkle.

Immunolocalization of PsCKX1

The localization of PsCKX1 was studied by confocal microscopy in mature root nodules. In 21 day-old nodules of Sparkle, the immunostaining, detected as a red colour (and green colour where indicated), was found mainly in the cytoplasm of infected cells (Figure 3.11- Figure 3.13). Specifically, the cytoplasm surrounding the nucleus and the symbiosomes, and that of the transfer cells located around the nodule vascular bundle (Guinel, 2009) were highlighted. PsCKX1 was not located within the symbiosomes; this was confirmed by the SYTO 13 counter-staining (Figure 3.12). There was also some punctuated immunofluorescence, usually around the nucleus in infected cells (Figure 3.12). The location of this punctuated staining appeared to coincide with that of the starch grains. Non-infected cells rarely showed any immunofluorescent signal; the starch grains in these cells were not labeled but autofluorescence around the grains was common. In R50 nodules, PsCKX1 was localized similarly to that in Sparkle nodules but the intensity of the immunofluorescent signal in the infected cells was much greater (Figure 3.14 – Figure 3.16). Control sections incubated only with secondary antibody or with pre-immune serum in place of primary antibody showed no or little labeling (Figures 3.11 B, 3.14 B, 3.15 B and 3.16 B).

Figure 3.11- Sagittal sections of Sparkle nodules 21 DAI, viewed either with differential interference contrast (DIC; A and C) or fluorescence (B and D) optics. Immunolocalization of PsCKX1 was performed using a polyclonal primary antibody to PsCKX1 and a secondary antibody AlexaFluor 635 (633/647).

A: A portion of a nodule exhibiting the inner cortex (C) recognized by the presence of tracheids (T) and part of the nitrogen fixation zone with infected cells (I) conspicuous by their larger vacuole (V). B: Same section but probed with pre-immune serum and secondary antibodies. Little detection was observed with fluorescence optics. C: The nitrogen fixation zone is shown with infected cells (I) and their large vacuoles (V); one uninfected cell (NI) is recognizable. D: Same section probed with the antibody to PsCKX1. The protein is localized to the cytoplasm of the infected cells and to vesicles which appear as bright punctuate labeling around the vacuole. The uninfected cell (NI) noticed in C has no PsCKX1 localization. Scale bar = 20 µm.

Figure 3.12 - Sagittal sections of Sparkle nodules 21 DAI were viewed with fluorescence optics. Sections were stained with SYTO 13 to label DNA (A and C) (495/519) and probed with a polyclonal primary antibody to PsCKX1 and a secondary antibody AlexaFluor 635 (633/647) (B and D).

A: A portion of a nodule exhibiting the nitrogen-fixation zone. The nuclei (N) and the bacteroids of the infected cells (I) are labeled green. A few starch grains (arrow) located in uninfected (NI) cells overlay the infected cells B: Same section probed with the antibody to PsCKX1. The protein was located to the cytoplasm in which the symbiosomes are suspended and to the cytoplasm around the nucleus in the infected cell (I). C: The nitrogen fixation zone is seen with infected cells (I) and their large vacuoles (V) and uninfected cells (NI) scattered among the infected cells. D: Same section probed with the antibody to PsCKX1. The protein was localized to the cytoplasm surrounding the bacteroids which are arranged around the periphery of the infected cell (I). A punctuate labeling for PsCKX1 was observed around the vacuole arranged in a pattern similar to the starch grains. Uninfected cells (NI) are not labeled with the antibody. Scale bar = 20 μm.
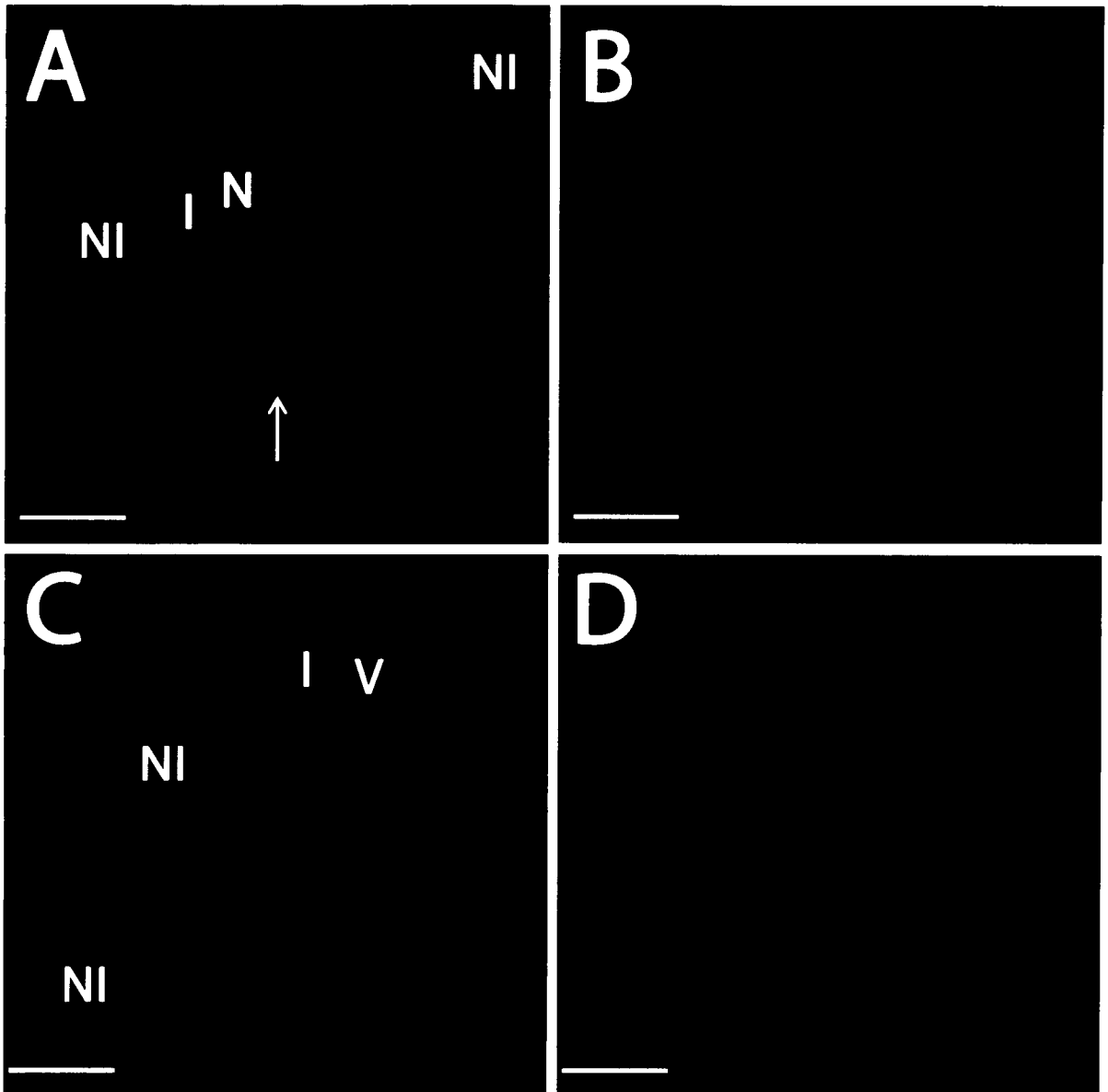
Figure 3.13 - Sagittal sections of Sparkle nodules 21 DAI, viewed with either differential interference contrast (DIC; A and C) or fluorescence (B and D) optics. Immunolocalization of PsCKX1 was performed using a polyclonal primary antibody to PsCKX1 and a secondary antibody AlexaFluor 488 (495/519).

A: A portion of a nodule exhibiting the nodule vasculature identified by the presence of tracheids (T). Adjacent to the tracheids are transfer cells of the pericycle (P) and large cells of the endodermis (E). B: Same section but probed with primary and secondary antibodies. A strong signal was observed in the cytoplasm of the pericycle cells and that of the endodermis, the cells of which appear to possess a large vacuole. C: A portion of a nodule exhibiting a vascular bundle viewed in cross-section. It is delimited by the cells of the pericycle (P) and of the endodermis (E). D: Same section probed with the antibody to PsCKX1 and examined with optics for AlexaFluor 488. PsCKX1 is localized to the cytoplasm at the periphery of the pericycle and endodermal cells. Scale bar = 20 μm.
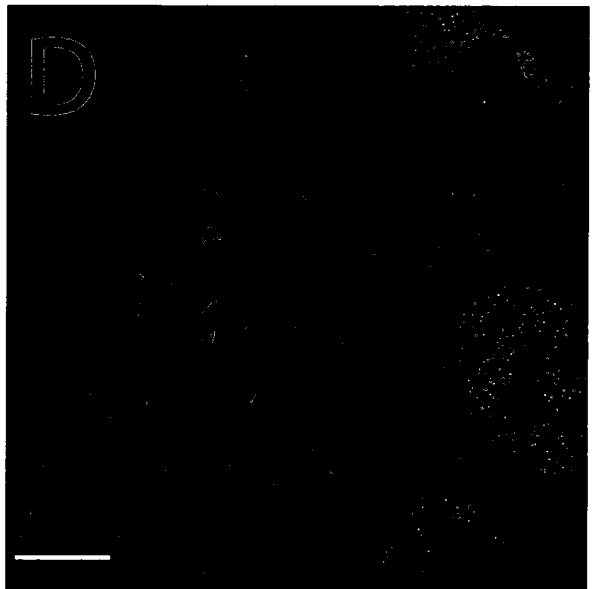
Figure 3.14 - Sagittal sections of R50 nodules at 21 DAI, viewed either with differential interference contrast (DIC; A and C) or fluorescence (B and D) optics. Immunolocalization of PsCKX1 was performed using a polyclonal primary antibody to PsCKX1 and a secondary antibody AlexaFluor 635 (633/647).

A: A portion of a nodule exhibiting the inner cortex recognized by the presence of tracheids (V) and a large portion of the nitrogen fixation zone with infected cells (I). B: Same section used as a control probed with pre-immune serum and secondary antibodies. Little detection was observed with fluorescence optics for AlexaFluor 635. C: A portion of a nodule exhibiting the nitrogen fixation zone is seen with infected cells (I) and a few uninfected cells (NI) scattered throughout. D: Same section probed with polyclonal antibodies to PsCKX1. The protein was localized to the infected cells, mainly to their cytoplasm. Notice the stronger signal than that of Sparkle (refer to Figure 3.11). Possible vesicles are observed as a bright punctuate labeling in organized patterns (refer to Figure 3.10). Uninfected cells (NI) are not labeled. Scale bar = 40 μm.
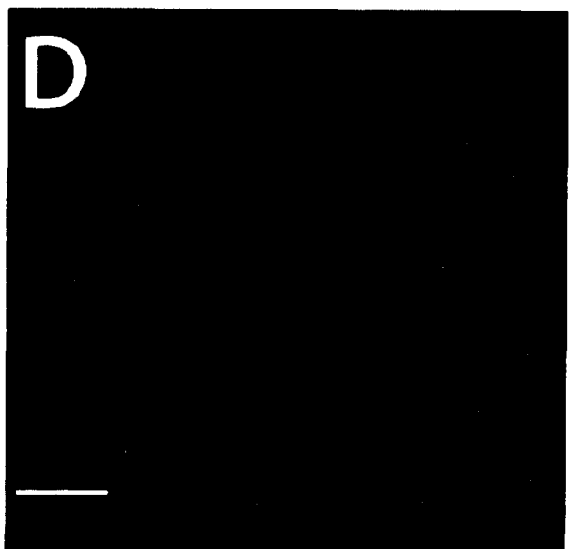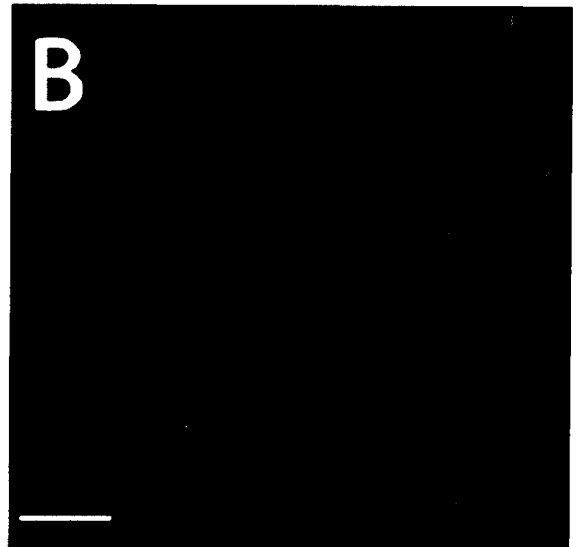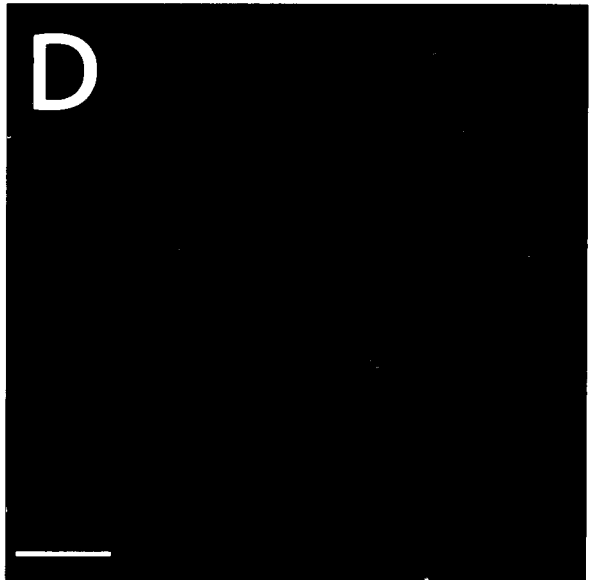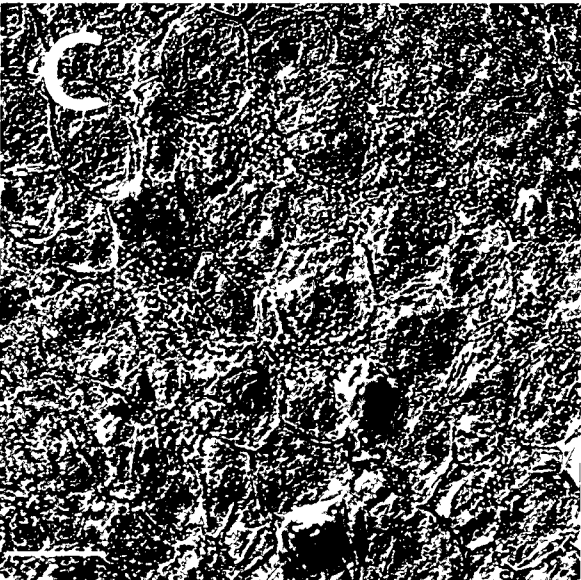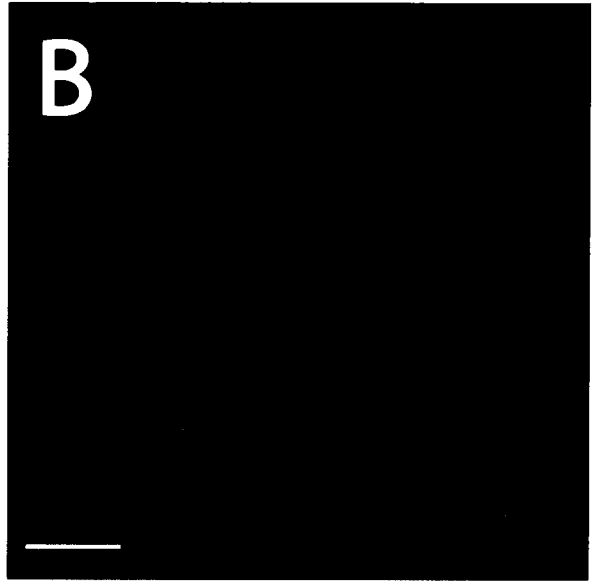
Figure 3.15 - Sagittal sections of R50 nodules 21 DAI viewed with fluorescence optics. Sections were stained with SYTO 13 to label DNA (A and C) (495/519) and probed using polyclonal primary antibodies to PsCKX1 and secondary antibodies AlexaFluor 635 (633/647) (B and D).

A: A portion of a nodule exhibiting the nitrogen fixation zone. The nucleus (N) of the infected cells (I) is labeled green. In these cells, the bacteroids (green) are arranged around the periphery of the vacuole (V). An infection thread (arrows) can be seen through the infected cells. B: Same section used as a control and probed with pre-immune serum. C: The nuclei (N) of infected cells (I) are green from SYTO 13. The vacuole (V) of the infected cells is not labeled. Some starch grains (S) can be made out as black outlines within the green fluorescence; those reside in the uninfected cells located on top of the infected cells. D: Same section probed with the antibody to PsCKX1. The protein is localized to the cytoplasm in which the symbiosomes are suspended, the cytoplasm around the nucleus, and possibly in vesicles which appear as punctuate labeling of the infected cells. The vesicles appear to surround the vacuole in the infected cell. There is no labelling where starch grains were located in the uninfected cells. Scale bar = 20 μm.
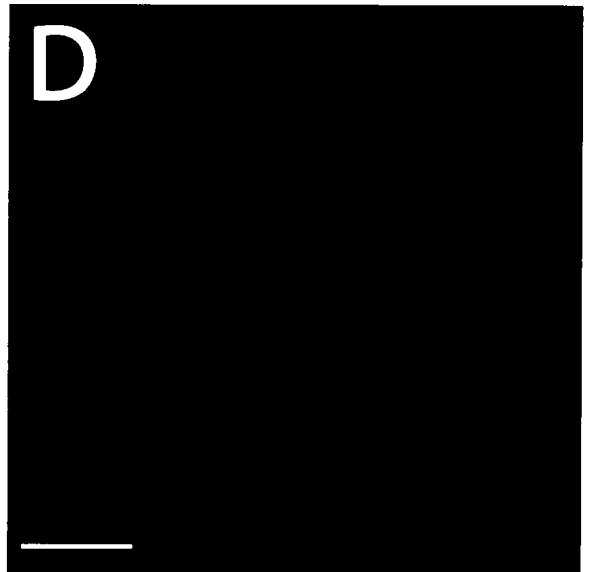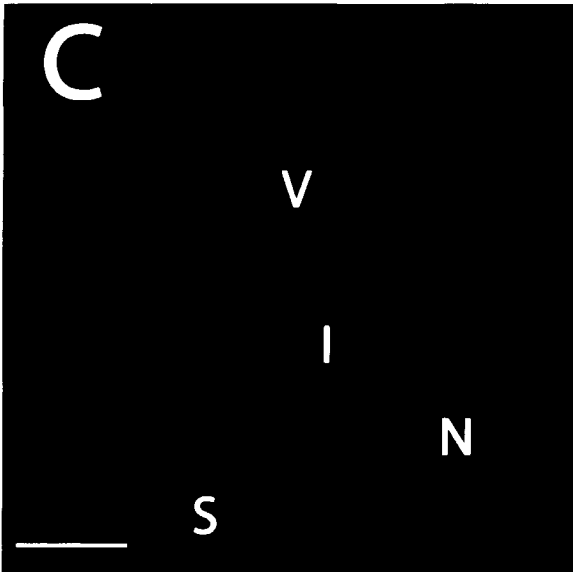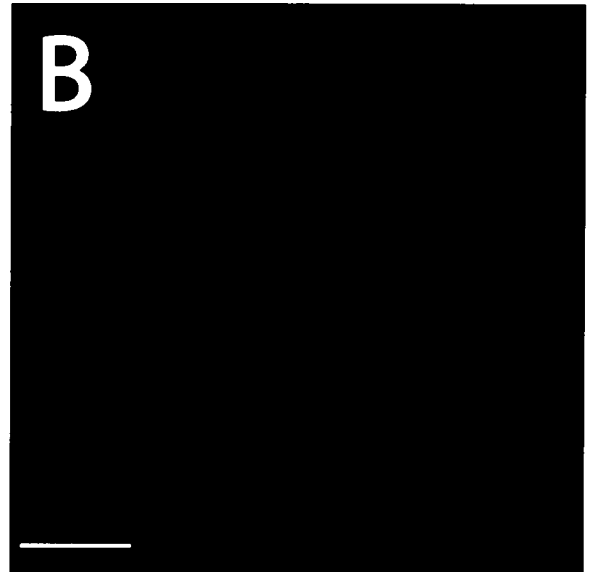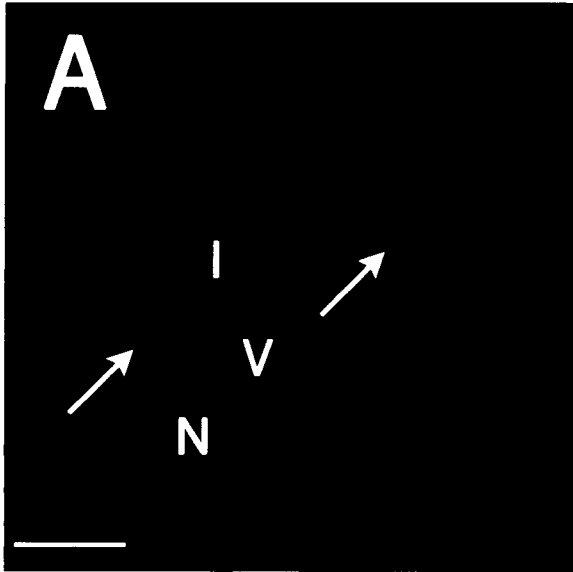
Figure 3.16 - Sagittal sections of R50 nodules 21 DAI viewed with fluorescence optics. Sections were stained with SYTO 13 to label DNA (A and C) (495/519) and probed using polyclonal primary antibodies to PsCKX1 and AlexaFluor 635 (633/647) secondary antibodies (B and D).

A: A portion of a nodule exhibiting the nitrogen fixation zone. The nuclei (N) of the infected cells (I) and bacteroids are labeled in green. A large infection thread (arrows) is seen in infected cells. B: Same section used as a control and probed with pre-immune serum. C: The bacteroids within the infected cells (I) are green. The vacuole (V) of an infected cell is not labeled. Some starch grains (arrow) can be made out as black outlines within the green fluorescence. D: Same section probed with the antibody to PsCKX1. The protein is localized to the cytoplasm of the infected cells. Punctuate labeling was observed close to the vacuole. No detection was observed in the vacuole of the infected cells (V). Scale bar = 10 μm.
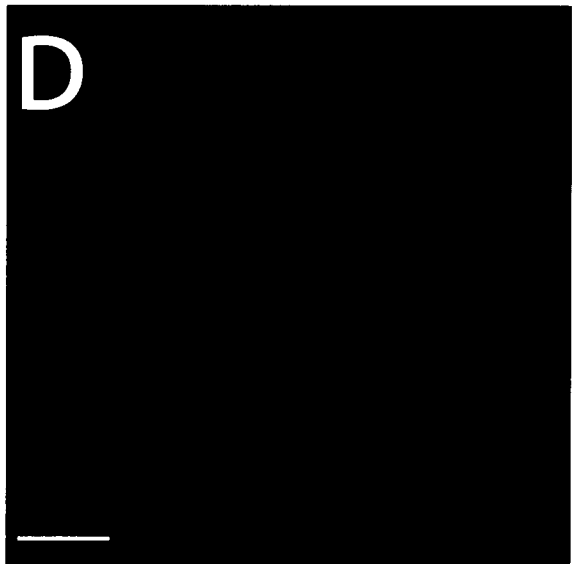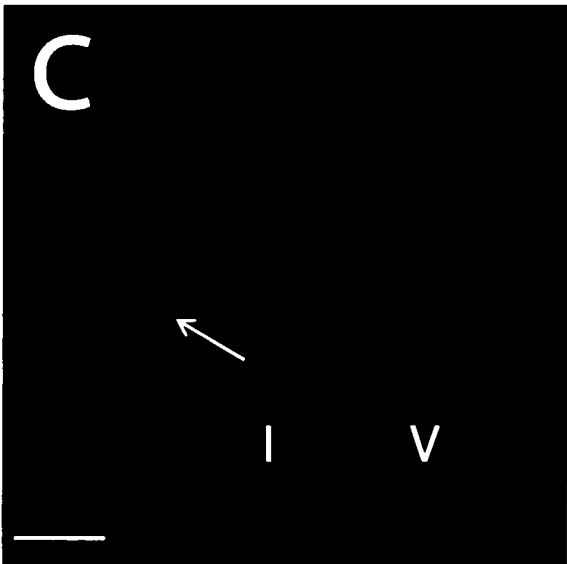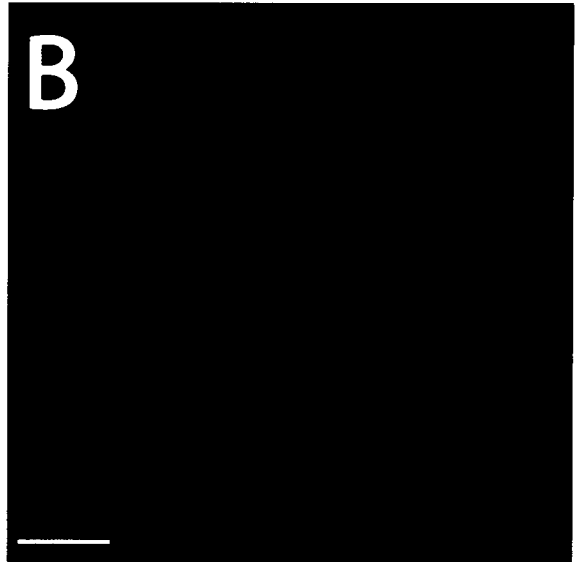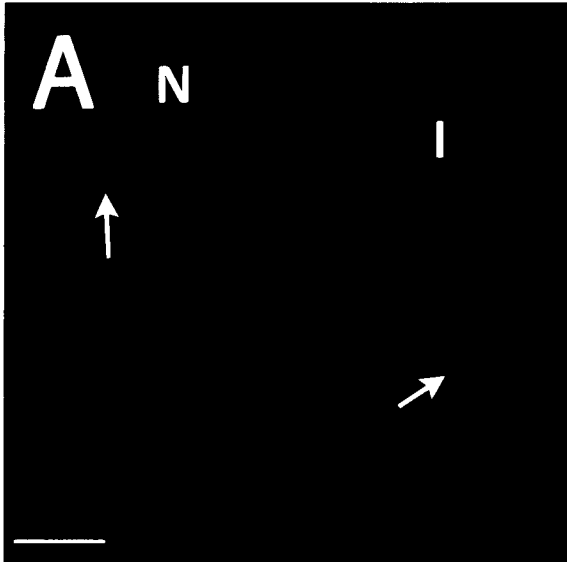
Western-blot analysis

A Western blot of PsCKX1 using total protein from Sparkle and R50 inoculated roots (21 DAI) is shown in Figure 3.17. When total protein from Sparkle was probed with antibodies (non-purified) to PsCKX1, two bands were observed around 58 kDa correspoding to the predicted protein mass of PsCKX1 (Held *et al.* 2008). When R50 was probed, a band barely visible was located at 58 kDa. Surprisingly, a strong band was visible around 42 kDa, well below the bands observed in Sparkle. This stronger signal detected in the R50 blot may explain the stronger signal obtained for PsCKX1 immunolocalization observed in Figures 3.15 – 3.16.

Expression analysis of CKX1

The expression of *PsCKX1* in the wild type increased as the lateral roots aged from 1 to 21 days after mock inoculation (Figure 3.18). In Sparkle, *PsCKX1* expression was always higher in spot-inoculated roots than in mock-inoculated plants, a trend that was observed as early as 24 HAI. The *PsCKX1* levels in the mock-inoculated roots of R50 were higher than those of Sparkle at all dates measured, agreeing with results reported by Held *et al.* (2008). In the mutant R50, there was also a spike of *PsCKX1* expression at 24 HAI. Unlike in the wild-type, *PsCKX1* expression in the mock-inoculated roots was similar to that found in inoculated roots by 14 DAI. The transcript levels of *PsCKX1* steadily increased overtime in both the non-inoculated and inoculated roots of R50 reaching levels twice those of Sparkle.

Figure 3.17 – Western blot of Sparkle and R50.

Western blot of total protein extracted from 21-day-old nodules of Sparkle and R50 probed with polyclonal primary PsCKX1 antibodies and secondary horseradish peroxidase antibodies which were detected with a enhanced chemiluminescent kit. Two bands were detected in Sparkle around the predicted weight for PsCKX1 of 58 kDa. However the PsCKX1 protein for R50 did not match the profile observed in Sparkle. A faint band (arrow) was detected beside the band of Sparkle and a brighter band was detected much lower on the blot (double arrow) close to 40 kDa. The blot was imaged for 10, 20 and 30 seconds.
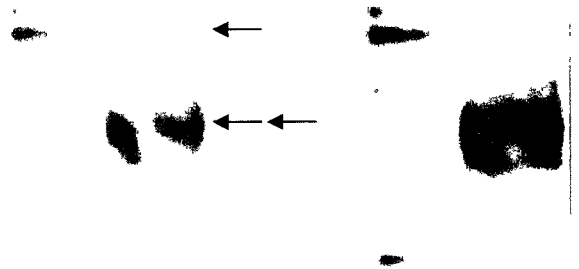
Figure 3.18 – *PsCKX1* transcript profile of Sparkle and R50 throughout nodule development

A. *PsCKX1* and *PsACTIN* transcripts of Sparkle and R50 were measured by semi-quantitative PCR. PCR program consisted of 26 cycles of 1 min denaturation (94°C) , 1 min annealing (54°C) and 30 sec extension (72°C) followed by a 6 min extension (72°C). Sparkle mock-inoculated (Sparkle N), Sparkle inoculated (Sparkle I), R50 mock-inoculated (R50 N) and R50 inoculated (R50 I) were examined at 1, 7, 14, and 21 days after inoculation.   B. The graph represents one of the four biological replicates. Inoculation up-regulates *PsCKX1* in Sparkle and R50.   As time after inoculation increases, the two lines differ. In WT, the transcript levels of infected roots remain higher than those of non-infected roots whereas in R50 they reach similar levels in the two types of roots. CKX1 transcript levels in both non-inoculated and inoculated R50 roots are higher than those of Sparkle at 14 and 21 DAI. This trend was observed in all replicates.
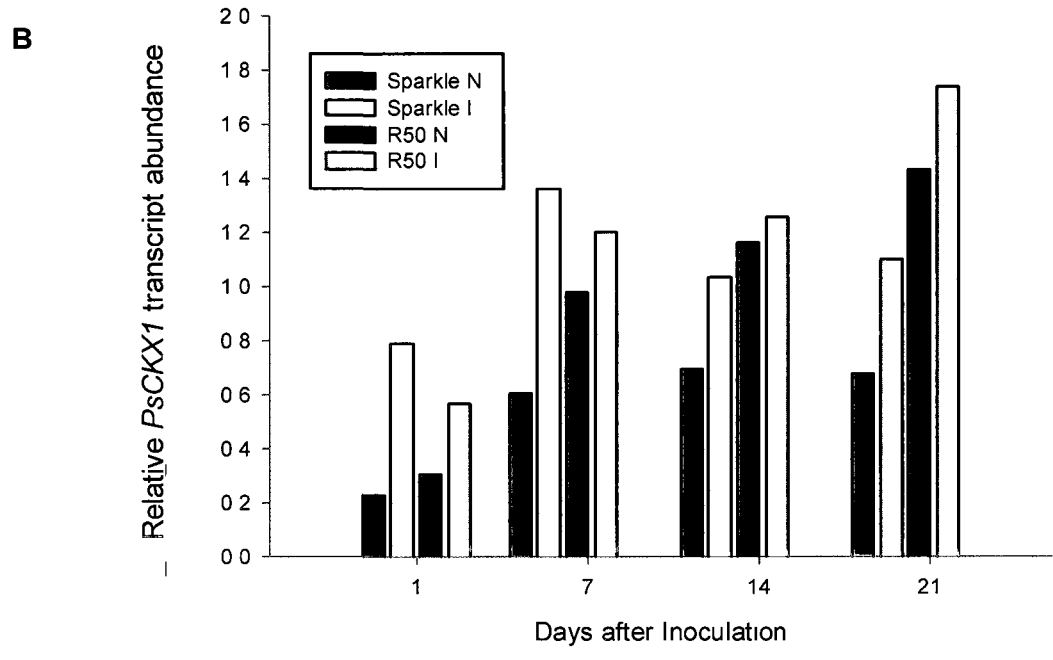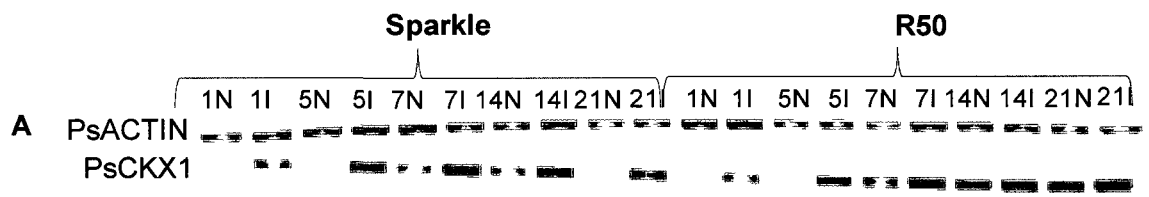
Discussion

This study set out to investigate the gene expression and the translated products of PsCKX1 in developing root nodules of Sparkle and R50. It had a successful outcome and the results are now making us reconsider the possibility of a mutation within the *PsCKX1* genomic sequence.

Sparkle nodule development occurred in the expected fashion, although the events leading to nodule development were captured much earlier than reported in the literature for pea likely because of the mechanism of rhizobia delivery (spot-inoculation). The cortical cells around the nodule vasculature and Zone II-III (Vasse *et al.* 1990) contain the highest density of starch grains although the infected cells and uninfected cells also possess some. The starch grains inside the infected cells are generally smaller than those of uninfected cells and they are located in a non-random fashion within the cell. PsCKX1 transcriptional expression is induced upon inoculation and remains higher in the infected roots than in non-inoculated roots at all time-points tested. Western blot reveals two protein bands, a strong reactive band of 58 kDa, the predicted mass of PsCKX1, and a second less abundant band a little higher than the first. PsCKX1 is mainly localized to the cytoplasm, i.e., around the nucleus and the symbiosomes, of the infected cells. PsCKX1 is also evident in the transfer cells of the nodule vasculature. A strong punctuate labeling is observed around the vacuole of the infected cells, in a pattern similar to that observed for the starch grains in sections that were stained with potassium iodine.

The events that lead to the development of a nodule are delayed in R50. Starch grains in the mature nodules are much bigger and more numerous than those of Sparkle. Like in Sparkle, the starch grains in the infected cells are smaller than those in uninfected

cells and their arranged patterns are more apparent. PsCKX1 transcription is also triggered upon inoculation in R50. However non-inoculated roots accumulate as much PsCKX1 transcripts as inoculated roots, reaching levels approximately twice as high as those of the infected roots of Sparkle by 21 DAI. The western blot for PsCKX1 in R50 is different from that of Sparkle. There is only a very faint band around 58 kDa that aligns with one of the Sparkle bands. There is, however, a strong immunoreactive band around 40 kDa (Figure 3.17). PsCKX1 is observed in the same cellular location as in Sparkle but the intensity of the label is stronger. The punctuate signal is also higher than that observed in the wild-type.

Because we were originally interested in the early stages of nodule development, the spot-inoculation technique was utilized for the first time. A developmental study for the timing of events required for a nodule to form was performed for Sparkle and R50. Root hairs of R50 did not curl as those of Sparkle; instead, they had an abnormal wavy appearance. Interestingly these root hairs appear similar to the abnormal root hairs of the pea *nin* mutant *SYM35* (Borisov *et al.* 2003). The spot-inoculation technique permitted me to observe very early events. Indeed, the pericycle cells are observed dividing periclinally 24 hours after inoculation and then anticlinally 48 HAI. I believe that these first cellular divisions in the outermost vascular layer are leading to the development of the nodule vasculature as they appear to be similar to the divisions described by Bond (1948) who studied in detail pea nodule organogenesis. To ensure that these divisions would indeed give rise to a nodule, an enzyme such as chalcone synthase, the first enzyme in the early flavonoid pathway, could be linked to a promoter fused with *gusA* as this type of labeling in *Trifolium repens* was successful at distinguishing sites of nodule

101

organogenesis before any cell division occurs (Mathesius *et al.* 1998). The divisions in the pericycle appear to precede those occurring in the inner cortex. As already described in the literature (Bond, 1948; Newcomb *et al.* 1979, Timmers *et al.* 1999), first anticlinal and then periclinal divisions were observed 48 HAI in the cortical cells. These events could not be captured in R50 as nodule development was rare. However, I believe that a more thorough investigation would uncover stages similar to those captured in the nodule development of Sparkle.

The western blots provided some interesting results. Two bands were produced when probing total Sparkle protein with PsCKX1 antibodies. Both bands appear close together, with a MW around 58 kDa, and could be a result of proteolysis. Alternatively, since PsCKX1 has three predicted glycosylation sites, the two bands may correspond to two different glycosylated forms which could exhibit different migration rates on an SDS-gel (Bilyeu *et al.* 2001). This could potentially mean that glycosylation regulates the activity of PsCKX1. The regulation of CKX by glycosylation was observed in *Nicotiana tabacum* calli whereby glycosylated CKX enzymes became more abundant when total cytokinin content increased (Motyka *et al.* 2003). When total R50 protein was probed with PsCKX1 antibodies, two bands were also observed. Surprisingly, none of these bands correlated well with the bands observed with Sparkle. Instead a strong immunoreactive band was detected around 40 kDa, while only a very faint band likely corresponding to PsCKX1 was observed around 58 kDa, the protein predicted mass. This result suggests that the protein is defective.

The high intensity signal obtained on the western blot for R50 supports the immunolocalization study. The immunofluorescence signal observed in R50 nodules was

greater than that of Sparkle. As predicted by Held *et al.* (2008), the majority of the signal was localized to the cytosol. The sheer abundance of immunofluorescent signal detected in both western blot and nodule tissue would suggest that the translation of PsCKX1 does occur in R50. The higher PsCKX1 protein detection in R50 also complements the abundance of *PsCKX1* transcript levels found in the mutant in this study and by Held *et al.* (2008). The accumulation of a possibly defective protein fits with the findings of Held *et al.* (2008) who demonstrated that total cytokinin oxidase activity in R50 was low compared to that of Sparkle. The abnormal PsCKX1 protein detected in R50 most likely fails to degrade cytokinin and thus the cytokinin negative feedback loop is continually engaged resulting in high transcript levels, high, potentially defective, protein levels, and no or little cytokinin inactivation. This would imply that PsCKX1 plays a major role in the overall homeostasis of cytokinin in nodules. However, the redundancy of the cytokinin oxidase genes most likely allows the plant to maintain most functions in growth and development (Werner *et al.* 2006).

The cause of the distinct enzymatic differences of PsCKX1 in R50 is still unknown. The cloning and subsequent sequencing of the coding region for PsCKX1 revealed no apparent mutations (Held *et al.* 2008). However, a single point mutation in *PsCKX1* could still be the cause of the R50 phenotype as it could have been missed during sequencing of the coding region. This could explain the large difference in MW seen in the immunoblot. Another possibility is that the two bands detected on the western blot for Sparkle could be alternative spliced forms of CKX. Yang *et al.* (2003) was the first to report such forms of cytokinin oxidase for DsCKX1 in the *Dendrobium* orchid, although the authors were unable to explain their functional significance. Since the

elucidation of CKX genes in legumes has been sluggish, the possibility of smaller CKX gene families compared to other plants exists as Lotus only has 3 CKX members (Heckmann, personal communication) compared to 7 CKX members in Arabidopsis. Then alternative splicing could serve to provide a variety of isoforms of CKX enzymes. AtCKX7, the closest homologue to PsCKX1, has 4 predicted introns (Bilyeu *et al.* (2001) and thus PsCKX1 could also have as many introns. A second report of alternative spliced cytokinin oxidase was made by Cueno *et al.* (2009) who studied the expression of the human immunodeficiency virus 1 trans-activator of transcription protein in tomato. Considering that the mutation in *sym16* is still unknown, and although no mutation was found in the coding region of PsCKX1 (Held *et al.* 2008), it is possible that the gene be mutated in one of its introns affecting the RNA splicing in R50 resulting in a truncated protein. In some cases, this type of mutation can still allow weak expression of the wild-type gene (Lal *et al.* 1999) as may be observed for R50 in the western blot. To determine if alternative splicing is in play for PsCKX1, one would have to obtain its genomic sequence and compare it to the cDNA used to draw previous conclusions.

When R50 nodules eventually develop, they contain vast amounts of starch grains that are much larger in size than those in Sparkle nodules. It is not clear why the starch grains are accumulating in the nodule of R50. It has been suggested that stressed nodules of the indeterminate type accumulate starch (Arrese-Igor *et al.* 1993). Boron-deficient pea plants also exhibit nodules which accumulate starch grains (Bolaños *et al.* 1994). Interestingly, there are numerous reports supporting a relationship between high cytokinin levels and starch synthesis. Sucrose-synthase is a highly active and stable enzyme

responsible for the conversion of sucrose, unloaded from the phloem, into UDP-glucose and fructose. Its activity increases the hexose pools of the cells, hexoses which will be used later to make starch (Copeland, 1990). Sucrose synthase has been localized to the vasculature and infected cells of indeterminate nodules (Hohnjec *et al.* 2003). *ENOD40*, stimulated by cytokinin, has been localized also to the vasculature and infected cells (Fang and Hirsh, 1998) and is known to have a protective effect on the degradation of sucrose-synthase (Koch, 2004). Furthermore, amyloplast formation has been synchronously induced by the addition of cytokinin benzyladenine (BA) to an auxin-depleted culture medium with cultured tobacco cells (Sakai *et al.* 1992). In contrast to auxin, cytokinin was shown to increase mRNA levels of three genes coding for enzymes responsible for starch synthesis, i.e., ADP-glucose pyrophosphorylase, granule-bound starch synthase, and starch branching enzyme (Miyazawa *et al.* 1999). Therefore, the elevated levels of cytokinin in R50 nodules could have induced elevated transcription of these genes which would have acted on the hexose pools formed by the activity of the sucrose-synthase enzyme leading ultimately to starch accumulation. It has been reported that cytokinin induces the expression of cell wall invertase and hexose transporters, the proteins of which are responsible for the mobilization and flow of sucrose into organs (Ehness and Roitsch, 1997; Godt and Roitsch, 1997; Roitsch and González, 2004). Thus, Zalewski *et al.* (2010), silencing the expression of HvCKX1 in barley, observed accumulation of starch grains in the endosperm. They suggested that increased cytokinin levels could enhance the activity of cell wall invertase and hexose transporters resulting in the accumulation of starch grains. Although in a different system, that of the endosperm of a monocot, it is possible that PsCKX1 localized in the transfer cells of the nodule

vasculature and in the cytoplasm of infected cells serve to regulate the transport and use of sucrose to and by the nodule. In R50, the defective PsCKX1 protein may not be able to regulate the import of sucrose by relieving the pressure of the cytokinin effect on the sucrose-synthase. If cytokinin promotes the formation of starch synthesis one would expect that a decrease in cytokinin content would result in starch catabolism. Thus, the strong punctuate labelling in R50 seen to co-localize with the starch grains in the infected cells could correspond to the localization of PsCKX1 attempting to regulate cytokinins to promote starch grain degradation. This punctuate immunolabelling was also observed in Sparkle but its signal was not as strong as in R50.

The relationship of cytokinin and cytokinin oxidase in the regulation of plant growth and development has been well documented (e.g. Mok and Mok, 2001; Werner *et al.* 2003), including the rapid mobilization of cytokinin and the subsequent transcription of cytokinin-induced genes (e.g. *ENOD40*) upon Nod factor perception for nodules to develop properly (Fang and Hirsch, 1998). The present study reports an increase in cytokinin oxidase transcript levels 24 hours after inoculation, reinforcing the concept that cytokinin levels are tightly regulated during nodule organogenesis. *PsCKX1* transcripts continued to increase as the nodules aged which suggests that cytokinin remains tightly regulated throughout nodule development; this is in agreement with the findings of Syõno *et al.* (1976) who reported peak levels of cytokinin 14 DAI in pea.

References

Arrese-Igor, C., Royuela, M., de Lorenzo, C., de Felipe, M. R., and Aparicio-Tejo, P. M. 1993. Effect of low rhizosphere oxygen on growth, nitrogen fixation and nodule morphology in lucerne. *Physiologia Plantarium*. **89**:55-63.

Bilyeu, K. D., Cole, J. L., Laskey, J. G., Riekhof, W. R., Esparza, T. J., Kramer, M. D., and Morris, R. O. 2001. Molecular and biochemical characterization of a cytokinin oxidase from maize. *Plant Physiology*. **125**: 378-386.

Bond, L. 1948. Origin and developmental morphology of root nodules of *Pisum sativum*. *Botanical Gazette*. **109**: 411-434.

Bolaños, L., Esteban, E., de Lorenzo, C., Fernández-Pascual, M., de Felipe, M. R., Gárate, A., and Bonilla, I. Essentiality of boron for symbiotic dinitrogen fixation in pea (*Pisum sativum*) Rhizobium nodules. *Plant Physiology*. **104**:85-90.

Borisov, A. Y., Madsen, L. H., Tsyganov, V. E., Umehara, Y., Voroshilova, V. V., Batagov, A. O., Sandal, N., Mortensen, A., Schauser, L., Ellis, N., Tikhonovich, I. A., and Stougaard, J. 2003. The *Sym35* gene required for root nodule development in pea is an ortholog of Nin from *Lotus japonicus*. *Plant Physiology*. **131**:1009-1017.

Bozdarov, J. 2008. (BSc Thesis). Cloning of the full-length CKX1 gene from pea (*Pisum sativum*) and comparison of the sequence from the nodulation mutant R50. Wilfrid Laurier University, Ontario, Canada.

Brownlee, B. G., Hall, R. H., and Witty, C. D. 1975. 3-Methyl-2-butenal: an enzymatic degradation product of the cytokinin, N-6-(delta-2 isopentenyl)adenine. *Canadian Journal of Biochemistry*. **53**:37-41.

Copeland, L. 1990. Enzymes of sucrose metabolism. *Methods in Plant Biochemistry*. **3**:73:85.

Cueno, M. E., Hibi, Y., Imai, K., Laurena, A. C., Okamoto, T. Impaired plant growth and development caused by human immunodeficiency virus type 1 Tat. *Transgenic Research*. **19**-903-913.

Dolgikh, E. A., Leppyanen, I. V., Osipova, M. A., Savelyeva, N. V., Borisov, A. Y., Tsyganov, V. E., Geurts, R., and Tikhonovich, A. 2010. Genetic dissection of *Rhizobium*-induced infection and nodule organogenesis in pea based on *ENOD12A* and *ENOD5* expression analysis. *Plant Biology*. Article first published online: 17 AUG 2010; doi: 10.1111/j.1438-8677.2010.00372.x

Ehness R., and Roitsch T. 1997. Co-ordinated induction of mRNAs for extracellular invertase and a glucose transporter in *Chenopodium rubrum* by cytokinins. *The Plant Journal*. **11**:539–548.

Fang, Y., and Hirsch, A. M. 1998. Studying early nodulin gene *ENOD40* expression and induction by nodulation factor and cytokinin in transgenic alfalfa. *Plant Physiology*. **116**:53-68.

Ferguson, B.J., Wiebe, E.M., Emery, N., and Guinel, F.C. 2005. Cytokinin Accumulation and an Altered Ethylene Response Mediate the Pleiotropic Phenotype of the Pea Nodulation Mutant R50 (*sym16*). *Canadian Journal of Botany*. **83**: 989-1000.

Galuszka, P., Frébortová, J., Werner, T., Yamada, M., Strnad, M., Schmülling, T., and Frébort, I. 2004. Cytokinin oxidase/dehydrogenase genes in barley and wheat: cloning and heterologous expression. *European Journal of Biochemistry*. **271**:3990-4002.

Godt, D.E., and Roitsch, T. 1997. Regulation and tissue-specific distribution of mRNAs for three extracellular invertase isoenzymes of tomato suggests an important function in establishing and maintaining sink metabolism. *Plant Physiology*. **115**:273–282.

Guinel, F.C. 2009. Getting around the legume nodule: I. The structure of the peripheral zone in four nodule types. *Botany*. **87**:1117-1138.

Guinel, F., and Geil, R. 2002. A model for the development of the rhizobial and arbuscular mycorrhizal symbioses in legumes and its use to understand the roles of ethylene in the establishment of these two symbioses. *Canadian Journal of Botany*. **80**: 695-720.

Guinel, F.C. and Sloetjes, L.L. 2000. Ethylene is involved in the nodulation phenotype of *Pisum sativum* R50 (*sym16*), a pleiotropic mutant that nodulates poorly and has pale green leaves. *Journal of Experimental Botany*. **51**: 885-894.

Haynes, J. G., Czymmek, K. J., Carlson, C. A., Veereshlingam, H., Dickstein, R., and Sherrier, D. J. 1994. Rapid analysis of legume root nodule development using confocal microscopy. *New Phytologist*. **163**:661-668.

Held, M., Pepper, A. N., Bozdarov, J., Smith, M. D., Emery, R. J. N., Guinel, F. C. 2008. The pea nodulation mutant R50 (*sym16*) displays altered activity and expression profiles for cytokinin dehydrogenase. *Journal of Plant Growth and Regulation*. **27**:170-180.

Hohnjec, N., Perlick, A. M., Pühler, A., and Küster, H. 2003. The *Medicago truncatual* sucrose synthase gene *MtSucS1* is activated both in the infected region of root nodules and in the cortex of roots colonized by arbuscular mycorrhizal fungi. *Molecular Plant-Microbe Interactions*. **16**:903-915.

Karas, B., Murray, J., Gorzelak, M., Smith, A., Sato, S., Tabata, S., and Szczyglowski, K. 2005. Invasion of *Lotus japonicus root hairless 1* by *Mesorhizobium loti* involves the nodulation factor dependent induction of root hairs. *Plant Physiology*. **137**:1331-1344.

Kneen, B. E., Weeden, N. F., and LaRue, T. A. 1994. Non-nodulating mutants of *Pisum sativum* (L.) cv. Sparkle. *Journal of Heredity*. **85**: 129-133.

Koch, K. 2004. Sucrose metabolism: regulatory mechanisms and pivotal roles in sugar sensing and plant development. *Current Opinion in Plant Biology*. **7**:235-246.

Lal, S., Choi, J-H., and Hannah, L. C. 1999. The AG dinucleotide terminating introns is important but not always required for Pre-mRNA splicing in the Maize endosperm. *Plant Physiology*. **120**: 65-72.

Lohar, D. P., Schaff, J. E., Laskey, J. G., Kieber, J. J., Bilyeu, K. D., and Bird, D. M. 2004. Cytokinins play opposite roles in lateral root formation, and nematode and Rhizobial symbioses. *The Plant Journal*. **38**:203-214.

Lorteau, M-A., Ferguson, B.J., and Guinel, F.C. 2001. Effects of cytokinin on ethylene production and nodulation in pea (*Pisum sativum*) cv. Sparkle. *Physiologia Plantarum*. **112**: 421-428.

Mathesius, U., Bayliss, C., Weinman, J., Schlaman, R. M., Spaink, H. P., Rolfe, B. G., McCully, M. E., and Djordjevic, M. A. 1998. Flavonoids synthesized in cortical cells during nodule initiation are early developmental markers in white clover. *Molecular Plant-Microbe Interactions*. **12**:1223-1232.

McGaw, B. A. And Horgan, R. 1983. Cytokinin catabolism and cytokinin oxidase. *Phytochemistry*. **22**:1103-1105.

Miyazawa, Y., Sakai, A., Miyagishima, S-y., Takano, H., Kawano, S., and Kuroiwa, T. 1999. Auxin and cytokinin have opposite effects on amyloplast development and the expression of starch synthesis genes in cultures bright yellow-2 tobacco cells. *Plant Physiology*. **121**:461-469.

Mok, D. W., and Mok, M. C. 2001. Cytokinin metabolism and action. *Annual Review of Plant Physiology and Plant Molecular Biology*. **52**:89-118.

Motyka, V., Faiss, M., Strnad, M., Kamínek, M., and Schmülling. 1996. Changes in cytokinin content and cytokinin oxidase activity in response to derepression of *ipt* gene transcription in transgenic tobacco calli and plants. *Plant Physiology*. **112**:1035-1043.

Murray, J. D., Karas, B. J., Sato, S., Tabata, S., Amyot, L., Szczyglowski, K. 2007. A cytokinin perception mutant colonized by Rhizobium in the absence of nodule organogenesis. *Science*. **315**:101-104.

Newcomb, W., Sippell, D., and Peterson, R. L. 1979. The early morphogenesis of *Glycine max* and *Pisum sativum* root nodules. *Canadian Journal of Botany*. **57**:2603-2616.

Pepper, A. N., Morse, A. P., and Guinel, F. C. 2007. Abnormal root and nodule vasculature in R50 (*sym16*), a pea nodulation mutant which accumulates cytokinins. *Annals of Botany*. **99**:765-776.

Sakai, A., Kawano, S., and Kuroiwa, T. 1992. Conversion of protoplastids to amyloplasts in tobacco cultured cells is accompanied by changes in the transcriptional activities of plastid genes. *Plant Physiology*. **100**:1062-1066.

Schmülling, T., Werner, T., Riefler, M., Krupková, E., and Bartrina y Manns, I. 2003. Structure and function of cytokinin oxidase/dehydrogenase genes of maize, rice, *Arabidopsis* and other species. *Journal of Plant Research*. **116**:241-252.

Syõno, K., Newcomb, W., and Torrey, J. G. 1976. Cytokinin production in relation to the development of pea root nodules. *Canadian Journal of Botany*. **54**:2155-2162.

Syõno, K., and Torrey, J. G. 1976. Identification of cytokinins of root nodules of the garden pea, *Pisum sativum* L. *Plant Physiology*. **57**:602-606.

Roitsch, T., and Gonzalez, M.S. 2004. Function and regulation of plant invertases: sweet sensations. *Trends in Plant Science*. **9**:606–613.

Timmers, A. C. J., Auriac, M-C., and Truchet, G. 1999. Refined analysis of early symbiotic steps of the *Rhizobium-Medicago* interaction in relationship with microtubular cytoskeleton rearrangements. *Development*. **126**:3617-3628.

Tirichine, L., Sandal, N., Madsen, L. H., Radutoiu, S., Albreksten, A. S., Sato, S., Asamizu, E., Tabata, S., and Stougaard, J. 2007. A gain-of-function mutation in a cytokinin receptor triggers spontaneous root nodule organogenesis. *Science*. **315**:104-107.

van Brussel, A., Bakhuizen, R., van Spronsen., Spaink, H. P., Tak, T., Lugtenberg, B., Kijne, J. W. 1992. Induction of pre-infection thread structures in the leguminous host plant by mitogenic lipo-oligosaccharides of *Rhizobium*. *Science*. **257**: 70-72.

Vasse, J., de Billy, F., Camut, S., and Truchet, G. 1990. Correlation between ultrastructural differentiation of bacteroids and nitrogen fixation in alfalfa nodules. *Journal of Bacteriology.* **172**:4295-4306.

Vincent, J., and Brewin, N. 2002. Immunolocalization of a cysteine protease in vacuoles, vesicles, and symbiosomes of pea nodule cells. *Plant Physiology.* **123**:521-530.

Voroshilova, V. A., Demchenko, K. N., Brewin, N. J., Borisov, A. Y., and Tikhonovich, I. A. 2009. Initiation of a legume nodule with an inderterminate meristem involves proliferating host cells that harbour infection threads. *New Phytologist.* **181**:913-923.

Werner, T., Motyka, V., Laucou, V., Smets, R., Van Onckelen, H., Schmülling, T. 2003. Cytokinin-deficient transgenic Arabidopsis plants show multiple developmental alterations indicating opposite functions of cytokinins in the regulation of shoots and root meristem activity. *The Plant Cell.* **15**:2532-2550.

Werner,T, Köllmer, I, Bartrina, I., Holst, K., and Schmülling. 2006. New insights into the biology of cytokinin degradation. *Plant Biology.* **8**:371-381.

Yang, S., Yu, H., Goh, C. J. 2003. Functional characterization of a cytokinin oxidase gene DsCKX1 in *Dendrobium* orchid. *Plant Molecular Biology.* **51**:237-248.

Zalewski, W., Galuszka, P., Gasparis, S., Orczyk, W., and Nadolska-Orczyk, A. 2010. Silencing of the HvCKX1 gene decreases the cytokinin oxidase/dehydrogenase level in barley and leads to higher plant productivity. *Journal of Experimental Botany.* **61**:1839-1851.

Zhukov, V., Radutoiu, S., Madsen, L. H., Rychagova, T., Ovchinnikova, E., Borisov, A., Tikhonovich, I., and Stougaard, J. 2008. The pea *sym37* receptor kinase gene controls infection-thread initiation and nodule development. *Molecular Plant-Microbe Interactions.* **21**: 1600-1608.

CHAPTER 4

Agrobacterium rhizogenes transformation of *Pisum sativum*

Methodology

Transformation of *Pisum sativum*.

Scott R. Clemow[1], Lene Madsen[2], and Frédérique C. Guinel[1]

Addresses:

1. Department of Biology, Wilfrid Laurier University, 75 University Avenue West, Waterloo, N2L 3C5, Ontario, Canada.

2. Laboratory of Gene Expression, Department of Molecular Biology, University of Aarhus, Gustav Wieds Vej 10, 8000 Aarhus C, Denmark

Email: Scott R. Clemow – clem5940@mylaurier.ca

Frédérique C. Guinel – fguinel@wlu.ca

Lene H. Madsen – lhm@mb.au.dk

Abstract

Background

The use of model legume plants, such as *Medicago truncatula* and *Lotus japonicus*, has greatly advanced our knowledge of nodule development and regulation over the last decade. The transformation of these species has proven to be a powerful tool for the identification of genes involved in nodule organogenesis. However, this technology has not easily been used with pea, as with many of the agriculturally-relevant legumes. While many hairy-root transformation protocols have been explored for pea, the implementation of its genes into *Medicago truncatula* is currently the most efficient method to study the orthology of the nodulation genes. We have therefore developed a practical procedure for the production of pea composite plants which are useful to study pea nodulation genes.

Results

A protocol modified from Collier *et al.* (2005) was developed for the *Agrobacterium rhizogenes* transformation of pea. The technique relied on the insertion of decapitated

pea plants into Fibrgro© cubes (rockwool) saturated with *A. rhizogenes* carrying the *PsSYM10* gene to complement the non-nodulation mutants of Frisson P5 and P56. The plants, upon transfer to pots, were inoculated with *Rhizobium leguminosarum* bv. *viciae* and scored for nodulation three weeks later.

Conclusion

We successfully complemented the mutation responsible for P5 and P56. A transformation efficiency of 50-80% was achieved with each composite plant possessing at least 1 hairy-root with nodules. We foresee the transformation technique to provide valuable insight into the many nodulation and mycorrhizal mutants which are known in pea, as well as in the hormonal regulation of the developmental program underlying these two symbioses.

Introduction

The transformation of plants is a powerful technique used to study gene function and it serves as an important crop improvement tool (e.g. Somers *et al.* 2003). Pea, like most other large legume plants, have been considered to be recalcitrant to transformation (de Kathen and Jacobsen, 1995; Švábová and Griga, 2008; Akcay *et al.* 2009), although, as summarized in a recent paper (Krejčí *et al.* 2007), several successful methods have been developed by infecting explants with *Agrobacterium tumefaciens*. Unfortunately, most of these procedures are plagued by long shoot regeneration periods; 4 months (Davies *et al.* 1993; Bean *et al.* 1997), 6 months (Puonti-Kaerlas *et al.* 1990; Polowick *et al.* 2000), 7 months (Grant *et al.* 1995), or 9 months (Schroeder *et al.* 1993; de Kathen and Jacobsen, 1995) are required before rooting can take place. Bean *et al.* (1997) reported additional drawbacks including low fertility, phenotypic abnormalities, altered ploidy and loss of transgene activity in subsequent generations. The pitfalls attached to these techniques make them too labor-intensive and too inefficient to be used for research applications.

If the gene of interest is involved in root biology, e.g. in rhizobial and mycorrhizal symbioses, a convenient way to avoid the difficulties encountered with *A. tumefaciens* transformation techniques is by using *Agrobacterium rhizogenes*, the culprit responsible for hairy root disease (Jensen *et al.* 1986). Pea is susceptible to this type of transformation; Wen *et al.* (1999) produced hairy roots from a sterile stem segment that was inverted in agar. This technique has limitations; it requires the removal of the shoot and thus is only useful for root-organ cultures. These have been extensively used in

mycorrhizal studies (Fortin *et al.* 2002); however, they are not useful in the study of mutants, the symbiosis phenotype of which is controlled by the shoot. Also, this technique is not useful for the study of nodules as their development requires photosynthates to be produced by the shoot. To address this problem, techniques have been developed for the creation of composite plants that have transformed roots but a wild-type shoot (Boisson-Dernier *et al.* 2001). These chimeric plants have proven to be useful in studies of root nutrient uptake, hormone transport and the nodulation and mycorrhizal symbiotic pathways (Somers *et al.* 2003). Nicoll *et al.* (1995) obtained transformed hairy roots in pea by stab-inoculating the epicotyl near the cotyledons but this technique was intended for root-organ cultures and has never been built-upon for the purposes of studying the nodulation of transformed hairy roots. Complementation in mutant legumes deficient in nodulation, which has proven to be a good tool for elucidating the steps involved in the nodulation program, has never been accomplished in pea. This has forced researchers studying pea to resort to the transformation of pea genes into its close relatives such as *Trifolium repens* (Diaz *et al.* 1989) or *Medicago truncatula* (Edwards *et al.* 2007) or has prevented their complementation altogether, a hurdle Zhukov *et al.* (2008) encountered with *sym37* and Dolgikh *et al.* (2010) with *sym7*.

Since the first report of *A. rhizogenes* transformation in *Lotus corniculatus* (Jensen *et al.* 1986) and the subsequent nodule production on its transformed roots (Hansen *et al.* 1989), the technology has been transferred to other legumes [e.g. *Trifolium repens* (Díaz *et al.* 1989), *Vigna aconitifolia* (Lee *et al.* 1993), *Glycine max* (Cheon *et al.* 1993), *Vicia hirsute* (Quandt *et al.* 1993), *Lotus japonicus* (Stiller *et al.* 1997)], "for a short cut to study transgenic nodules" as described by many. To our knowledge, there has been only

one report of successful nodule formation on composite pea plants (Hohnjec *et al.* 2003); unfortunately, no transformation efficiency was provided by these authors and the methodology was not detailed. In this paper, we present a protocol for the rapid development of transformed hairy roots on composite plants for *Pisum sativum* using *A. rhizogenes*. We show that the transformed roots of non-nodulating pea mutants are efficiently complemented with the appropriate wild-type gene and are nodulated with *Rhizobium leguminosarum*.

Results and Discussion

At first we tried the most common approach for the *A. rhizogenes* transformation of plants, i.e., the stab-inoculation of different organs (epicotyls and radicle) to produce composite pea plants. Although numerous roots were visible at the location of the wound, they did not grow well and none tested positive for transformation. Similar observations were made for *Medicago truncatula* (barrel medic) (Boisson-Dernier *et al.* 2001). The best method at producing transformed composite plants (Figure 4.1) relied on the infection of 10 day-old pea seedlings using Fibrgro® cubes imbibed with *Agrobacterium* as in Collier *et al.* (2005). The treated plants were maintained in high humidity after a wilting period until roots develop ~10 days after infection. In the first few attempts, we utilized *A. rhizogenes* ARqual carrying a *gusA* intron reporter gene (generously provided by David Barker, INRA/CNRS, Toulouse, France) to transform the pea cultivar Sparkle. The composite plants were healthy as numerous roots developed from the callus and were able to produce nodules. To determine if the resulting roots were transformed, they were subjected to a histochemical GUS assay. However, this type of staining provided mixed results. A long incubation time (up to 48 hours) was needed to observe any colour change. Because of this long incubation time, abnormal staining was observed, such as speckled staining on the control roots. Collier *et al.* (2005) generated hairy roots successfully on two legumes, *Glycine max* (soybean) and barrel medic, obtaining transformation efficiencies (at least one transformed root per plant) of ~80% and 56%, respectively. The average number of transformed roots per plant was between 2 and 4 for soybean and below 2 for the barrel medic.

To assess the validity of our technique, we used Frisson and its mutants P5 (Duc and Messager, 1989) and P56 (Sagan *et al.* 1994) as a tool to score for transformation efficiency. As described by Madsen *et al.* (2003), P5 and P56 are *sym10* mutants that are defective in nod factor perception and thus are non-nodulating plants. The complementation of these mutants with the wild-type SYM10 gene should revert their nodulation phenotype; the presence of nodules would serve as the ultimate scoring for transformation success. *A. rhizogenes* strains AR12 and AR1193 carrying the *sym10* genes were both used to transform the mutant plants. Using the described protocol, we could induce the formation of transgenic roots on composite plants; when inoculated, these roots were nodulated. We were thus able to complement successfully the *sym10* mutants P5 and P56. In our experiments, strain AR12 was less efficient than strain AR1193 at producing transformed roots as less nodules were observed on roots transformed with AR12 (data not shown). To improve the transformation efficiencies using AR12, we attempted to use antibiotic counterselection to inhibit the growth of non-transformed roots in favour of transformed roots. A range of kanamycin concentrations (2 to 15 µg/mL) was tested but produced no satisfactory results, as treatments caused significant growth retardation of the roots and shoots compared to that of non-treated plants. Because AR1193 was more efficient than AR12 at transforming pea, we pursued our experiments using it solely.

IAA is commonly used in rooting media to promote root growth (e.g. Limpens *et al.* 2004). To trigger the growth of transformed roots, we treated plants for 48 hours with IAA (0.1 - 10 µM) two days after AR1193 infection. Furthermore, we tried cutting the roots off after their protrusion from the Fibrgro® cube as most of the roots that

regenerated were adventitious (e.g., Wasson *et al.* 2006; Kereszt *et al.* 2007). We also provided plants with only water to determine the impact of the other treatments. Plants that received exogenous IAA had transformation efficiencies between 14 and 40% with at least one transformed root, whereas plants that received only water had the lowest transformation efficiencies with 15-30% of the plants with at least one transformed root. Overall, the highest transformation efficiencies, 70% for P56 and 73% for P5 with at least one transformed root per plant, were obtained when all of the roots appearing through the Fibrgro® cube were excised; this pruning seemingly promoted root growth from the callus while it limited most adventitious root development. These new roots were subsequently inoculated with *Rhizobium leguminosarum* and were analyzed 21 days after inoculation for nodule formation. Using this method we have thus been able to complement two non-nodulating *sym10* mutants, P5 and P56, with the wild-type gene (Table 4.1). That is, hairy roots protruding from the callus were capable of forming nodules (Figure 4.1) where non-transformed roots could not. This high throughput transformation system is the first to show gene complementation in pea; it should be possible to use it for similar studies in the future.

Future directions should focus on a reliable marker for the selection of transformed roots. At the moment we are investigating an additional pea background for our technique as it has been reported that different pea backgrounds have varying degrees of susceptibly to *Agrobacterium tumefaciens* (Hawes *et al.* 1980). As a proof-of principle, we are testing if the pea mutant *Pssym7* (E69 background Sparkle) (Kneen *et al.* 1994) can be complemented via our transformation method. E69 (*sym7*) is a mutant defective in root hair curling and consequently no nodules develop on its roots (Walker *et*

Table 4.1 – Success rate of *sym10* complementation in pea mutants P5 and P56

Decapitated P5 and P56 plants were exposed to AR1193 carrying the *SYM10* gene for transformation. Because P5 and P56 are non-nodulating mutants with a defective *sym10* gene, successful transformation should restore nodulation. Hairy roots developed approximately 10 days after inoculation with AR1193. Transformation efficiencies were the highest when the regenerating roots were excised before inoculating with rhizobia. Plants with at least one transformed root, indicated by the presence of nodules, were considered as transformed plants. With each passing trial, adjustments were made to fine-tune the protocol. Thus the latest trial is distinguished from the other trials. In that trail the average number of nodules per plant was 9.6 for P5 and 7.29 for P56.

Plant	Treatments	Number of Plants	Number of Transformed Plants	Transformation efficiency (%)
P5	Water	36	10	28
P5	IAA	21	4	19
P5	Roots removed	22	12	55
P56	Water	20	4	20
P56	IAA	14	5	36
P56	Roots Removed	14	10	71
Latest Trial				
P5	Roots removed	22	16	73
P56	Roots removed	10	7	70

Figure 4.1 - Macro-photography of developing nodules

The non-nodulation mutants P56 (A and B) and P5 (C and D) with their nodulation capabilities restored through *A. rhizogenes* transformation. Nodules (arrows) on roots that have emerged from the callus should not be confused with pieces of vermiculite (arrowheads).
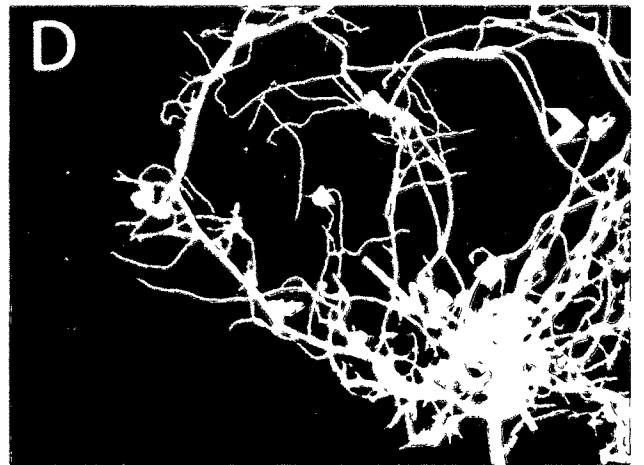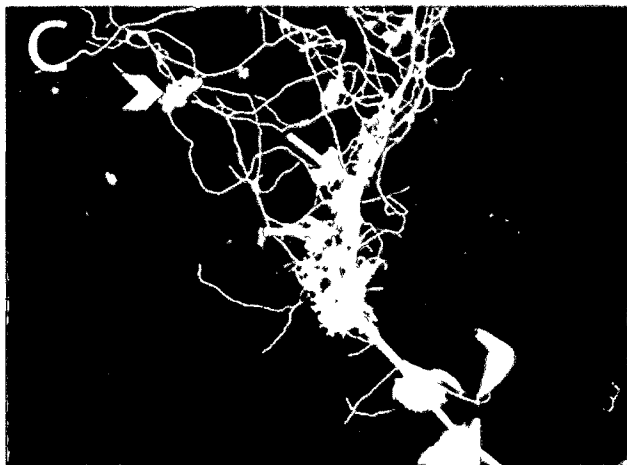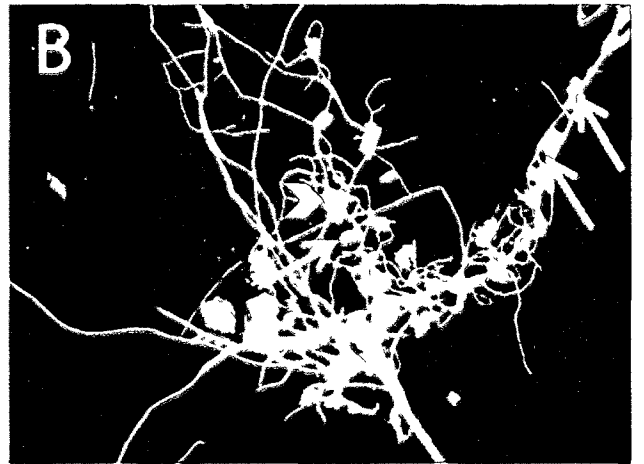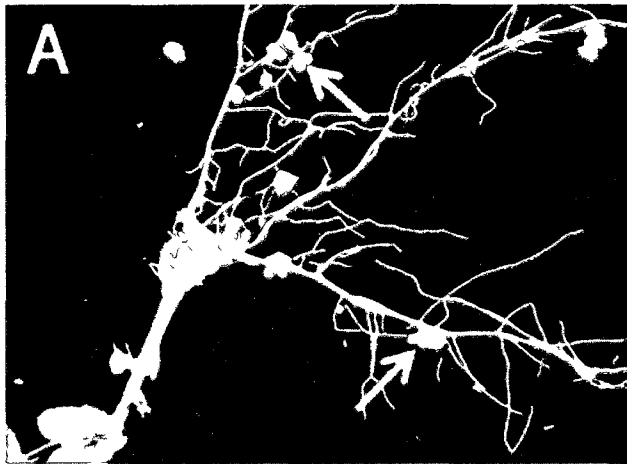
al. 2000). SYM7 is apparently a transcriptional regulator of important genes involved in nodulation; it is encoded by *NSP2* in *L. japonicus* and barrel medic (e.g., Dolgikh *et al.* 2010). If we are successful in the complementation of *Pssym7*, we will have additional support for the efficiency of our technique.

New insight in the roles of genes involved in nodulation should likely be provided with the transformation of legumes which once were thought to be recalcitrant, such as *Glycine max* (e.g., Kereszt *et al.* 2007), *Phaseolus vulgaris* L. (Estrada-Navarrete *et al.* 2007), *Aeschynomene indica* (Bondali *et al.* 2010) and now pea. Now that model legumes have opened the molecular way to nodulation studies, it is hoped that the transformation of other legumes will bring plenty of knowledge to this intricate developmental process.

MATERIALS AND METHODS

Plants, bacterial strains, and vectors

Seeds of *Pisum sativum* L. cv. Frisson and its mutants P5 and P56 [generous gift from Gérard Duc (Dijon, France)] were subjected to a 5-min surface-sterilization in 10% bleach followed by 3 rinses in sterile water. After a 24-hour imbibition period, seeds were planted in sterile vermiculite to germinate.

Agrobacterium rhizogenes AR1193 containing *SYM 10* was cultured in 100 mL of Luria Burtani (LB) broth (Bioshop, Burlington, ON) with 100 μg/mL rifampicin and 100 μg/mL spectinomycin (Bioshop, Burlington, ON). As a control, AR1193 with no vector containing the *SYM 10* insert was grown in LB with 100 μg/mL rifampicin. Cultures were grown at 28°C for 24 hours on an orbital shaker (New Brunswick Scientific, Edison, NJ) at 200 rpm until the culture reached an absorbance, read at 600 nm on a spectrophotometer (Varian, Inc., Mississauga, ON), between 0.6 and 0.8. The bacterial culture was then transferred to sterile centrifuge tubes and spun at 6000 x g for 15 min, 4°C. The pellet was resuspended in ice cold, ¼ x Murashige and Skoog basal medium (Sigma-Aldrich M5524), pH 5.8, until an optical density of 0.3 at 600 nm was reached.

Rhizobium leguminosarum bv. *viciae* 128C53K (gift from Dr. S. Smith, EMD Crop Bioscience, Milwaukee, WI) was cultured in 20 mL of yeast-mannitol broth (YMB), consisting of (g/L) mannitol 10.0, K_2HPO_4 0.5, $MgSO_4$ 0.2, NaCl 0.1, yeast extract 0.4 and of pH 6.8. The medium inoculated with a loop-full of culture, stored at -20°C, was placed on an orbital shaker (100 rpm) at 25°C for 48 hours.

Production of composite plants

The following steps represent the protocol with which we obtained the highest transformation efficiencies.

Imbibed seeds were planted at a depth of 1-2 cm and grown in the dark until the seedlings were ~ 8 cm tall (about 7 days, Figure 4.2, A). The dark treatment promoted etiolation and thus facilitated the decapitation of the plant at a later step. The plants were then moved into a controlled growth-room with a cycle of 16 hours of light at 23°C and 8 hours of dark at 18°C for 3 days to provide time for the leaves to develop.

Fibrgro® cubes (Homegrown Hydroponics Inc., Breslau, ON) were cut into smaller cubes (~ 2.5 cm^3). A dissecting probe was used to make a small starter hole, a quarter to half way through the cube, into which the stem of the plant was inserted. Without this hole the stems of the plants broke easily when inserted. Nine days after planting, the culture of *Agrobacterium rhizogenes* was prepared. Two to 4 sterile Fibrgro® cubes (prevacuum cycle for 20 min in the autoclave), with the holes facing up, were placed in 12 cm sterile petri plates. The cubes were inoculated with the diluted *A. rhizogenes* culture until complete saturation; 4 to 7 mL of inoculant was usually sufficient per cube (Figure 4.2, B). The 10-day old plants were decapitated above node 2 with a clean razor blade and the stem gently placed in the hole of the Fibrgro® cube (Figure 4.2, C). When the distance between node 2 and 3 was too short, the plant was cut above node 1 instead so that the leaves were never in contact with the inoculated cube.

Figure 4.2 - Schematic representation of important steps in the protocol for the production of composite pea plants.

A. Plants grown for 10 days in vermiculite (6 days in dark followed by 4 in light); B. Fibrgro® cubes saturated with *A. rhizogenes*; C. A 10 day-old plant decapitated above node 2 and inserted into Fibrgro® cube; D. A wilted pea plant about to receive water for recovery; E. Plants placed in growth tray under dome; F. High humidity provided by closed plastic lid and metal tray with water; G. A root protruding through a Fibrgro® 10 days after *A. rhizogenes* infection; and H. Rootless plants placed in an upright position in vermiculite and inoculated with *Rhizobium leguminosarum* 3 days later.
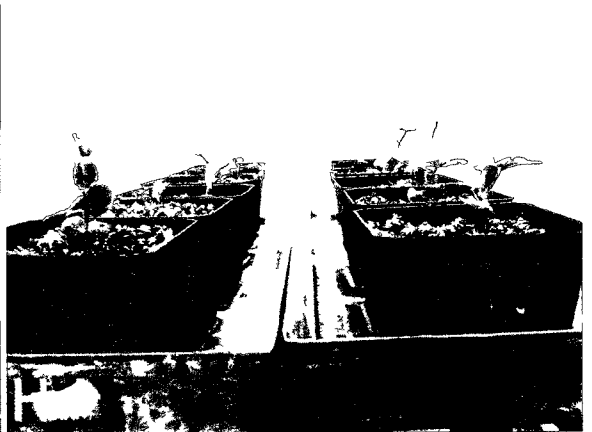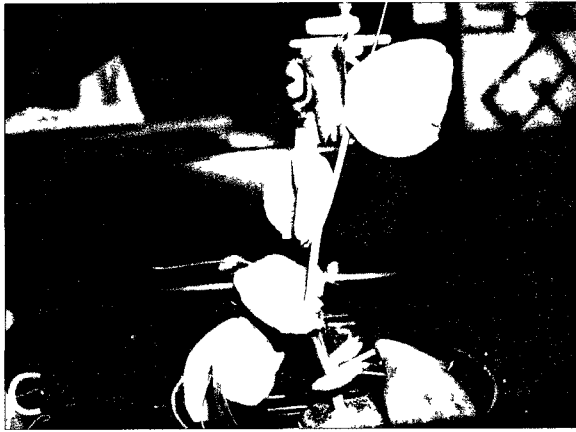
The petri plates containing the plant/cubes were placed in a plastic tray containing drainage holes and were covered with a transparent dome with ventilation holes closed. The tray was left on the lab bench for 24 hours. The following day the lid was removed and the plants were left for an additional 24 hours on the bench to promote wilting of the shoots (Figure 4.2, D). The wilting period was required for a callus to develop as it probably drew the inoculant into the plant (Collier *et al.* 2005). Once the stems were wilted, sterile water was added to the petri plates and the dome returned for an additional 24 hours (Figure 4.2, E). The plastic tray containing the plants was then placed into a metal watering tray and moved back to the growth room (Figure 4.2, F). Water was added to the metal tray until it emerged through the drainage holes to cover the bottom of the plastic tray. The plastic dome was kept snug to the plastic tray and the ventilation holes were closed to increase humidity, which increases transgenic yield (Kereszt *et al.* 2007).

Once roots were visible (~10 days after inoculation) (Figure 4.2, G), the Fibrgro® cube was carefully dissected with a pair of tweezers away from the roots and all the roots were excised with a sterile blade. At this stage most of the roots were adventitious and their removal promoted root growth from the callus. The callus with its epicotyl was transferred to a large pot filled with sterile vermiculite which was tightly packed around the rootless callus so that the shoot was kept upright (Figure 4.2, H). The plants were inoculated with 5 mL of 5% *Rhizobium leguminosarum* three days after being moved to vermiculite. They were harvested 21 days after inoculation and the roots arising from the callus were carefully examined; roots with nodules were counted and the number of nodules per root were recorded.

References

Akcay, U. C., Mahmoudian, M., Kamci, H., Yucel, M., and Oktem, H. A. 2009. *Agrobacterium tumefaciens*-mediated genetic transformation of a recalcitrant grain legume, lentil (*Lens culinaris* Medik). *Plant Cell Reports.* **28**:407-417.

Bean, S. J., Gooding, P. S., Mullineaux, P. M., and Davies, D. R. 1997. A simple system for pea transformation. *Plant Cell Reports.* **16**:246-252.

Boisson-Dernier, A., Chabaud, M., Garcia, F., Bécard, G., Rosenberg, C., and Barker, D. G. 2001. *Agrobacterium rhizogenes*-transformed roots of *Medicago truncatula* for the study of nitrogen-fixing and endomycorrhizal symbiotic associations. *Molecular Plant-Microbe Interactions.* **6**:695-700.

Bondali, K., Gherbi, H., Franche, C., Bastien, G., Fardoux, J., Barker, D., Giraud, E., and Cartieaux, F. 2010. The nod factor-independent symbiotic signaling pathway: Development of *Agrobacterium rhizogenes*-mediated transformation for the legume *Aeschynomene indica*. *Molecular Plant-Microbe Interactions.* **23**:1537-1544.

Cheon, C. I., Lee, N. G., Siddique, A. M., Bal, A. K., and Verma, D. P. S. 1993. Roles of plant homologues of Rab1p and Rab7p in the biogenesis of the peribacteroid membrane, a subcellular compartment formed de novo during root nodule symbiosis. *The EMBO Journal.* **12**:4125-4135.

Collier, R., Fuchs, B., Walter, N., Lutke, W. K., and Taylor, C. G. 2005. *Ex vitro* composite plants: an inexpensive, rapid method for root biology. *The Plant Journal.* **43**:449-457.

Davies, D. R., Hamilton, J., and Mullineaux, P. 1993. Transformation of peas. *Plant Cell Reports.* **12**: 180-183.

de Kathen, A., and Jacobsen, H. 1995. Cell competence for *Agrobacterium*-mediated DNA transfer in *Pisum sativum* L. *Transgenic Research.* **4**:184-191.

Díaz, C. L., Melchers, L. S., Hooykaas, P. J. J., Lugtenberg, B. J. J., and Kijne, J. W. 1989. Root lectin as a determinant of host-plant specificity in the *Rhizobium*-legume symbiosis. *Nature.* **338**:579-581.

Dolgikh, E. A., Leppyanen, I. V., Osipova, M. A., Savelyeva, N. V., Borisov, A. Y., Tsyganov, V. E., Geurts, R., and Tikhonovich, A. 2010. Genetic dissection of *Rhizobium*-induced infection and nodule organogenesis in pea based on *ENOD12A* and *ENOD5* expression analysis. *Plant Biology.* Article first published online: 17 AUG 2010; doi: 10.1111/j.1438-8677.2010.00372.x

Duc, G., and Messager, A. 1989. Mutagenesis of pea (*Pisum sativum* L.) and the isolation of mutants for nodulation and nitrogen fixation. *Plant Science.* **60**:207-213.

Edwards, A., Heckmann, A. B., Yousafzai, F., Duc, G., and Downie, J. A. 2007. Structural implications of mutations in the pea *SYM8* symbiosis gene, the *DMI1* ortholog, encoding a predicted ion channel. *Molecular Plant-Microbe Interactions.* **20**: 1183-1191.

Estrada-Navarrete, G., Alvarado-Affantranger, X., Olivares, J., Guillen, G., Diaz-Camino, C., Quinto, C., Gresshoff, P.M., Sanchez, F. 2007. Fast, efficient and reproducible genetic transformation of *Phaseolus* spp. by *Agrobacterium rhizogenes*. *Nature Protocols.* **2**: 1819-1824.

Fortin, J. A., Bécard, G., Declerck, S., Dalpé, Y., St-Arnaud, M., Coughlan, A. P., and Piché Y. 2002. Arbuscular mycorrhiza on root-organ cultures. *Canadian Journal of Botany.* **80**:1-20.

Grant, J. E., Cooper, P. A., McAra, A. E., Frew, T. J. 1995. Transformation of pea (*Pisum sativum* L) using immature cotyledons. *Plant Cell Reports.* **15**:254-258.

Hansen, J., Jorgensen, J.-E., Stougaard, J., and Marcker, K. A. 1989. Hairy roots – a short cut to transgenic root nodules. *Plant Cell Reports.* **8**:12-15.

Hawes, M. C., Robbs, S. L., and Pueppke, S. G. 1980. Use of root tumorigenesis assay to detect genotypic variation susceptibility of thirty-four cultivars of *Pisum sativum* to crown gall. *Plant Physiology.* **90**:18-184.

Hohnjec, N., Perlick, A. M., Pühler, A., and Küster, H. 2003. The *Medicago truncatula* sucrose synthase gene *MtSucS1* is activated both in the infected region of root nodules and in the cortex of roots colonized by arbuscular mycorrhizal fungi. *Molecular Plant-Microbe Interactions.* **16**:903-915.

Jensen, J. S., Marcker, K. A., Otten, L., and Schell, J. 1986. Nodule-specific expression of a chimaeric soybean leghaemoglobin gene in transgenic *Lotus corniculatus. Nature.* **321**:669-674.

Kereszt, A. Li, D. Indrasumunar, I. Nguyen, C. D. Nontachaiyapoom, S. Kinkema, M., and Greshoff, P. M. 2007. *Agrobacterium rhizogenes*-mediated transformation of soybean to study root biology. *Nature Protocols.* **2**: 948-952.

Kneen, B. E., Weeden, N. F., and LaRue, T. A. 1994. Non-nodulating mutants of *Pisum sativum* (L.) cv. Sparkle. *Journal of Heredity.* **85**:129-133.

Krejčí, P., Matušková, P., Hanáček, P., Reinöhl, V., Procházka, S. 2007. The transformation of pea (*Pisum sativum* L.): applicable methods of *Agrobacterium tumefaciens*-mediated gene transfer. **29**:157-163.

133

Lee, N. G., Stein, B., Suzuki, H., and Verma, D. P. S. 1993. Expression of antisense nodulin-35 RNA in *Vigna aconitifolia* transgenic root nodules retards peroxisome development and affects nitrogen availability to the plant. *The Plant Journal.* 3:599-606.

Limpens, E., Ramos, J., Franken, C., Raz, V., Compaan, B., Franssen, H., Bisseling, T., and Geurts, R. 2004. RNA interference in *Agrobacterium rhizogenes*-transformed roots of *Arabidopsis* and *Medicago truncatula. Journal of Experimental Botany.* **55**:983-992.

Madsen, B. E., Madsen, L. H., Radutoiu, S., Olbryt, M., Rakwalska, M., Szczglowski, K., Sato, S., Kaneko, T., Tabata, S., Sandal, N., and Stougaard, J. 2003. A receptor kinase gene of the LysM type is involved in legume perception of rhizobial signals. *Nature.* **425**:637-640

Nicoll, S. M., Brigham, L. A., Wen, F., and Hawes, M. C. 1995. Expression of transferred genes during hairy root development in pea. *Plant Cell, Tissue and Organ Culture.* **42**:57-66.

Polowick, P. L., Quandt, J., and Mahon, J. D. 2000. The ability of pea transformation technology to transfer genes into peas adapted to western Canadian growing conditions. *Plant Science.* **153**: 161-170.

Puonti-Kaerlas, J., Eriksson, T., and Engström, P. 1990. Production of transgenic pea (*Pisum sativum* L.) plants by *Agrobacterium tumefaciens*-mediated gene transfer. *Theoretical and Applied Genetics.* **80**:246-252.

Quandt, H. J., Pühler, A., and Broer, I. 1993. Transgenic root nodules of *Vicia hirsute.* A fast and efficient system for the study of gene expression in indeterminate-type nodules. *Molecular Plant-Microbe Interactions.* **6**:699-703.

Sagan, M., Huguet, T., and Duc, G. 1994. Phenotypic characterization and classification of nodulation mutants of pea (*Pisum sativum* L.). *Plant Science.* **100**:59-70.

Schroeder, H. E., Schotz, A. H., Wardley-Richardson, T., Spencer, D., and Higgins, T. J. V. 1993. Transformation and regeneration of two cultivars of pea (*Pisum sativum* L.). *Plant Physiology.* **101**:751-757.

Somers, D. A., Samac, D. A., and Olhoft, P. M. 2003. Recent advances in legume transformation. *Plant Physiology.* **131**: 892-899.

Stiller, J., Martirani, L., Tuppale, S., Chian, R.-J., Chiurazzi, M., and Greshoff, P. M. 1997. High frequency transformation and regeneration of transgenic plants in the model legume *Lotus japonicus. Journal of Experimental Botany.* **48**:1357-1365.

Švábová, L., and Griga, M. 2008. The effect of cocultivation treatments on transformation efficiency in pea (*Pisum sativum* L). *Plant Cell, Tissue and Organ Culture*. **95**:293-304.

Walker, S. A., Viprey, V., and Downie, J. A. 2000. Dissection of nodulation signaling using pea mutants defective for calcium spiking induced by Nod factor and chitin oligomers. *Proceedings of the National Academy of Sciences*. **97**:13413-13418

Wasson, A. P., Pellerone, F. I., and Mathesius, U. 2006. Silencing the flavonoid pathway in *Medicago truncatula* inhibits root nodule formation and prevents auxin transport regulation by Rhizobia. *The Plant Cell*. **18**:1617-1629.

Wen, F., Zhu, Y., and Hawes, M. C. 1999. Effect of pectin methylesterase gene expression on pea root development. *The Plant Cell*. **11**:1129-1140.

Zhukov, V., Radutoiu, S., Madsen, L. H., Rychagova, T., Ovchinnikova, E., Borisov, A., Tikhonovich, I., and Stougaard, J. 2008. The pea *sym37* receptor kinase gene controls infection-thread initiation and nodule development. *Molecular Plant-Microbe Interactions*. **21**: 1600-1608.

CHAPTER 5

Final Discussion and Conclusion

Conclusion

This thesis used an integrative approach to further identify the problems associated with cytokinin homeostasis in the pea mutant R50. The overall goal was to determine if PsCKX1 was differentially regulated during nodule development and to pinpoint the localization of its protein product. To accomplish this task, a few short-term objectives which will be discussed throughout this chapter had to be met.

As described in the introduction, an intricate program of events is required for a nodule to develop. Pea, a major agricultural crop, especially in western Canada, was once used as a main model plant to study nodulation (Fred and Haas, 1919; Bond, 1948). However, its popularity as a model organism has declined over the last two decades because it has not been amenable to many techniques used in other plant species. Spot-inoculation, one of these tools, is routinely used on the small legume plants barrel medic and *Lotus* which are now the legumes of choice to study nodulation. As discussed in chapter two, spot-inoculation has been used on pea in the past (van Brussel *et al.* 1992; Geurts *et al.* 1997; Albrecht *et al.* 1998), but I could not reproduce the results following the methods that these authors reported. When their techniques, along with those used to spot-inoculate soybean, barrel medic and *Lotus*, were used on pea, nodules rarely or never formed. Thus my objective was to develop an easy-to-use spot-inoculation technique, one that would be successful at nearly every attempt. The common approach to grow plants on agar plates and the primary root chosen to be spot-inoculated were not suitable for pea. A few modifications to accommodate the growth of a healthy pea in a pouch (Turgeon and Bauer, 1989) and the choice to spot-inoculate its lateral roots rather than its primary

roots proved to be successful. I am now able to induce the formation of a nodule on every spot-inoculated root (Chapter 2).

Spot-inoculation was a key tool to the experiments in chapter 3. I first had to determine the timing of the histological events (Timmers *et al.* 1999) throughout nodule organogenesis for pea and its mutant R50 (refer to table 3.1). With the spot-inoculation of pea that I performed, the timing of the histological events was on par to what was observed in barrel medic with the first events occurring in the pericycle 1 DAI; nodule primordium was established 2 DAI; infection threads and nodule meristem 3 DAI and an emerging nodule 5 DAI (Timmers *et al.* 1999). The time taken by the nodules to emerge that I report does not parallel those results from studies using flood-inoculation (e.g. Guinel and LaRue, 1991; Voroshilova *et al.* 2009). For example, in their recent study, Voroshilova *et al.* (2009) flood-inoculated 7-day-old plants and compared the cellular events needed for nodules to develop in three pea mutants. The authors depict an infection thread and resumption of cell proliferation in the inner cortex 5 DAI, a nodule primordium at 9 DAI and an emerging nodule at 12 DAI. The difference in the timing of the events is most likely a result of the time it takes for the mobilization of the flood-inoculated rhizobia to the zone of the root that is most susceptible to infection. When describing the phenotype of mutant lines with defective nodulation, the spot-inoculation technique could be used to standardize inoculation timing allowing for more precise comparisons with their wild-types.

Using this approach the early events in the nodule development for Sparkle was compared those of R50. The root hairs of R50 did not seem to respond to rhizobia in the same fashion as those of Sparkle. Most R50 root hairs appeared to have a crinkly or

wavy appearance to them compared to the curled hairs of Sparkle. These root hairs resemble those observed in the nodule inception regulator (*nin*), s*ym35*, pea mutant (Borisov *et al.* 2003). R50 root hairs also appear to be much longer than those of Sparkle, but this was not investigated in detail. Since the root hairs of R50 do not curl properly in response to the spot-inoculation, the first infection threads appear in the cortical cells three days later than in the cells of Sparkle. These infection threads were coiled masses as reported by Guinel and Sloetjes (2002) and as time progressed, the infection threads appeared to be blocked in the middle cortical cells with no cell divisions occurring in the inner cortical cells. Sparkle can be induced to form similar infection threads with high levels of exogenous cytokinin. Coiled infection threads and uncoordinated cell divisions have also been reported for the hyperinfection mutant *Lotus japonicus hit1* which has a defective cytokinin receptor (LHK1) (Murray et al 2007). This mutant thus lacks the required cytokinin perception to activate NIN essential for proper nodule development.

The spot-inoculation technique was a must for the accurate assessment of *PsCKX1* transcript levels throughout development of Sparkle and R50 nodules. It was interesting to assess the upregulation of PsCKX1 upon inoculation; this observation emphasized the importance of cytokinin oxidase in the development of a nodule. Over time *PsCKX1* levels in R50 nodules were shown to accumulate, supporting the data from Held *et al.* (2008). This makes sense as R50 is known to accumulate cytokinin which would trigger a negative feed-back loop (Ferguson *et al.* 2005). Moreover, Held *et al.* (2008) reported that compared to Sparkle the total cytokinin oxidase activity was low in R50 even though PsCKX1 transcripts were accumulating. Since Held *et al.* (2008) also reported that there

was no mutation in the coding region of PsCKX1 for R50, these results were difficult to explain.

To investigate this R50 conundrum, we placed our attention on the translation and localization of the PsCKX1 protein. A western blot with total proteins from R50 and Sparkle nodules was probed with polyclonal antibodies generated against PsCKX1. Surprisingly, two bands were detected in the Sparkle total protein around the predicted mass of 58 kDa for PsCKX1. Unexpectedly, for R50 there was only a very weak signal at 58 kDa, which aligned with one of the Sparkle bands, and a very large chemiluminescence signal around 40 kDa. Supporting the results of the western blot, the immunofluorescent detection was significantly higher in R50 nodules than in Sparkle nodules. PsCKX1 was localized to the same cellular locations in both pea lines, mainly to the cytoplasm as predicted by Held *et al.* 2008, at the periphery of the infected cells. PsCKX1 was also localized to the cytoplasm in the transfer cells of the nodule vasculature. I suggested earlier that the peculiarities observed on the western blot for both R50 and Sparkle could point toward post-transcriptional regulation of PsCKX1 by alternative RNA splicing. This would explain the two bands observed for Sparkle that migrated in close proximity to one another. In R50 a mutation in one of the introns could lead to a truncated protein during RNA splicing. It has been shown that mutations resulting in abnormal RNA splicing near an intron/exon border could result in a leaky expression of the wild-type gene (e.g. Lal *et al.* 1999). Lal *et al.* (1999) studying the mutant *shrunken2* of maize reported that the RNA splicing machinery only recognized approximately 10% of transcripts authentic splice sites. This would account for the odd PsCKX1 bands observed for R50 in the immuno blot. The big knock against this

hypothesis is the fact that Held *et al.* (2008) were able to get a clean sequence for PsCKX1 for R50 which showed no mutation. I remember Bozdarov (2008) having great difficulty in obtaining a full length clone of PsCKX1 from R50. He finally succeeded by using three overlapping primer pairs based on the sequence of Sparkle. Based on this methodology, if leaky expression did occur in R50, it is entirely possible that Bozdarov (2008) would have selected for the leaky, wild-type product rather than the truncated product that I am proposing results from alternative RNA splicing. Although the mutation of R50 remains elusive, its irregular cytokinin homeostasis is likely a result of a non-functional PsCKX1 protein.

It would be interesting to see if the implementation of a functional PsCKX1 from Sparkle into R50 could reduce the high cytokinin levels of R50. It would also be of interest to observe the impacts of silencing *PsCKX1* in Sparkle through RNAi transformation. However, at the moment, these experiments are not possible as there is no efficient transformation system for pea. This is why a protocol for the production of transformed composite plants was created (Chapter 4). This technique would permit the rapid transformation of roots making gene complementation a possibility. The lack of such a technique has frustrated many researchers working on pea symbioses (e.g. Zhukov *et al.* 2010 and Dolgikh *et al.* 2010). I was able to complement *SYM10* in the mutants P5 and P56 (background Frisson) and this could be considered a major breakthrough for researchers working on pea nodulation. It is important for such a technique to exist since there are pea mutants that have novel mutations affecting their nodulation that are not seen in barrel medic or *Lotus* (Dolgikh *et al.* 2010). We are currently testing the complementation of *SYM7* in the pea mutant E69 (background Sparkle) which Dolgikh *et*

al. (2010) attempted in barrel medic, however, without success. I trust the transformation technique that I have developed holds much promise but there is still room for improvement. I do believe that GUS is an inefficient marker for transformed roots in pea as it never seemed to work properly. I have also tried using GFP and DsRED to detect transformed roots, but I did not have the appropriate instrumentation to view the roots. The only manner by which I knew with certainty whether a root was transformed or not was by making a non-nodulating pea mutant form nodules. A good screening application needs to be formulated for pea. To this end, I suggest that the search for a useful selectable marker should be combined with the *sym10* transformation reported in chapter 4. Although the transformation technique is still in the developmental phase, it has allowed the complementation of a pea mutant with its wild-type gene. A quick transformation technique to obtain transformed roots would be a luxury that has not yet been available for researchers studying pea. For R50 it should serve to identify the problems with its cytokinin homeostasis with the insertion of a functional wild-type PsCKX1. I hope that the two techniques I developed during this thesis will help remove some of the barriers that researchers have encountered when studying pea nodulation.

In conclusion, if I had to speculate on the function of PsCKX1 in nodule organogenesis in the wild-type, I would propose that it is extremely important because it tightly regulates the levels of cytokinin in roots waiting to be infected. It is known that cytokinin is essential for the initiation of nodule organogenesis as its perception opens the path for successful nodulation (Frugier *et al.* 2008). Cytokinin stimulates the expression of *NIN* (Murray *et al.* 2007) in the cortex and, as suggested by Oldroyd (2010, personal communication), *NIN* would be translocated to the vasculature promoting cortical cell

divisions. Cytokinin also up-regulates *ENOD40* (Fang and Hirsch, 1998) in the vasculature.

NIN and cytokinin are also known to co-localize in the epidermis, therefore likely playing a role in the epidermal program. *NIN* may possibly control nodule number by restricting the zone that is susceptible to infection in wild-type plants (Marsh *et al.* 2007). In the mutant R50, a defective cytokinin oxidase would cause cytokinin to accumulate in abnormally high levels which would result in the over-expression of *NIN*. Such high levels of this transcription factor would negatively regulate infection and prevent cortical cell divisions. The cortical program would be inhibited by the ineffective recruitment of NIN by the vasculature. The rare nodules observed in R50 may be explained by a leaky expression of the wild-type protein PsCKX1.

References

Albrecht, C., Geurts, R., Lapeyrie, F., Bisseling, T. 1998. Endomycorrhizae and rhizobial Nod factors both require SYM8 to induce the expression of the early nodulin genes *PsENOD5* and *PsENOD12A*. *The Plant Journal*. **15**:605-614.

Bond, L. 1948. Origin and developmental morphology of root nodules of *Pisum sativum*. *Botanical Gazette*. **109**: 411-434.

Borisov, A. Y., Madsen, L. H., Tsyganov, V. E., Umehara, Y., Voroshilova, V. V., Batagov, A. O., Sandal, N., Mortensen, A., Schauser, L., Ellis, N., Tikhonovich, I. A., and Stougaard, J. 2003. The *Sym35* gene required for root nodule development in pea is an ortholog of Nin from *Lotus japonicus. Plant Physiology*. **131**:1009-1017.

Bozdarov, J. 2008. (BSc Thesis). Cloning of the full-length CKX1 gene from pea (*Pisum sativum*) and comparison of the sequence from the nodulation mutant R50. Wilfrid Laurier University, Ontario, Canada.

Dolgikh, E. A., Leppyanen, I. V., Osipova, M. A., Savelyeva, N. V., Borisov, A. Y., Tsyganov, V. E., Geurts, R., and Tikhonovich, A. 2010. Genetic dissection of *Rhizobium*-induced infection and nodule organogenesis in pea based on *ENOD12A* and *ENOD5* expression analysis. *Plant Biology*. Article first published online: 17 AUG 2010; doi: 10.1111/j.1438-8677.2010.00372.x

Fang, Y., and Hirsch, A. M. 1998. Studying early nodulin gene *ENOD40* expression and induction by nodulation factor and cytokinin in transgenic alfalfa. *Plant Physiology*. **116**:53-68.

Ferguson, B.J., Wiebe, E.M., Emery, N., and Guinel, F.C. 2005. Cytokinin accumulation and an altered ethylene response mediate the pleiotropic phenotype of the pea nodulation mutant R50 (*sym16*). *Canadian Journal of Botany*. **83**: 989-1000.

Fred, E. B., and Haas, A. R. C. 1919. The etching of marble by roots in the presence and absence of bacteria. *The Journal of General Physiology*. **1**:631-638.

Frugier, F., Kosuta, S., Murray, J. D., Crespi, M., and Szczyglowski, K. 2008. Cytokinin: secret agent of symbiosis. *Trends in Plant Science*. |:115-120.

Geurts, R., Heidstra, R., Hadri, A-E., Downie, J. A., Franssen, H., van Kammen, A., Bisseling, T. 1997. Sym2 of pea is involved in a nodulation factor-perception mechanism that controls the infection process in the epidermis. *Plant Physiology*. **115**:351-359.

Guinel, F. C, and LaRue, T. A. 1991. Light microscopy study of nodule initiation in *Pisum sativum* L. cv Sparkle and its low nodulating mutant E2 (*sym5*). *Plant Physiology.* **97**:1206-1211.

Guinel, F.C. and Sloetjes, L.L. 2000. Ethylene is involved in the nodulation phenotype of *Pisum sativum* R50 (*sym16*), a pleiotropic mutant that nodulates poorly and has pale green leaves. *Journal of Experimental Botany.* **51**: 885-894.

Held, M., Pepper, A. N., Bozdarov, J., Smith, M. D., Emery, R. J. N., Guinel, F. C. 2008. The pea nodulation mutant R50 (*sym16*) displays altered activity and expression profiles for cytokinin dehydrogenase. *Journal of Plant Growth and Regulation.* **27**:170-180.

Lal, S., Choi, J-H., and Hannah, L. C. 1999. The AG dinucleotide terminating introns is important but not always required for Pre-mRNA splicing in the Maize endosperm. *Plant Physiology.* **120**: 65-72.

Marsh, J. F., Rakocevic, A., Mitra, R. M., Brocard, L., Sun, J., Eschstruth, A., Long, S. R., Schultze, M., Ratet, P., and Oldroyd, G. E. D. 2007. *Medicago truncatula* NIN is essential for rhizobial-independent nodule organogenesis induced by autoactive calcium/calmodulin-dependent protein kinase. *Plant Physiology.* **144**:324-335.

Murray, J. D., Karas, B. J., Sato, S., Tabata, S., Amyot, L., and Szczyglowski, K. 2007. A cytokinin perception mutant colonized by *Rhizobium* in the absence of nodule organogenesis. *Science.* **315**:101-104.

Timmers, A. C. J., Auriac, M-C., and Truchet, G. 1999. Refined analysis of early symbiotic steps of the *Rhizobium-Medicago* interaction in relationship with microtubular cytoskeleton rearrangements. *Development.* **126**:3617-3628.

Turgeon, B. and Bauer, W. 1983. Spot inoculation of Soybean roots with *Rhizobium japonicum. Protoplasma.* **115**: 122-128.

van Brussel, A. A. N., Bakhuizen, R., van Spronsen, P.C., Spaink, H.P., Tak, T., Lugtenberg, B. J. J., Kijne, J. W. 1992. Induction of pre-infection thread structures in the leguminous host plant by mitogenic lipo-oligosaccharides of *Rhizobium. Science.* **257**:70-72.

Voroshilova, V. A., Demchenko, K. N., Brewin, N. J., Borisov, A. Y., and Tikhonovich, I. A. 2009. Initiation of a legume nodule with an inderterminate meristem involves proliferating host cells that harbour infection threads. *New Phytologist.* **181**:913-923.

Zhukov, V., Radutoiu, S., Madsen, L. H., Rychagova, T., Ovchinnikova, E., Borisov, A., Tikhonovich, I., and Stougaard, J. 2008. The pea *sym37* receptor kinase gene controls infection-thread initiation and nodule development. *Molecular Plant-Microbe Interactions.* **21**: 1600-1608.